

**ARE ENZYMES ACCURATE INDICATORS
OF POSTMORTEM INTERVAL?
A BIOCHEMICAL ANALYSIS**

A Thesis

**Submitted to the Graduate Faculty of the
Louisiana State University and
Agricultural and Mechanical College
in partial fulfillment of the
requirements for the degree of
Master of Arts**

in

The Department of Geography and Anthropology

**by
Karly Laine Buras
B.S., Louisiana State University, 2001
May 2006**

ACKNOWLEDGEMENTS

I would like to thank the members of my thesis committee for their continued encouragement and help throughout my program. My heartfelt thanks go out to Bob Tague, Mary Manhein, and Grover Waldrop for helping me along the way. I would especially like to thank Grover Waldrop for his contributions to my thesis expenses, as well as for the use of his lab for my research. I would not have been able to do any of this without his help. To my statistics professor, Dr. Lynn Lamotte, I owe my eternal gratitude for all of his help with my data and statistical procedures. I would also like to thank the people at the Louisiana State University School of Veterinary Medicine, who helped me with my initial research on the rats used in the study. Finally, I would like to thank my family and friends who have supported me along the way. I couldn't have done this without each of them.

TABLE OF CONTENTS

Acknowledgements.....	ii
List of Tables.....	iv
List of Figures.....	v
Abstract.....	vii
Introduction.....	1
Literature Review.....	6
Materials and Methods.....	16
Results.....	20
Discussion.....	75
Works Cited.....	80
Vita.....	83

LIST OF TABLES

4.1. PI Values of Knots in Figure 4.1.....	21
4.2. PI Values of Knots in Figure 4.2.....	23
4.3. PI Values of Knots in Figure 4.3.....	23
4.4. PI Values of Knots in Figure 4.4.....	25
4.5. PI Values of Knots in Figure 4.5.....	27
4.6. PI Values of Knots in Figure 4.6.....	27
4.7. PI Values of Knots in Figure 4.7.....	29
4.8. PI Values of Knots in Figure 4.8.....	29
4.9. PI Values of Knots in Figure 4.9.....	31
4.10. PI Values of Knots in Figure 4.10.....	33
4.11. PI Values of Knots in Figure 4.11.....	33
4.12. PI Values of Knots in Figure 4.12.....	35
4.13. PI Values of Knots in Figure 4.13.....	35
4.14. PI Values of Knots in Figure 4.14.....	37
4.15. PI Values of Knots in Figure 4.15.....	39
4.16. PI Values of Knots in Figure 4.16.....	39
4.17. PI Values of Knots in Figure 4.17.....	41
4.18. PI Values of Knots in Figure 4.18.....	43
4.19. PI Values of Knots in Figure 4.19.....	43
4.20. PI Values of Knots in Figure 4.20.....	45

LIST OF FIGURES

4.1. LDH activity in outside liver samples.....	22
4.2. LDH activity in cold room liver samples.....	24
4.3. CK activity in outside liver samples.....	26
4.4. CK activity in cold room liver samples.....	28
4.5. AST activity in outside liver samples.....	30
4.6. AST activity in cold room liver samples.....	32
4.7. ADH activity in outside liver samples.....	34
4.8. ADH activity in cold room liver samples.....	36
4.9. LDH activity in outside muscle samples.....	38
4.10. LDH activity in cold room muscle samples.....	40
4.11. CK activity in outside muscle samples.....	42
4.12. CK activity in cold room muscle samples.....	44
4.13. AST activity in outside muscle samples.....	46
4.14. AST activity in cold room muscle samples.....	47
4.15. LDH activity in outside heart samples.....	48
4.16. LDH activity in cold room heart samples.....	49
4.17. CK activity in outside heart samples.....	50
4.18. CK activity in cold room heart samples.....	51
4.19. AST activity in outside heart samples.....	52
4.20. AST activity in cold room heart samples.....	53

4.21. Lactate Dehydrogenase (Outside Liver Samples).....	55
4.22. Lactate Dehydrogenase (Cold Liver Samples).....	56
4.23. Creatine Kinase (Outside Liver Samples).....	57
4.24. Creatine Kinase (Cold Liver Samples).....	58
4.25. Aspartate Aminotransferase (Outside Liver Samples).....	59
4.26. Aspartate Aminotransferase (Cold Liver Samples).....	60
4.27. Alcohol Dehydrogenase (Outside Liver Samples).....	61
4.28. Alcohol Dehydrogenase (Cold Liver Samples).....	62
4.29. Lactate Dehydrogenase (Outside Muscle Samples).....	63
4.30. Lactate Dehydrogenase (Cold Muscle Samples).....	64
4.31. Creatine Kinase (Outside Muscle Samples).....	65
4.32. Creatine Kinase (Cold Muscle Samples).....	66
4.33. Aspartate Aminotransferase (Outside Muscle Samples).....	67
4.34. Aspartate Aminotransferase (Cold Muscle Samples).....	68
4.35. Lactate Dehydrogenase (Outside Heart Samples).....	69
4.36. Lactate Dehydrogenase (Cold Heart Samples).....	70
4.37. Creatine Kinase (Outside Heart Samples).....	71
4.38. Creatine Kinase (Cold Heart Samples).....	72
4.39. Aspartate Aminotransferase (Outside Heart Samples).....	73
4.40. Aspartate Aminotransferase (Cold Heart Samples).....	74

ABSTRACT

There are numerous ways to estimate postmortem interval (PMI), or time since death, including body temperature, rigor mortis, insect activity, and decomposition. Individually, many of these indicators are prone to inaccuracy due to the influence of the external environment upon them. This study proposed that in addition to or in conjunction with these and other indicators, certain enzymes could be used to accurately determine PMI, namely aspartate aminotransferase (AST), alcohol dehydrogenase (ADH), creatine kinase (CK), and lactate dehydrogenase (LDH).

In this project, 18 rats were studied postmortem to determine how ethanol consumption and different environments affect decomposition and enzyme activity. Three groups of six rats each were studied at three different times. Two rats in each group of six received Treatment 1 (0 mg/dL ethanol), two received Treatment 2 (75 mg/dL ethanol), and two received Treatment 3 (200 mg/dL ethanol). One hour after treatments were given, the rats were euthanized in a CO₂ chamber. After euthanasia one rat from each treatment pair was put into a cold room (approximately 40° F) and the other was put outside. Liver tissue, cardiac muscle, and skeletal muscle samples were taken periodically and frozen at -80° C.

Samples were homogenized and centrifuged at 12x g for one hour and put back into -80° C until analysis on the spectrophotometer. After this analysis, the data were compiled using the SAS/IML version 9.1 program. Graphs for each enzyme and tissue type were made, illustrating the positions of all data points in relation to the prediction interval deduced from the statistical computations. Visually and statistically, the graphs

did not seem to exhibit any discernible pattern with regard to enzyme velocity. Alcohol did not appear to affect the enzyme activity.

This study did not find a pattern for using enzyme velocity to determine PMI. Further research projects could attempt to study other variables not considered in this project. Studies using larger animals, different environments, and different taphonomic conditions would all be projects that could enhance this subfield of forensics.

INTRODUCTION

Postmortem interval (PMI), or time since death, is a matter of crucial importance in any death investigation, but especially those involving homicide. In the investigation of deaths from any cause, the evaluation of changes in the body requires careful consideration of all variables one may encounter. One must record pertinent variables such as ambient temperature, relative humidity, covering or clothing of the body, general structure and supporting structure of the body, presence and activity of scavengers, wind currents, and other influencing factors. Also considered must be additional items, including events which occurred prior to death: existence of injury; relationship of injury and death; interval between injury and death; cause, mode, and manner of death; musculature activity of the deceased prior to injury or death; and health of the person before death (Lyle et al. 1958). Such information, accompanied by a thorough study of the body, can help to both identify a victim and convict or exonerate suspects. Even in natural deaths, PMI can have implications in legal matters, such as inheritance and insurance issues (Wells and Lamotte 2001).

Postmortem changes in a body depend on several factors, many of which are listed above, and PMI can be extremely difficult to determine (Bass 1984). Any physical or biological change that is a function of time since death provides a potentially useful clue in determining PMI. Initially, the most reliable PMI indicators are usually the predictable physical and chemical consequences of death (Henssge et al. 1995). Coe noted in his 1974 review that “extensive studies by many workers have shown that postmortem variations occur quite rapidly in most enzymes” (p 27). This study intends to determine whether certain enzymes are accurate indicators of early PMI, defined by Jetter

(1959) as “that period extending [from death] to the onset of hemolysis” (p 341), in spite of the different circumstances under which a death can occur. If found to be predictable, these enzymes could be used in conjunction with other PMI indicators to estimate more accurately the time since death.

Most environmentally dependent indicators are too unreliable to be used by themselves to reach an accurate PMI estimate. For example, the entomological evidence at the scene of an investigation can be altered by one factor or another. Fire ants present a major problem to investigators—they will eat the larvae of other insects, and if they are exposed to the body long enough, they can alter the entomological evidence so much that PMI estimates may show a time of death much later than when it actually occurred. They can also attack the body itself, leaving strange marks that are often undecipherable to those who would normally examine the body. The vast majority of cases are autopsied only by local pathologists and are never seen or examined by a forensic pathologist or other trained physician whose examination could be of value to recognize such a phenomenon (Lyle et al. 1958). In addition, Wells and Lamotte (2001) state that “In its most conservative form, [insect age estimation] does not estimate the maximum PMI because an unknown period of time may elapse between death and the deposition of eggs or larvae” (p 264). Insects also do not normally lay eggs in the rain or in cold weather, and if a body is stored and disposed of later, insect activity will not correspond to the actual time of death. Weather, body temperature, geographic region, drugs and other toxins, food type, and so forth, can also play a part in carrion insect activity (Wells and Lamotte 2001), as well as enzyme activity (Young et al. 1975).

Unfortunately, these are not the only ways in which a PMI estimate can be skewed. Every visual or external indicator is affected too heavily by the environment to be reliable by itself, and, even if used together with another indicator, both the accuracy and precision of the estimate may be called into question in a forensic case.

Location is also an important piece of the PMI puzzle. How different must a body that has been left outside look from one which has been in a cool, dark room, or even underwater? When bodies are located in different places, some indicators may become invalid. Putrefaction is one such variable—it can occur anywhere from a few hours to a few days after death, depending on the environment. The classic “triad of death”—algor mortis, rigor mortis, and livor mortis—is subject to unpredictable variations, and decomposition is partially determined by the conditions of the local environment. Most of the forensic investigators who have written on physical changes that occur after death have based estimates of time since death on appearance of livor mortis, rigor mortis, changes in the eyes, and putrefaction (Lyle et al. 1958). However, these “classic” signs of death (SOD) are “fickle beyond the imagination,” (Burton 1974, p 529) and many authorities on the subjects of rigor, algor, and livor mortis do not agree on their appearance and progression except within wide limits. The consensus, according to Burton (1974), is that the average human body cools at a rate of 2½ to 3½ degrees per hour for the first 2-3 hours, and 1 degree each hour thereafter until reaching ambient temperature. He also states that no two authorities on the subject of algor mortis agree. Rigor is a tricky subject as well, because it is so unpredictable. Often, it occurs instantly, and other times not at all (especially in the extremely obese or emaciated). Rigor must

also not be confused with stiffening due to cold. As with other enzymatic or biological processes, cold temperatures will retard rigor, and warm temperatures accelerate it (Burton 1974).

Even before Burton, Camps (1959) was writing about the limited reliability of the PMI indicators being used at the time. He stated that the three most common were fixation of hypostasis, state of rigor mortis, and temperature changes from heat loss. As stated above, these indicators are not always reliable, and one should proceed with caution when using them to fix a time of death. Burton (1974) goes so far as to say, “it is this total unreliability of such frivolous factors as the SOD that makes it unwise to use them in fixing the time of death” (p 29).

Also complicating the PMI estimate is the notion that the longer the postmortem interval, the more unreliable the timetable becomes, until the question arises as to whether the signs are worthwhile at all anymore. SOD and PMI indicators are to be used with caution in fixing the time of death. Accuracy can only come with experience and a combination of those SOD and PMI indicators which are the least variable. Postmortem changes are variable, and, at times, deceiving. To fix the time of death by only one or a few signs of death, with any degree of certainty, would be almost impossible (Burton 1974). Further study of these external signs, as well as biochemical ones, is needed to accurately assess time since death in the future. The fewer the factors that vary widely under different conditions and the greater the number of bodily changes evaluated, the greater will be the accuracy of the time of death estimate.

Each known factor for which an approximate correction can be made carries with it a margin of error that is inherent in assessing the effects of environmental factors and

needs to always be taken into account. All of the errors will not likely be in the same direction, and the probable error will undoubtedly be less than the maximum possible error (Camps 1959). Even so, the aim of the forensic scientist should always be to limit the margin of error as much as possible. The only method by which to decrease this margin is by combining numerous internal and external indicators, always selecting the most reliable ones.

LITERATURE REVIEW

Biochemical analysis of postmortem body fluids offers an alternative to highly environmentally dependent indicators. Occasionally, there are no visible changes or only minor changes found at autopsy, and the pathologist is pressed for an opinion on whether certain antemortem conditions may have been present (Naumann 1950). Decomposition, insect activity, and other PMI indicators are not always present, and, therefore, cannot be used to determine time since death in such cases. Pathologists and medical examiners are also confronted with cases in which postmortem anatomic changes are inconclusive and in which “further elucidation of the problem depends on the recognition and interpretation of chemical changes in the tissues and body fluids” (Jetter and McLean 1942, p 178). Biochemical changes have proven themselves in the medical field as indicators of various types of disease, necrosis, or infarction. It stands to reason that these changes would also be reliable in the field of forensic science.

Work has been done on enzymes as far back as the 1940s and 1950s. Camps (1959, p 80-81) refers to an unpublished work by Kolmen and Parr, who state that “the use of enzymes for the estimation of the time of death is a possibility...one might thus make some estimate of the time elapsing since death by measuring the activities of a small group of selected enzymes, and then consulting experimentally derived graphs which relate enzymic activity with time after death”. Since then, much work has been done on postmortem activity of various enzymes, and new technology has improved both accuracy and reliability. Enticknap (1960) correlated postmortem serum enzyme accumulation in the blood from arm veins to the time elapsed between death and necropsy. Other studies have been done in an attempt to compare enzyme levels in

various areas of the body and correlate them with PMI (Backer et al. 1980, Budd 1982, Stone and Rooney 1984, Gilliland and Bost 1993). Decomposing fluid recovered from the chest has at times been used as a substitute when blood is not obtainable from the vascular system because of decomposition (Gilliland and Bost 1993).

Determination of postmortem chemical values may be of use in a variety of situations. “Results of studies may demonstrate biochemical abnormalities responsible for death when no autopsy is performed, establish a cause of death where autopsy reveals no significant anatomic pathology, help in evaluation of physiological effects of recognizable anatomic lesions, and assist in estimation of time of death” (Coe 1974, p 13). Development of automation in laboratories, availability of commercial assay kits, ease of performance, and low cost have all made routine examination of postmortem blood and body fluids both practical and desirable (Coe 1974). A sizable body of knowledge has been published to enable an investigator to interpret postmortem values for a wide variety of substances. Coe (1974) compiled an extensive review of the literature on postmortem chemistry of blood, vitreous humor, and cerebrospinal fluid. Unfortunately, there is a lack of published information on postmortem enzyme concentrations in tissues, as opposed to body fluids.

Researchers have found that some biochemical markers remain remarkably stable after death while others show varying degrees of change. Jetter (1959) claimed that these biochemical changes that occur are the result of three things: “the agonal period of anoxia, the continuation of biochemical changes in the early postmortem period, and the distribution of easily diffusible substances between erythrocytes and plasma as well as between interstitial fluid, tissue cells, and the blood” (p 340). These changes, he said, are

never uniform, following a predictable pattern for some materials while being erratic for others. Therefore, the question arises: Is postmortem chemical analysis more reliable than other methods of evaluation, or is it just as susceptible to environmental variables? These changes do seem to follow some general rules, at least in the early postmortem time (Schleyer 1963), the period on which this study will focus.

Cerebrospinal fluid (CSF) was first studied and found to be useful for certain medical or antemortem abnormalities such as heart conditions. However, collection is inconvenient and obtaining a sample free of blood or other contaminants may be difficult, especially in certain postmortem circumstances. Changes in cerebrospinal fluid also occur fairly rapidly and tend to be erratic, not allowing it to be used reliably or for very long in determining PMI (Coe 1974).

Vitreous humor has increasingly been used as an alternative to CSF in chemical analysis. The eye is isolated and well protected so that vitreous humor is normally preserved despite severe trauma, and less subject to contamination or putrefactive change than blood or CSF. Researchers have also found that for many substances chemical changes occur more slowly here than in blood or CSF, allowing for longer periods of reliable PMI assessment (Coe 1974).

The purpose of this project is to determine whether study of enzymes can be used in combination with standard physical examinations and other PMI indicators during the early PMI to estimate time since death, and if and to what degree enzyme activity is affected by environmental conditions. Tissues were chosen for this study because enzyme content in them may differ significantly, depending on the tissues from which the sample is taken. For example, the activity levels of certain enzymes that are produced in

the liver may be higher in tissues taken from the liver than tissues taken from elsewhere because they do not have a chance to be circulated throughout the bloodstream postmortem because of coagulation, body position, or other factors.

This study will examine the activity levels of four enzymes present in body tissues immediately postmortem and compare these levels to those found at other postmortem time points to determine whether there is a significant change among them. If significant differences are shown, the researcher will then examine whether there is a predictable pattern by which activity increases or decreases as a function of time. The four enzymes to be studied are aspartate aminotransferase (AST), alcohol dehydrogenase (ADH), creatine kinase (CK), and lactate dehydrogenase (LDH). Each of these enzymes serves a unique regulatory function in the body and can be easily measured using commercially available assay kits.

Aspartate Aminotransferase—The function of an aminotransferase, or transaminase, is to transfer a preexisting amino group from one amino acid to another. This occurs during synthesis of nonessential amino acids or in the degradation of amino acids. AST functions in amino acid catabolism, which involves degradation of foodstuffs or stored fuels such as carbohydrates, lipids, and proteins into either usable or storable forms of energy (Devlin 2002). It is found in heart and skeletal muscle, as well as liver, kidney, erythrocytes, and brain tissue, and acts to catalyze the reaction that converts aspartate to glutamate.

AST is presently used in medicine as an indicator of heart and liver damage due to myocardial infarction, necropsy, and carcinogenesis. Raised serum levels may be associated with damage or disease to the heart, liver, skeletal muscle, kidneys, and

erythrocytes due to myocardial infarction, viral hepatitis, liver necrosis, cirrhosis, and muscular dystrophy (Zilva and Pannall 1979). The amount of enzyme released depends on the degree of cellular damage, the intracellular concentrations of the enzymes, and the mass of affected tissue. The nature of the insult (viral infection, hypoxia, or surgical, chemical, or mechanical trauma) has no bearing on the enzymes released into circulation (Bhagavan 2002). However, the nature of the enzyme released is reflected in the severity of damage. Mild conditions release cytoplasmic enzymes, whereas necrotic conditions release mitochondrial enzymes as well. In severe liver damage, the serum AST level is extremely high because both isoenzymes are released. Erythrocytes contain high concentrations of AST; therefore, hemolysis can elevate its levels as well. Such is also the case with postmortem tissue decomposition. As the tissue degrades and cells lyse, more AST is released into the area directly surrounding tissues containing it (Bhagavan 2002). Enticknap (1960) noted a “striking” progressive postmortem increase in concentration of AST, stating that the increase was roughly linear for the first 60 hours postmortem, so that a crude PMI estimate was possible.

Alcohol Dehydrogenase—A dehydrogenase is a subclassification of oxidoreductases. Oxidoreductases catalyze oxidation-reduction reactions, while dehydrogenases catalyze specifically the oxidation of an alcohol to an aldehyde. ADH functions in the first step of alcohol metabolism by oxidizing ethanol to acetaldehyde and producing NADH; hence, it is found only in the liver, and almost exclusively in the cytosol of the liver’s parenchymal cells (Devlin 2002). There are three families of ADH activity, one of which is found in mammals. This family, known as the medium and long chain ADHs, is further broken down into six classes, coded for in over seven distinct

genes and making up at least 20 different isozymes. Many of these isozymes have been found in human tissue (Riveros-Rosas et al. 1997).

ADH activity in the liver is widely regarded as the principal process by which ethanol is removed from circulation (Lands 1998). Because much of the acetate made from ethanol escapes the liver to the blood, diagnostic implications could be to establish circulating levels of ethanol in cases of suspected intoxication, as well as tissue concentrations in suspected alcohol poisoning. “The concentration of ethanol in the water of the body at steady state is the same everywhere, both within and without the cell” (Deitrich and Harris 1996, p 1). A statistical analysis by Briglia et al. (1992) did not find any significant differences among various postmortem blood sites tested for alcohol. Gilliland and Bost (1993) cited numerous studies in their paper in which ratios among fluid or tissue and blood, as well as vitreous or bile and urine, were calculated, attempting to correlate concentration of ethanol in body fluids or tissues with blood alcohol content (BAC). Ethanol is naturally present in low concentrations in mammals due to gastrointestinal flora fermentation and endogenous production, especially by the liver (Riveros-Rosas et al. 1997). Gilliland and Bost (1993) concluded that endogenous alcohol production may result in a blood concentration as high as 0.15% in some cases.

Formation of acetaldehyde adducts with proteins in liver and blood of animals and humans drinking alcohol has been demonstrated. Such adducts may provide a marker for past drinking activity of an individual (Devlin 2002). Gilliland and Bost (1993) urge caution, however, because some cases may reflect uneven distribution from either very recent or far prior ingestion. It is not necessary “that a person die at the height of his brain-alcohol concentration for death to have been caused by alcohol poisoning” (Jetter

and McLean 1942, p 178). Lands (1998) also pointed out that alcohol clearance rates are significantly different among different ethnic groups, and that ethanol clearance is not continually constant, changing as a nonlinear function of blood alcohol level.

No studies could be found on postmortem levels of ADH with implications for determining PMI. However, Jetter and McLean (1942) have tested body fluids and tissues for changes in alcohol levels. They suggest that if the concentration of alcohol in blood, brain, or urine can be determined, then the possibility exists for one to assume that such a concentration existed at the moment of death and, therefore, could be an adequate explanation of death in the absence of other conditions incompatible with life. Riveros-Rosas et al. (1997) cautioned researchers, however, stating that the expression of ADH genes is regulated by some important metabolites, but the physiological roles of the ADH systems “scarcely begin to be understood” (p 466). Gilliland and Bost (1993) stated that investigators should exercise extreme caution when interpreting postmortem alcohol results, especially those from decomposing bodies.

Creatine Kinase—Kinases are enzymes that catalyze the transfer of a phosphoryl group from ATP or other nucleoside triphosphate to alcohol or amino group acceptors. CK catalyzes the transfer of phosphate from ATP to creatine, to form phosphocreatine. It has two isozymes, one present in heart and skeletal muscle, and the other in the brain. If the metabolic process is insufficient to keep up with an organism’s energy demand, the creatine phosphokinase system serves as a “buffer” to maintain cellular levels of ATP. When a sudden demand of energy depletes ATP, phosphocreatine serves as a source of phosphoryl groups to make ATP, helping to stimulate respiration when muscle activity increases (Bhagavan 2002).

Increased CK levels are associated with myocardial infarction (MI), becoming evident four to six hours after onset of pain, peaking after 18-30 hours, and lasting for about ten days (Kachmar and Moss 1976). CK leaks from injured heart cells and is the first enzyme to appear in the blood after MI. Above normal levels are also associated with all types of muscular dystrophy, hypothyroidism, liver disease, pernicious anemia, pulmonary infarction, and acute cerebrovascular disease (Erickson and Morales 1961, Zimmerman and Henry 1979). Jetter and McLean (1942) noted that small amounts of creatine are found in the urine of children and sometimes in the urine of normal adult females, but large amounts indicate body tissue breakdown such as starvation, diabetes, goiter, fever, physical exertion, and so forth. They also noted that creatine is not formed in the urine after death as a result of postmortem change.

Bollinger and Carrodus (1938) were the first to observe a postmortem rise in creatine serum levels. Naumann (1950) and Karkela (1993) later supported this result with similar studies on CSF. Naumann (1950) stated that although there is a “rough” correlation between increases in creatine levels and the PMI, extending up to a maximum of about ten hours, the variation in individual cases showed that this enzymatic reaction does not depend on time alone and therefore could not be used to estimate accurately the time since death. Schleyer (1963) substantiated Naumann’s work but felt the correlation could serve as a rough indicator of the time between death and withdrawal of the sample.

Lactate Dehydrogenase—As stated above, dehydrogenases catalyze the oxidation of an alcohol to an aldehyde. The role of LDH in metabolism is to catalyze the terminal step in glycolysis under anaerobic conditions to produce more NAD⁺ for glycolysis. Pyruvate is reduced to L-lactate, and NADH is oxidized to NAD⁺. LDH also

serves in the first step of the reverse process, gluconeogenesis, by converting lactate back to pyruvate. LDH is found in skeletal and heart muscle, liver, kidneys, erythrocytes, pancreas, and lungs (Devlin 2002). LDH is a tetrameric enzyme containing only two distinct subunits: those designated 'H' for heart, and 'M' for muscle. These two subunits are combined in five different ways and numbered LDH1 through LDH5. Elevated levels of each isoenzyme indicate particular disorders: myocardial infarction, renal cortical infarction, pernicious anemia, hemolysis, late stage muscular dystrophy (involving LDH1 and LDH2, frequently levels of LDH1 > LDH2), liver disease, skeletal muscle damage, some cancers (LDH5), some neoplastic diseases, lymphoproliferative disorders, platelet-related disorders (elevated levels of LDH3, frequently LDH3 > LDH2), pulmonary infarction (LDH2 and LDH3), and widespread tissue injury (all isoenzymes elevated) (Bhagavan 2002).

No studies could be found on postmortem LDH concentrations in body tissues, and few studies have been done on LDH in the blood (Naumann 1950, Camps 1959, Coe 1974). Enticknap (1960) found there to be a patterned increase in activity for the first 60 hours after death. He suggested the following equation to predict the number of Wroblewski units of LDH:

$$\text{Wroblewski units of LDH}/1000 = 2.69 + 0.24 (\text{time after death in hours}).$$

He found that LDH accumulated in cadaver sera in three phases, beginning with a rapid rise within a few hours. Next, a slower, usually linear increase occurred for the next two to three days, and levels finally peaked around the fourth day postmortem. His work was reviewed and supported by Schleyer (1963), who added that because red blood cells are the main source of serum LDH, its postmortem increase must be ascribed to red blood

cell autolysis. No significant difference in activity, attributable to the cause of death, was observed. Karkela (1993), studying postmortem changes in LDH in cisternal fluid, concluded that total LDH activity increased linearly and statistically significantly after death, and that freezing and storage of samples may reduce LDH activity.

MATERIALS AND METHODS

Animals and Treatments— Male Sprague-Dawley rats, age 9 weeks, were used in this study. They were bred and housed in Division of Laboratory Animal Medicine (DLAM) facilities at Louisiana State University School of Veterinary Medicine during the course of the study. The total sample of 18 rats was subdivided into three groups of six animals each, utilizing one group at a time. Within a group of six animals, two received treatment (Trt.) one, two received treatment two, and two received treatment three. Treatments consisted of 0 mg/dl ethanol (Trt. 1), 75 mg/dl ethanol (Trt. 2), and 200 mg/dl ethanol (Trt. 3). Water was used as the vehicle. Total volume did not exceed 1.5% of body weight, and treatments were administered through a 3 inch, 18 gauge gavage needle. Treatments were given to determine whether different levels of alcohol consumption would alter ADH activity. Alcohol administered was in the form of the alcoholic beverage “Everclear,” which is 200 proof, or 100% ethanol.

Blood and Tissue Samples— Blood collection was done under anesthesia, and the animals were gavaged as they recovered from anesthesia and regained their cough reflexes. Utilizing anesthesia, one ~0.5 ml blood sample was collected prior to treatment administration. After the first blood sample was collected and treatment was applied, animals were allowed to recover in their cages. Forty-five minutes later, a second ~0.5 ml sample was collected using anesthesia, followed by CO₂ euthanasia. Blood was collected via retroorbital bleeding for antemortem samples. Anesthesia was delivered first into a chamber, followed by nose cone administration. Anesthesia consisted of 3.0% isofluorine delivered at 0.7 L/min. After euthanasia, one animal from each treatment pair

was placed in a cold room (approximately 8° C) and the other placed outside (underneath a milk crate to prevent animal scavenging).

Tissue samples of approximately 1 gram were taken from skeletal muscle, cardiac muscle, and the liver, and were collected at increasing postmortem time points. They were immediately frozen and stored at -80°C. To isolate the cytosolic extract, tissues were first minced. They were then mixed with 3 ml of buffer composed of 50 mmol Hepes, pH 7.5, with 1 mmol EDTA. Tissues were ground using an Elvehjem tissue homogenizer. Mixtures were centrifuged at 12×g for one hour, and supernatants were removed and stored at -80°C immediately after centrifugation.

The decision was made not to use the antemortem blood samples drawn under anesthesia from the rats via retroorbital bleeding. The reason is that the samples would not provide a legitimate comparison with the tissue samples obtained postmortem. The focus of this research was enzyme concentrations in the tissues; therefore, blood enzyme levels would have been inappropriate for study.

Enzymatic Assays— The activity for each enzyme was measured using a continuous spectrophotometric assay specific for the enzyme. Enzyme activities were reported as specific activity, that is, $\mu\text{moles}/\text{min}/\text{mg}$ protein. Initial velocities for each enzyme assay were measured. The reagents for each enzyme assay are commercially available from Sigma Chemical Co., St. Louis, Missouri. Enzyme velocities were monitored using a UV/visible spectrophotometer interfaced to a computer equipped with a data acquisition program. The temperature of the enzymatic reaction was maintained at 25°C by a circulating water bath with the capacity to heat and cool the thermospace of the cell compartment. Specifics for each assay are as follows:

Aspartate Aminotransferase—AST catalyzes the transfer of the amino group from aspartate to α -ketoglutarate, forming oxaloacetate and glutamate. Production of oxaloacetate by AST is coupled to malate dehydrogenase, which uses NADH to reduce oxaloacetate to malate and NAD⁺. Decrease in NADH was followed at 340nm.

Alcohol Dehydrogenase—ADH catalyzes oxidation of ethanol by NAD⁺, which forms acetaldehyde and NADH. Increase in absorbance of NADH was followed at 340nm.

Creatine Kinase—CK catalyzes transfer of a phosphoryl group from phosphocreatine to ADP to make ATP and creatine. Production of ATP is coupled to hexokinase, which transfers a phosphate group from ATP to glucose to make ATP and glucose-6-phosphate. Production of glucose-6-phosphate was monitored using glucose-6-phosphate dehydrogenase, which uses NADP⁺ to oxidize glucose-6-phosphate to form 6-phosphogluconate and NADPH. Increase in absorbance of NADPH was followed at 340nm.

Lactate Dehydrogenase—LDH utilizes NADH to reduce pyruvate to lactate and NAD⁺. Decrease in absorbance by NADH was followed at 340nm.

Statistical Analysis—The models are linear splines, or straight lines, linked by knots, or bends, at different points. The models fit are enzyme velocity vs. PMI and linear splines in PMI with knots at 1.5, 5, 11, 21, 29, 48, 55, and 68 hours. The reason for this is that enzymes were assayed at different times, for example, at 1, 1.25, 1.5, and 1.92 hours postmortem, and then at 4.5, 5, and 5.7 hours postmortem. This linear spline model enables comparisons of estimated velocities at fixed, common PMIs—for

example, at 5 h vs. 11 h. This implicitly entails a little linear interpolation for observations near, but not exactly at, 5 h, 11 h, etc, and the model does this.

Considerable effort was spent identifying outliers with this model. The model was fit by least squares to the data points after excluding the outliers. Initial calculations to identify outliers and examine sub-models were done in PROC REG in SAS, version 9.1. The graphs were generated by programs written in SAS's programming language, SAS/IML. A critical value of approximately 3.3 was used for outlier t -statistics, corresponding approximately to a Bonferroni critical value for about 50 comparisons at the 5% level of significance (*i.e.* any data point with a t -value beyond 3.3 was labeled an outlier). The Bonferroni correction is used when multiple comparisons are done on a single set of data (LaMotte 2004, personal communication). This was a cumulative process, in which the first model was run with all data; outliers identified by this criterion were deleted and the model was run again. This was repeated until no more cases were identified by this criterion.

I examined and tried sub-models identified by the all-possible-regressions variable selection procedure, a procedure which removed some knots in the various regression models. I did this to try to identify simpler and smoother models. However, after several trials, I decided to go back to including all knots, the argument being that the purpose of the knots was to facilitate linear interpolation among near-neighbors, not to attempt smoothing between observations at different PMIs.

RESULTS

Results of this study suggest that the four enzymes in question would not be reliable for PMI estimations. Visually, the graphs did not appear to exhibit a discernible pattern with reference to enzyme velocity as a function of time; that is, there was no steady increase or decrease in velocity as time progressed. This is opposed to what Karkela (1993) found.

Each graph shows enzyme velocity vs. PMI (shown in Appendix 1). Data points are identified by rat ID (1 to 9 for those from cold (C) storage and 10 to 18 for those left outside (OS)). Cases used to fit the spline models are shown in blue. Cases classified as outliers are plotted in red; they were not used in the estimation of the model and prediction values. The solid black line shows predicted values of enzyme velocity at each value of PMI. The red lines roughly parallel this black line, and depict a 95% prediction-interval limit on PMI. This prediction interval gives a formula that, for any PMI, gives a predicted value of velocity (the points on the solid black line of the graph). Upper and lower prediction limits are computed based on the fitted model (LaMotte 2004, personal communication).

For use in estimating PMI of an unknown specimen, approximate confidence bounds would be obtained as follows. Denote the specimen's enzyme velocity by y^* . On the graph for that enzyme, draw a horizontal line at height y^* (LaMotte 2004, personal communication). The PMI range(s) where that line is not between the upper and lower red lines are PMIs that are not tenable for this specimen. That is, it could be said that any of these PMIs is not reasonable for this specimen. Those values not eliminated form an approximate 95% confidence set on PMI for this specimen. This method can be applied

to other enzyme concentration studies as well, even though this particular set of enzymes did not appear to give significant positive results for PMI estimation.

Figure 4.1: LDH Liver Outside Samples—There are two outliers above the upper limit that were not used in the determination of the 95% prediction interval (PI). The graph does not follow the steeply sloping line that would be ideal for enzyme velocity determination. There does appear to be an overall decrease in velocity over time, but the points fluctuate inconsistently. At the farthest time points the tissues were too decomposed to take samples. As time increased, the velocity fluctuated. PI values at the knots are given in Table 4.1. The knots are measured in hours, and the upper and lower limits and predicted value are measured in $\mu\text{moles/ml/mg}$ protein.

Table 4.1: PI Values of Knots in Figure 4.1

Knot	1.5	5	11	21	29	48	55	68
Lower Limit	0.3247	0.2738	0.2690	0.1636	0.0027	-0.0211	0.1100	0.2163
Predicted Value	1.1584	1.0327	1.0244	0.8903	0.7563	0.7396	0.8447	0.9648
Upper Limit	1.9921	1.7917	1.7797	1.6171	1.5099	1.5003	1.5794	1.7133

Figure 4.2: LDH Liver Cold Samples—The values in this graph are more spread out than the values from the outside LDH liver samples. There were no outliers above the upper limit. There was a sharp decline in velocity between the first and second knots, followed by a zig-zag pattern, and finally a gradual decline in the PI. The reason for the spread out nature of the samples is unknown. PI values at the knots are given in Table 4.2. The knots are measured in hours, and the upper and lower limits and predicted value are measured in $\mu\text{moles/ml/mg}$ protein.

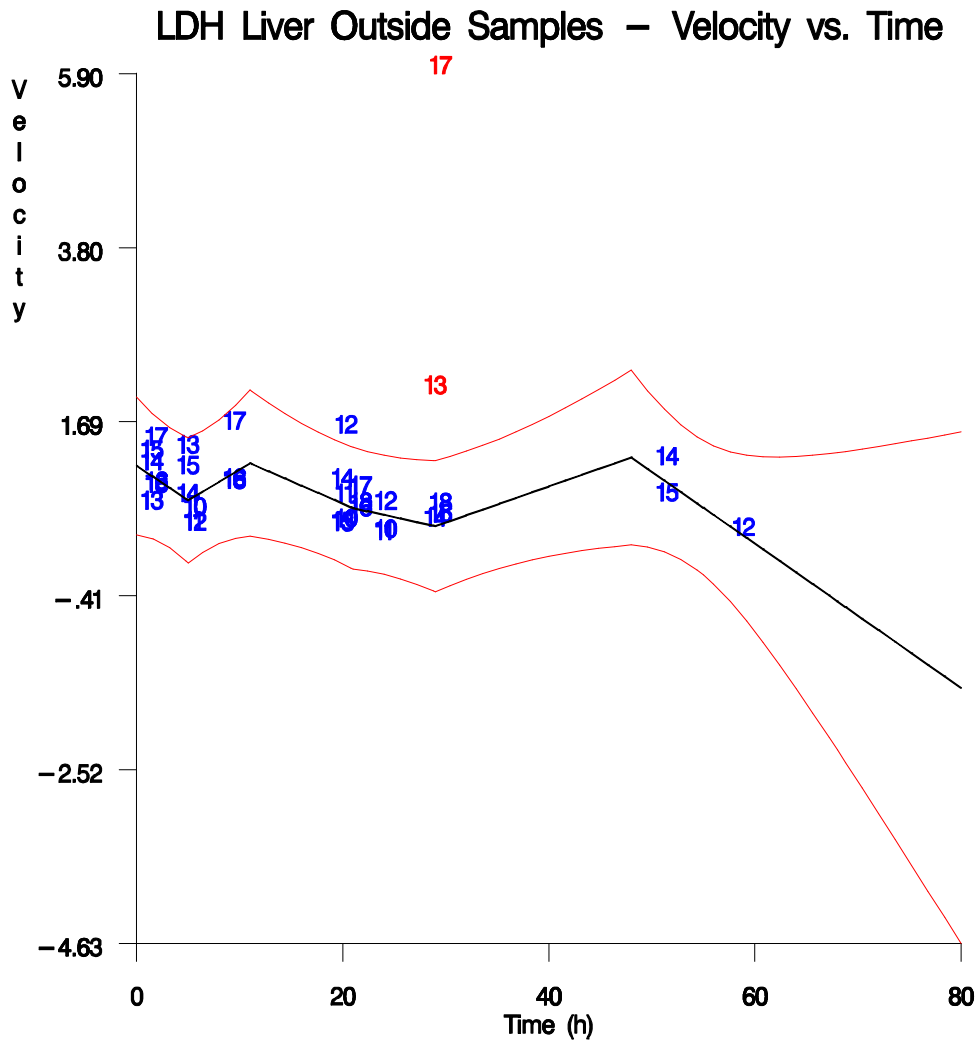


Figure 4.1: LDH activity in outside liver samples as a function of time. Two data points that fall outside the 95% prediction interval are excluded from computation of the regression line. The regression line is shown in black, and the 95% prediction interval is denoted by the two outer red lines. Data points in blue were used in computation of the prediction interval, while data points in red were considered outliers and excluded from the formula. Velocity is measured in $\mu\text{moles}/\text{min}/\text{mg}$ protein.

Table 4.2: PI Values of Knots in Figure 4.2

Knot	1.5	5	11	21	29	48	55	68
Lower Limit	0.4867	0.3381	0.3267	0.1167	-0.1167	-0.1836	-0.1210	-0.0701
Predicted Value	1.3532	1.1378	1.1235	0.8937	0.6639	0.6352	0.6654	0.6998
Upper Limit	2.2197	1.9376	1.9202	1.6707	1.4749	1.4540	1.4518	1.4698

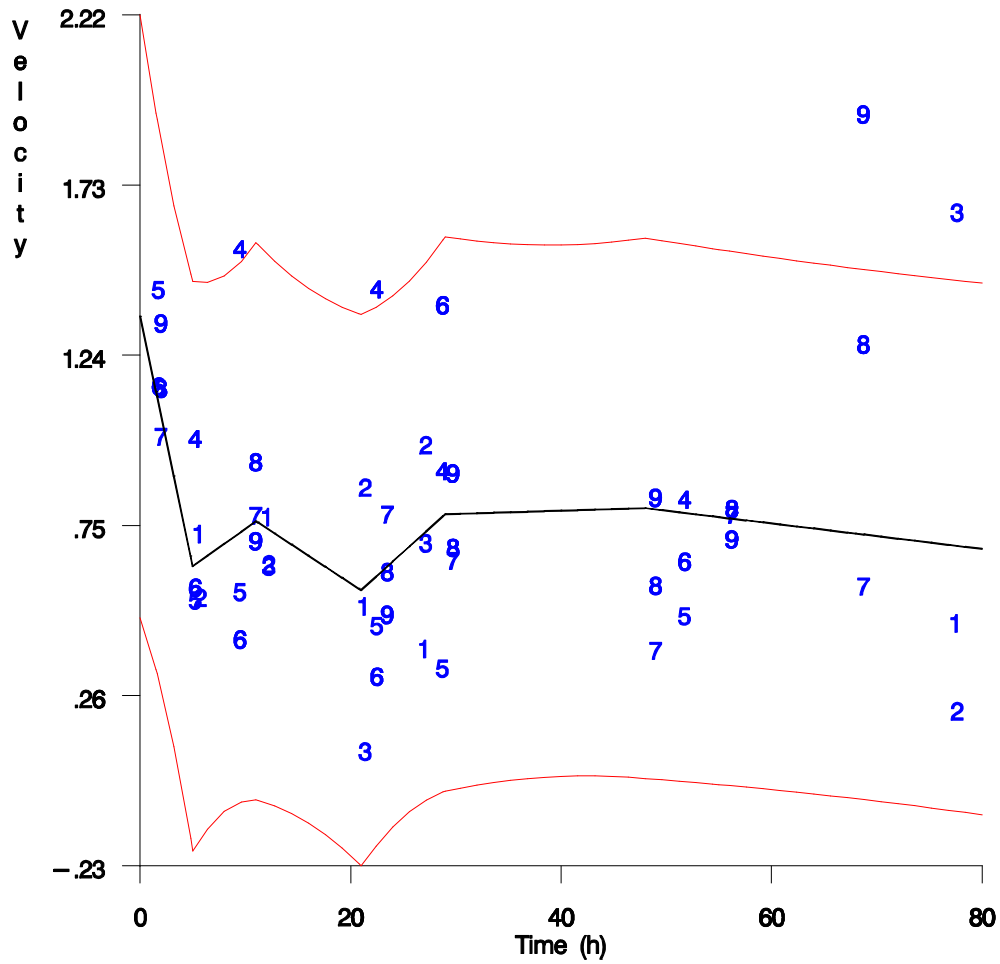
Figure 4.3: CK Liver Outside Samples—There were two outliers above the upper limit of the 95% PI. The graph displays an initial rise in velocity, followed by a general decrease and a final increase, although some of the individual rats show a different pattern. Rat 12 showed a higher average of all its points than all other samples. The PI is fairly narrow, and many areas within the PI have data points with similar values. However, there are not many time points toward the end of the graph, and the data points present have values similar to the others in the rest of the graph. PI values at the knots are given in Table 4.3. The knots are measured in hours, and the upper and lower limits and predicted value are measured in $\mu\text{moles/ml/mg}$ protein.

Table 4.3: PI Values of Knots in Figure 4.3

Knot	1.5	5	11	21	29	48	55	68
Lower Limit	-0.093	-0.0672	-0.0657	-0.0448	-0.0309	-0.0297	-0.0361	-0.0489
Predicted Value	0.0135	0.0297	0.0307	0.0480	0.0653	0.0675	0.0577	0.0466
Upper Limit	0.1199	0.1266	0.1272	0.1408	0.1615	0.1646	0.1515	0.1422

Figure 4.4: CK Liver Cold Samples—There are three outliers above the upper limit of the 95% PI. This PI range is smaller than the one from the outside CK liver samples, possibly because the temperature stayed within a range of a few degrees. This

LDH Liver Cold Room Samples – Velocity vs. Time



graph began with a slight overall increase in velocity, followed by a small dip and rise. There is a gradual decrease and finally a slight increase beginning around 48 hours postmortem. Rats 7, 8, and 9 were consistently grouped close together except for the last time point, and all their points were below the average except for the first and last samples from Rat 9. PI values at the knots are given below in Table 4.4. The knots are measured in hours, and the upper and lower limits and predicted value are measured in $\mu\text{moles/ml/mg}$ protein.

Table 4.4: PI Values of Knots in Figure 4.4

Knot	1.5	5	11	21	29	48	55	68
Lower Limit	-0.0675	-0.0445	-0.0431	-0.0234	-0.0088	-0.0074	-0.0104	-0.016
Predicted Value	0.0223	0.0385	0.0396	0.0569	0.0742	0.0763	0.0705	0.0639
Upper Limit	0.1121	0.1216	0.1224	0.1372	0.1572	0.1600	0.1514	0.1438

Figure 4.5: AST Liver Outside Samples—There are two outliers below the lower limit of the 95% PI for this graph, which shows a general upward trend. There are enough data points before ~ 30 hours to get a true sense of what the trend is, but there are only three data points past this ~ 30 hour time point on which the last part of the PI is based. The beginning of the graph shows a fairly sharp increase, followed by a partial decrease and then a gently sloping rise and fall with a final overall increase in velocity. PI values at the knots are given in Table 4.5. The knots are measured in hours, and the upper and lower limits and predicted value are measured in $\mu\text{moles/ml/mg}$ protein.

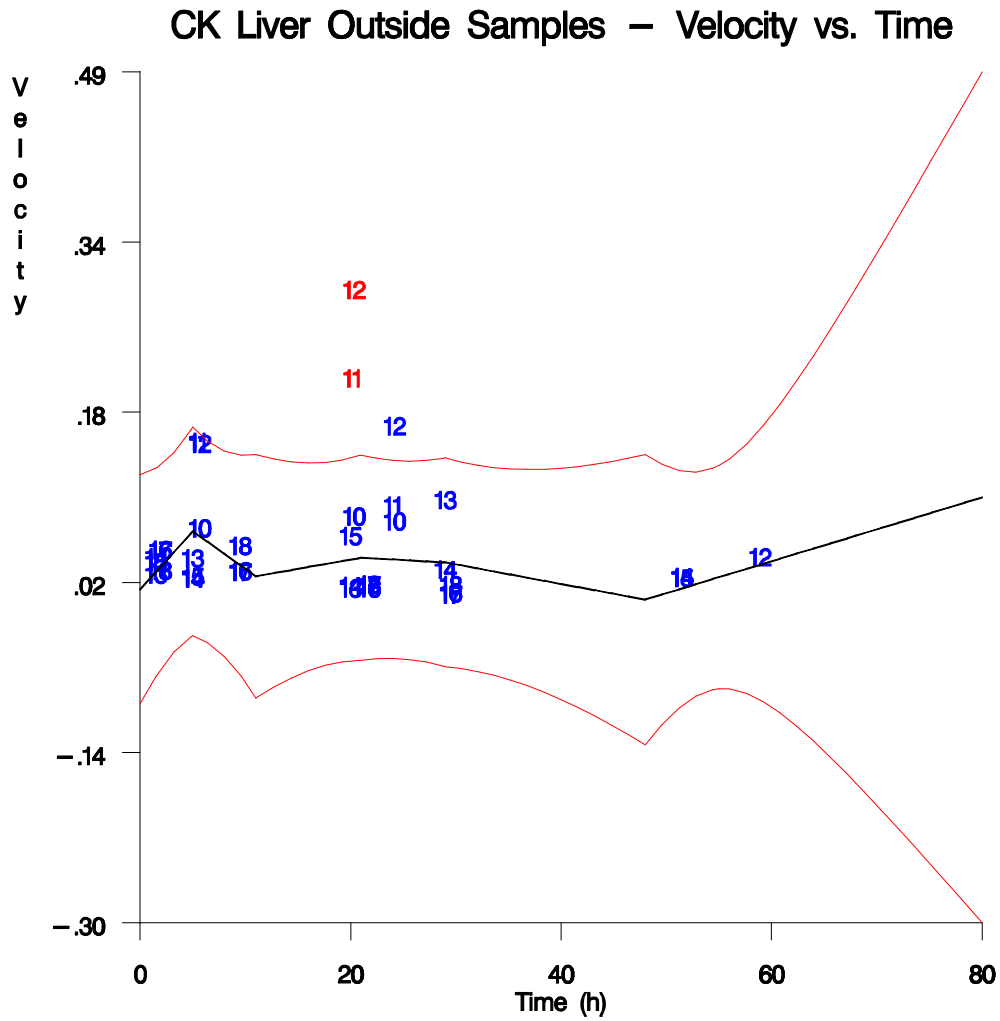


Figure 4.3: CK activity in outside liver samples as a function of time. Two data points that fall outside the 95% prediction interval are excluded from computation of the regression line. The regression line is shown in black, and the 95% prediction interval is denoted by the two outer red lines. Data points in blue were used in computation of the prediction interval, while data points in red were considered outliers and excluded from the formula. Velocity is measured in $\mu\text{moles}/\text{min}/\text{mg}$ protein.

Table 4.5: PI Values of Knots in Figure 4.5

Knot	1.5	5	11	21	29	48	55	68
Lower Limit	0.1647	0.1182	0.1146	0.0488	0.0346	0.0462	0.0187	0.0011
Predicted Value	0.4281	0.3579	0.3532	0.2783	0.2035	0.1941	0.2133	0.2353
Upper Limit	0.6914	0.5976	0.5918	0.5079	0.4415	0.4344	0.4454	0.4718

Figure 4.6: AST Liver Cold Samples—These data are more spread out than those for the outside samples. There are two outliers below the lower limit of the 95% PI. There are more samples available in this group than in the outside samples, allowing for a more accurate determination of the enzyme velocity. There is an initial increase and subsequent decrease in enzyme velocity, followed by a gradual steady increase for the remainder of the graph. PI values at the knots are given in Table 4.6. The knots are measured in hours, and the upper and lower limits and predicted value are measured in $\mu\text{moles/ml/mg protein}$.

Table 4.6: PI Values of Knots in Figure 4.6

Knot	1.5	5	11	21	29	48	55	68
Lower Limit	0.0190	0.0278	0.0280	0.0219	0.0006	0.0045	0.0281	0.0589
Predicted Value	0.2953	0.2835	0.2827	0.2701	0.2574	0.2559	0.2786	0.3047
Upper Limit	0.5717	0.5391	0.5374	0.5183	0.5155	0.5162	0.5292	0.5505

Figure 4.7: ADH Liver Outside Samples—The samples in this graph are clustered close together, all around a velocity near zero, indicating that there is little enzyme activity. There are only two outliers outside the upper limit of the 95% PI. The graph shows a gradual rise in average velocity until ~ 20 hours, where it then decreases

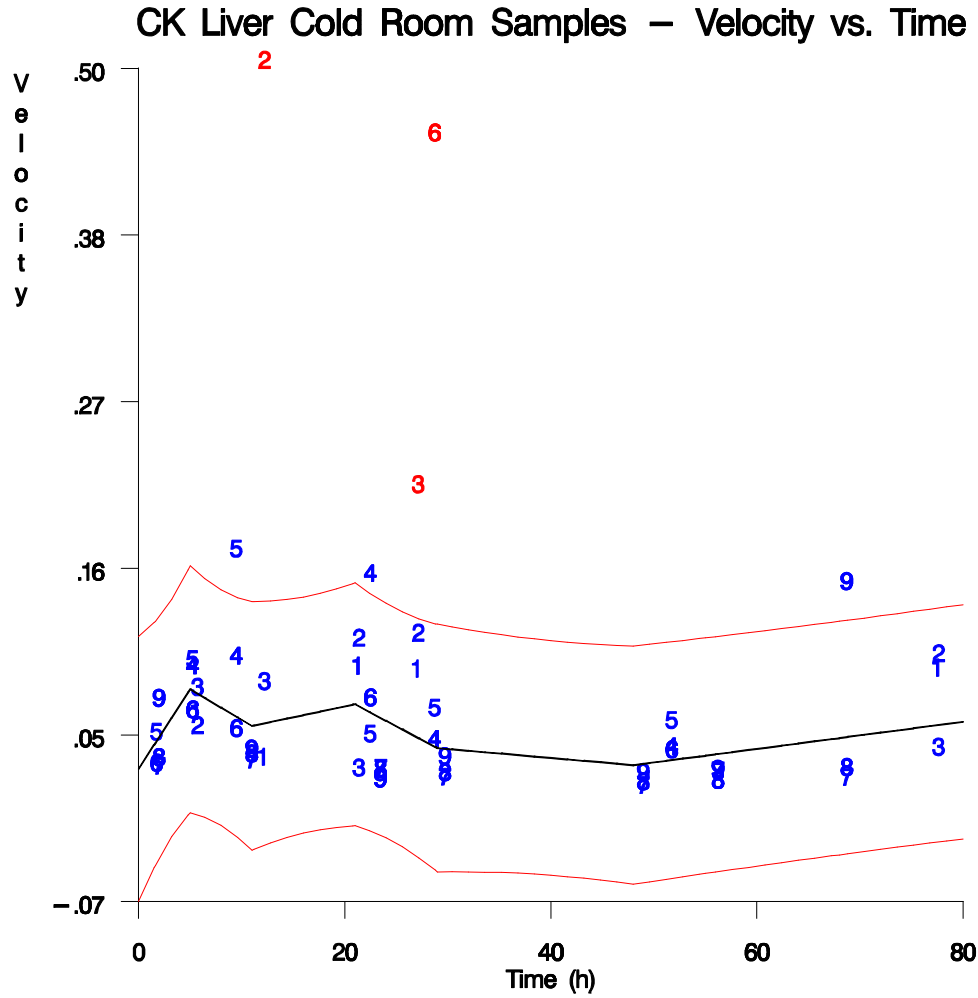


Figure 4.4: CK activity in cold room liver samples as a function of time. Three data points that fall outside the 95% prediction interval are excluded from computation of the regression line. The regression line is shown in black, and the 95% prediction interval is denoted by the two outer red lines. Data points in blue were used in computation of the prediction interval, while data points in red were considered outliers and excluded from the formula. Velocity is measured in $\mu\text{moles}/\text{min}/\text{mg}$ protein.

over the next 40 hours. As with some other outside sample groups, there are not many late postmortem samples available for analysis, so the graph is based on relatively few data points. PI values at the knots are given below in Table 4.7. The knots are measured in hours, and the upper and lower limits and predicted value are measured in $\mu\text{moles/ml/mg protein}$.

Table 4.7: PI Values of Knots in Figure 4.7

Knot	1.5	5	11	21	29	48	55	68
Lower Limit	-0.0021	-0.0015	-0.0015	-0.0011	-0.0008	-0.0008	-0.0007	-0.0007
Predicted Value	0.0001	0.0005	0.0005	0.0008	0.0012	0.0012	0.0012	0.0012
Upper Limit	0.0023	0.0024	0.0025	0.0027	0.0031	0.0032	0.0032	0.0032

Figure 4.8: ADH Liver Cold Samples—This graph has seven data points above the upper limit of the 95% PI. There are more outliers in this graph than in the graph for the outside samples, but there is still minimal activity in the enzymes. Rat 2 had three data points fall outside the PI. Although very slight, the graph displays an overall rise in enzyme velocity. Rats 7, 8, and 9 had all data points within the 95% PI. PI values at the knots are given in Table 4.8. The knots are measured in hours, and the upper and lower limits and predicted value are measured in $\mu\text{moles/ml/mg protein}$.

Table 4.8: PI Values of Knots in Figure 4.8

Knot	1.5	5	11	21	29	48	55	68
Lower Limit	-0.0011	-0.0008	-0.0008	-0.0005	-0.0003	-0.0003	-0.0003	-0.0004
Predicted Value	0.0001	0.0004	0.0004	0.0006	0.0009	0.0009	0.0008	0.0008
Upper Limit	0.0014	0.0015	0.0016	0.0018	0.0021	0.0021	0.0020	0.0019

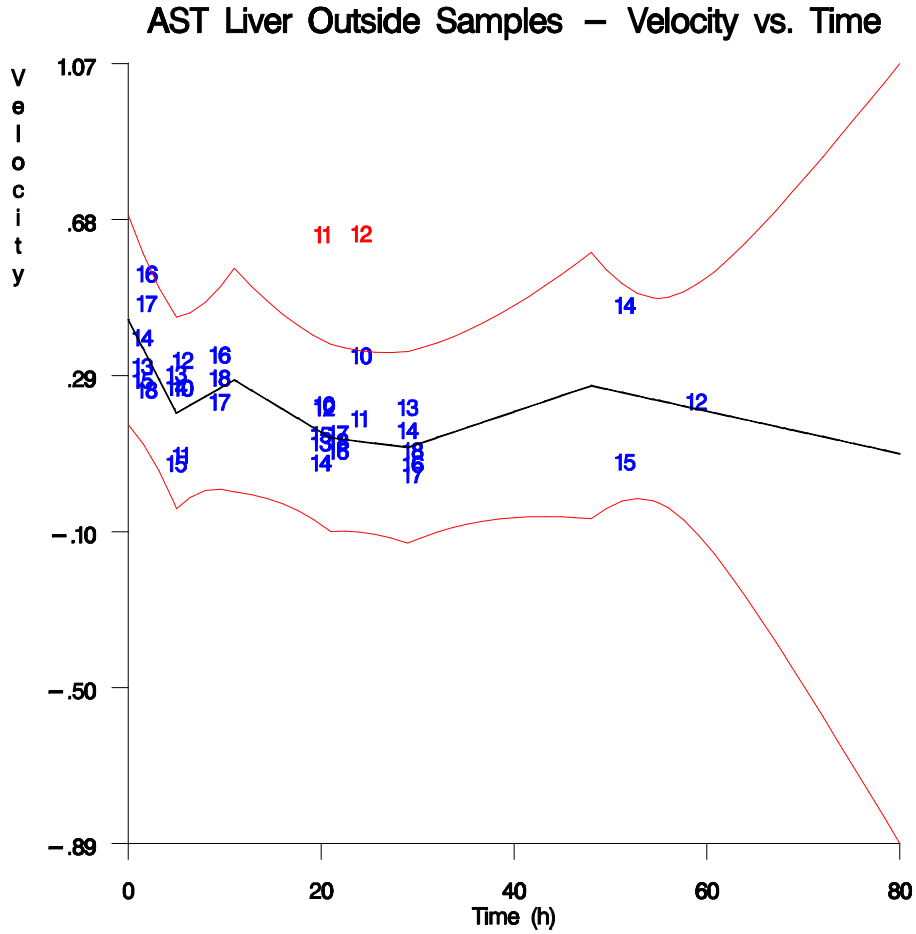


Figure 4.5: AST activity in outside liver samples as a function of time. Two data points that fell outside the 95% prediction interval are excluded from computation of the regression line. The regression line is shown in black, and the 95% prediction interval is denoted by the two outer red lines. Data points in blue were used in computation of the prediction interval, while data points in red were considered outliers and excluded from the formula. Velocity is measured in $\mu\text{moles}/\text{min}/\text{mg}$ protein.

Figure 4.9: LDH Muscle Outside Samples—There are three outliers above the upper limit of the 95% PI. There is a general downward slope to the graph, but there are a couple of places where it turns upward. The drops in the slope are sharp, whereas the increases in velocity are gradual, or slight. The graph ends with an upward trend starting at ~48 hours. The PI range is broad; PI values at the knots are given below in table 4.9. The knots are measured in hours, and the upper and lower limits and predicted value are measured in $\mu\text{moles/ml/mg}$ protein.

Table 4.9: PI Values of Knots in Figure 4.9

Knot	1.5	5	11	21	29	48	55	68
Lower Limit	1.4592	1.2501	1.2300	0.7845	0.0981	-0.0040	0.1778	0.1957
Predicted Value	5.0848	4.5506	4.5150	3.9452	3.3753	3.3041	3.3727	3.4511
Upper Limit	8.7104	7.8510	7.8000	7.1058	6.6526	6.6122	6.5676	6.7064

Figure 4.10: LDH Muscle Cold Samples—There are no data points outside the PI in this graph, although the values are spread out. Like the graph for the outside samples, this one shows a slight downward trend overall. This graph displays a zig-zag like pattern and ends in a decrease in velocity, which begins at ~48 hours. There are not many areas where data points are clustered together, indicating similar values; the data points are spread out throughout the area of the PI. PI values at the knots are given in Table 4.10. The knots are measured in hours, and the upper and lower limits and predicted value are measured in $\mu\text{moles/ml/mg}$ protein.

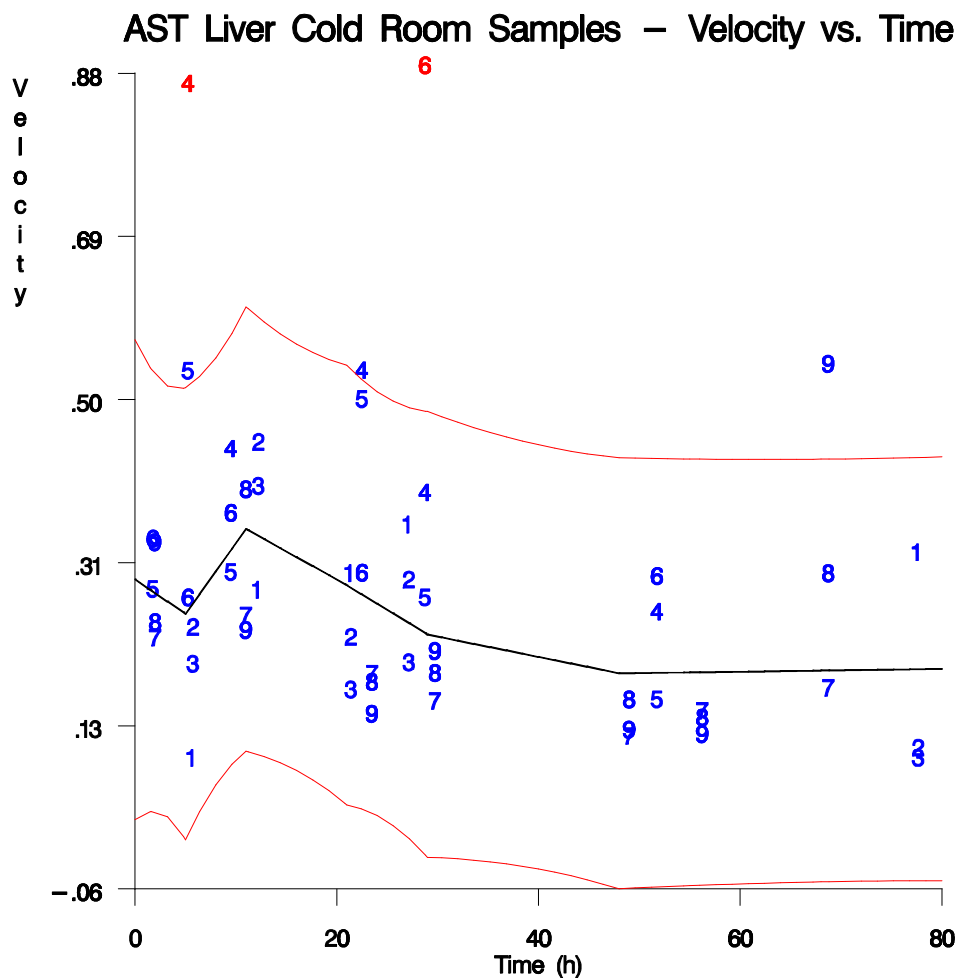


Figure 4.6: AST activity in cold room liver samples as a function of time. Two data points that fall outside the 95% prediction interval are excluded from computation of the regression line. The regression line is shown in black, and the 95% prediction interval is denoted by the two outer red lines. Data points in blue were used in computation of the prediction interval, while data points in red were considered outliers and excluded from the formula. Velocity is measured in $\mu\text{moles}/\text{min}/\text{mg}$ protein.

Table 4.10: PI Values of Knots in Figure 4.10

Knot	1.5	5	11	21	29	48	55	68
Lower Limit	0.1819	-0.1167	-0.1422	-0.6549	-1.3652	-1.4669	-0.9396	-0.4205
Predicted Value	3.6265	3.0980	3.0627	2.4989	1.9351	1.8647	2.2605	2.7129
Upper Limit	7.0712	6.3126	6.2677	5.6528	5.2354	5.1962	5.4606	5.8463

Figure 4.11: CK Muscle Outside Samples—There is one outlier above the upper limit for the 95% PI. This line is not as erratic as the line for the cold samples; that is, there are not as many changes in the velocity’s overall direction. The CK muscle graphs display a higher average velocity than the others; likewise, the CK muscle outside graph shows a higher velocity than the graph for the cold samples. The range for the PI is broad in this graph. PI values at the knots are given in table 4.11. The knots are measured in hours, and the upper and lower limits and predicted value are measured in $\mu\text{moles/ml/mg protein}$.

Table 4.11: PI Values of Knots in Figure 4.11

Knot	1.5	5	11	21	29	48	55	68
Lower Limit	5.3887	5.0438	4.9925	3.6148	1.1435	0.7608	-0.5925	-3.0006
Predicted Value	21.8453	20.0246	19.9033	17.9612	16.0191	15.7763	13.9093	11.7755
Upper Limit	38.3019	35.0054	34.8140	32.3076	30.8947	30.7919	28.4111	26.5516

Figure 4.12: CK Muscle Cold Samples—This graph also has high values compared to the others, although not as high as the graph for the outside samples. There are three data points above the upper limit of the 95% PI. The line has more directional changes in velocity (*i.e.*, increases or decreases), but the changes are not as pronounced

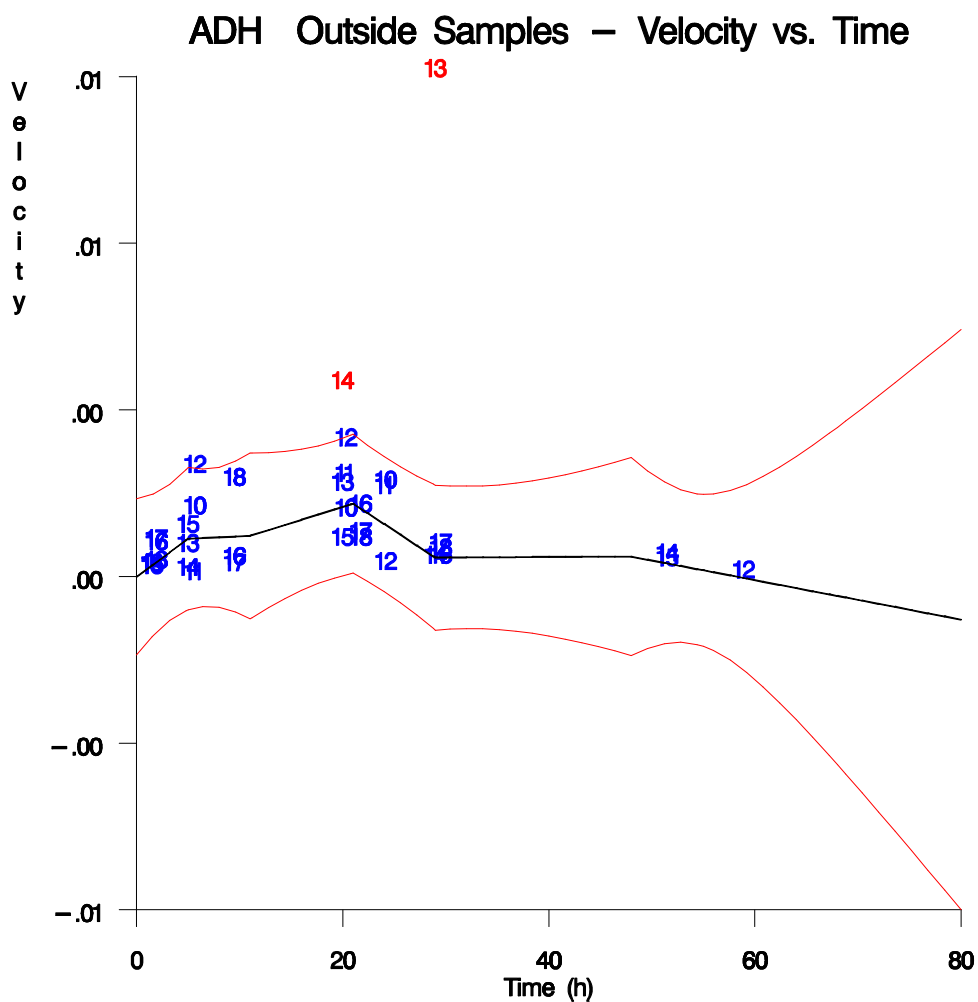


Figure 4.7: ADH activity in outside liver samples as a function of time. Two data points that fall outside the 95% prediction interval are excluded from computation of the regression line. The regression line is shown in black, and the 95% prediction interval is denoted by the two outer red lines. Data points in blue were used in computation of the prediction interval, while data points in red were considered outliers and excluded from the formula. Velocity is measured in $\mu\text{moles}/\text{min}/\text{mg}$ protein.

as those in the graph for the outside samples. This graph displays a fairly smooth regression line. PI values at the knots are given in Table 4.12. The knots are measured in hours, and the upper and lower limits and predicted value are measured in $\mu\text{moles/ml/mg}$ protein.

Table 4.12: PI Values of Knots in Figure 4.12

Knot	1.5	5	11	21	29	48	55	68
Lower Limit	2.0279	1.9748	1.9547	1.3221	0.1045	-0.0861	0.9239	1.8064
Predicted Value	12.1987	11.4659	11.4170	10.6353	9.8536	9.7559	10.3725	11.0771
Upper Limit	22.3695	20.9569	20.8793	19.9485	19.6026	19.5978	19.8210	20.3479

Figure 4.13: AST Muscle Outside Samples—This graph displays a sharp overall rise in enzyme velocity, although the range is smaller than most of the other graphs. There is an initial sharp rise in velocity, followed by a gradual drop beginning at about ten hours, and finally another sharp increase at around 48 hours. There is only one outlier below the lower limit of the 95% PI for this set of data points. PI values at the knots are given below in Table 4.13. The knots are measured in hours, and the upper and lower limits and predicted value are measured in $\mu\text{moles/ml/mg}$ protein.

Table 4.13: PI Values of Knots in Figure 4.13

Knot	1.5	5	11	21	29	48	55	68
Lower Limit	0.2968	0.2437	0.2397	0.1651	0.0711	0.0581	0.0214	0.0350
Predicted Value	0.5670	0.4890	0.4838	0.4007	0.3175	0.3071	0.2607	0.2076
Upper Limit	0.8373	0.7344	0.7280	0.6363	0.5639	0.5561	0.4999	0.4502

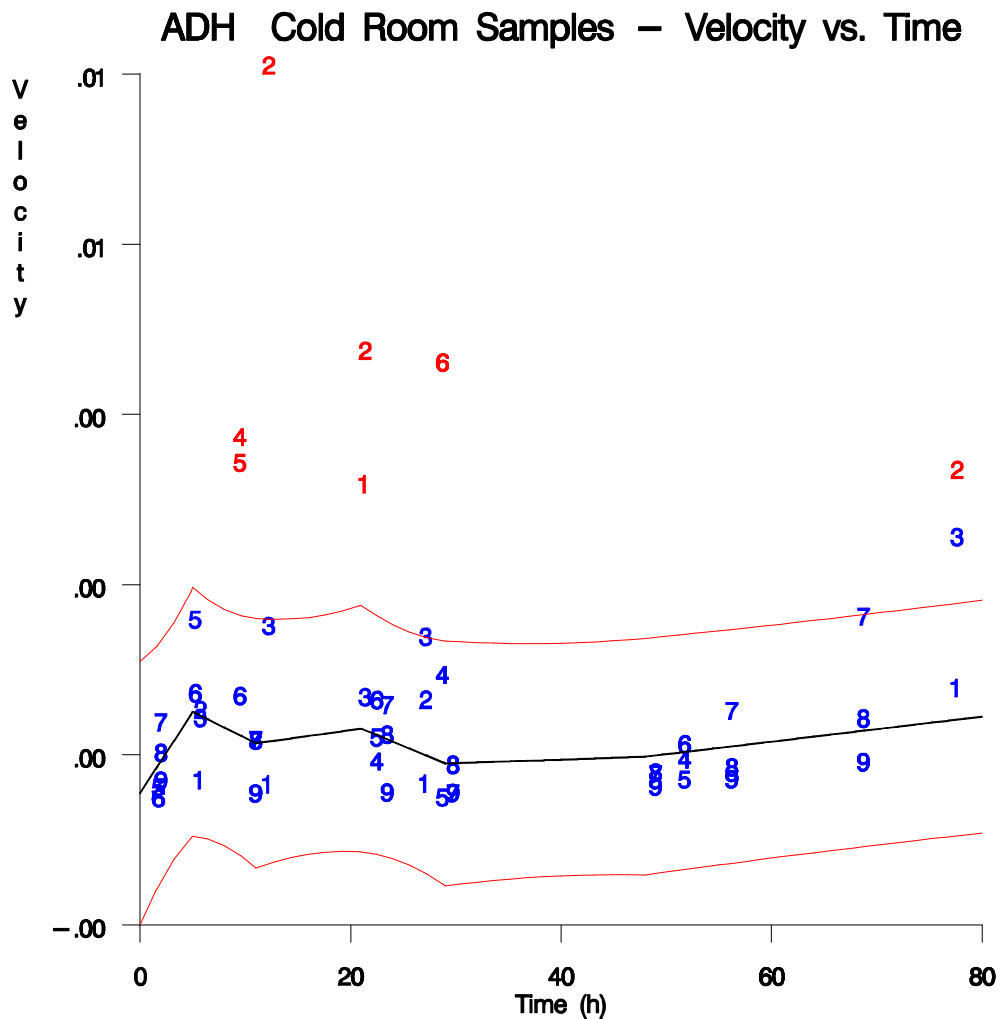


Figure 4.8: ADH activity in cold room liver samples as a function of time. Seven data points that fall outside the 95% prediction interval are excluded from computation of the regression line. The regression line is shown in black, and the 95% prediction interval is denoted by the two outer red lines. Data points in blue were used in computation of the prediction interval, while data points in red were considered outliers and excluded from the formula. Velocity is measured in $\mu\text{moles}/\text{min}/\text{mg}$ protein.

Figure 4.14: AST Muscle Cold Samples—There are four outliers below the 95% PI for this graph. There is a general increase in enzyme velocity over time, with a sharp rise and fall seen in the beginning of the line. From about 20 hours on, the graph values stay fairly constant. The values of the data points of rats 7, 8, and 9 seem to follow one another more closely than the rats in the other two groups for this graph. PI values at the knots are given below in Table 4.14. The knots are measured in hours, and the upper and lower limits and predicted value are measured in $\mu\text{moles/ml/mg}$ protein.

Table 4.14: PI Values of Knots in Figure 4.14

Knot	1.5	5	11	21	29	48	55	68
Lower Limit	0.2594	0.1776	0.1717	0.0662	0.0575	0.0741	0.0222	0.1243
Predicted Value	0.5543	0.4528	0.4460	0.3377	0.2294	0.2159	0.2987	0.3933
Upper Limit	0.8492	0.7279	0.7203	0.6092	0.5163	0.5059	0.5752	0.6623

Figure 4.15: LDH Heart Outside Samples—This graph has no outliers. The range is fairly small, but the pattern of the graph is erratic. There are not many data points from which to draw an inference past around 30 hours, but the samples prior to the 30 hour mark show dramatic groupings of data points, most notably at the first and third knots. None of the other graphs displays such obvious correlations of data points as the ones seen here. PI values at the knots are given in Table 4.15. The knots are measured in hours, and the upper and lower limits and predicted value are measured in $\mu\text{moles/ml/mg}$ protein.

LDH Muscle Outside Samples – Velocity vs. Time

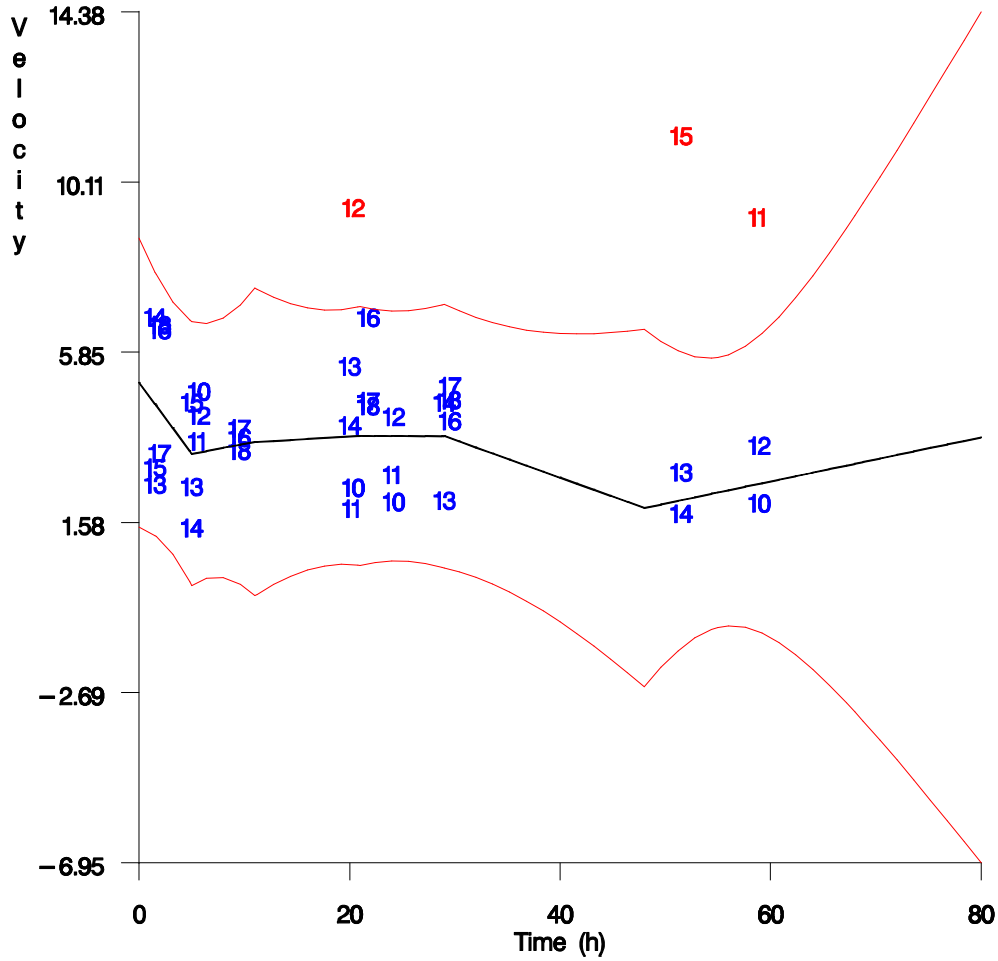


Figure 4.9: LDH activity in outside muscle samples as a function of time. Three data points that fall outside the 95% prediction interval are excluded from computation of the regression line. The regression line is shown in black, and the 95% prediction interval is denoted by the two outer red lines. Data points in blue were used in computation of the prediction interval, while data points in red were considered outliers and excluded from the formula. Velocity is measured in $\mu\text{moles}/\text{min}/\text{mg}$ protein.

Table 4.15: PI Values of Knots in Figure 4.15

Knot	1.5	5	11	21	29	48	55	68
Lower Limit	-0.4647	-0.6732	-0.6902	-1.0242	-1.4789	-1.5438	-1.1362	-0.7654
Predicted Value	1.3523	0.9808	0.9561	0.5598	0.1636	0.1140	0.4649	0.8659
Upper Limit	3.1693	2.6349	2.6024	2.1438	1.8060	1.7719	2.0660	2.4972

Figure 4.16: LDH Heart Cold Samples—There are no outliers above the 95% PI for the graph. The range of values for these samples is similar to the outside samples’ graph. For almost all the samples in this group, the data points of each individual rat fall either all or almost all above or below the line (*i.e.*, all data points from Rat 7 are all above the black line, and all data points from Rat 2 are below). This graph, like that of the outside samples, has a zig-zag pattern, but unlike the other graph it has a lot of data points past 30 hours. There is more drastic change in enzyme velocity prior to 30 hours, whereas after the 30 hour time point the changes are more gradual. PI values at the knots are given in Table 4.16. The knots are measured in hours, and the upper and lower limits and predicted value are measured in $\mu\text{moles/ml/mg}$ protein.

Table 4.16: PI Values of Knots in Figure 4.16

Knot	1.5	5	11	21	29	48	55	68
Lower Limit	-0.4333	-0.7531	-0.7778	-1.2341	-1.8074	-1.8867	-1.6035	-1.3289
Predicted Value	1.5870	1.1319	1.1016	0.6161	0.1307	0.0700	0.2771	0.5137
Upper Limit	3.6073	3.0169	2.9809	2.4663	2.0687	2.0266	2.1576	2.3564

Figure 4.17: CK Heart Outside Samples—There is a steady and constant decrease in enzyme velocity throughout the entire postmortem period, and there are no

LDH Muscle Cold Room Samples – Velocity vs. Time

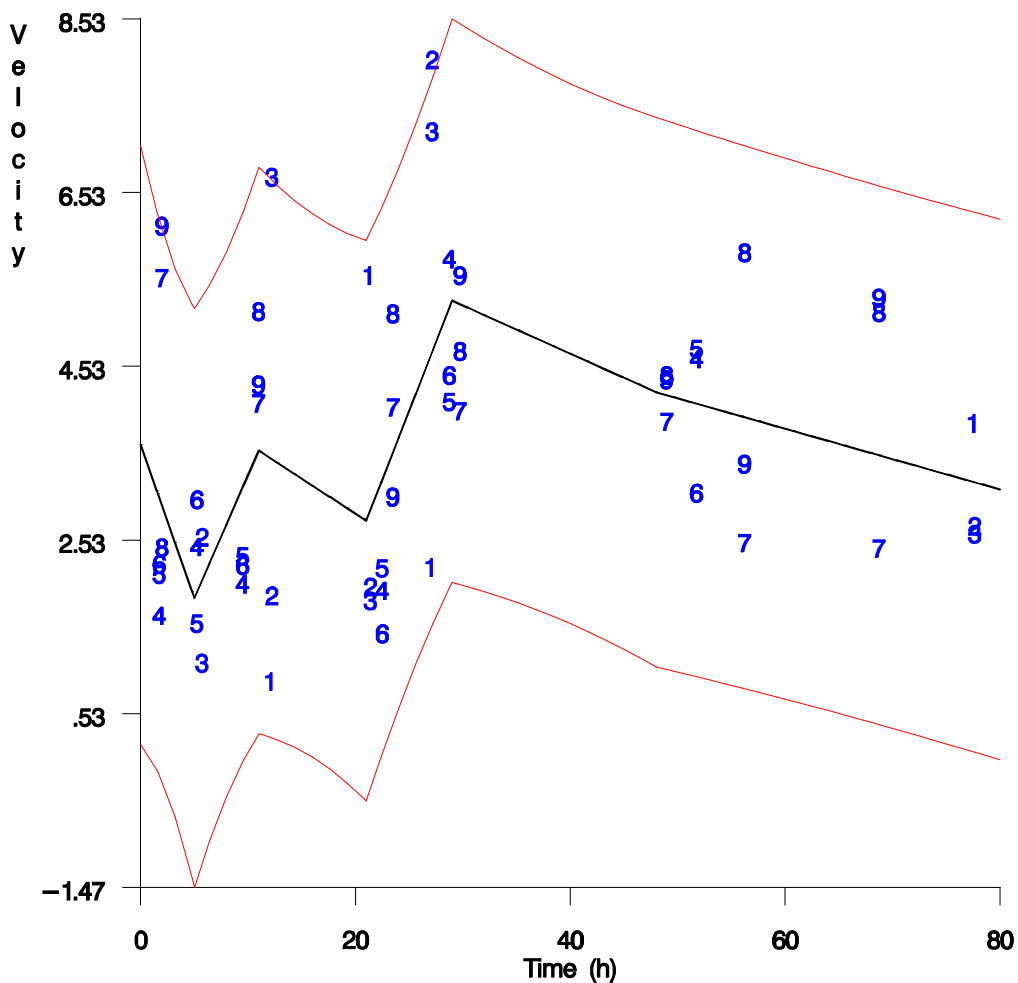


Figure 4.10: LDH activity in cold room muscle samples as a function of time. No data points fall outside the 95% prediction interval and none are excluded from computation of the regression line. The regression line is shown in black, and the 95% prediction interval is denoted by the two outer red lines. Data points in blue were used in computation of the prediction interval, while data points in red were considered outliers and excluded from the formula. Velocity is measured in $\mu\text{moles}/\text{min}/\text{mg}$ protein.

outliers beyond the PI range. The data points are clustered fairly evenly around the line, with a few samples having almost the same values at certain time points. Although there are not many data points past about the 30 hour mark, the ones that are present continue the downward trend seen in the earlier samples. PI values at the knots are given below in Table 4.17. The knots are measured in hours, and the upper and lower limits and predicted value are measured in $\mu\text{moles/ml/mg}$ protein.

Table 4.17: PI Values of Knots in Figure 4.17

Knot	1.5	5	11	21	29	48	55	68
Lower Limit	0.6240	0.7075	0.7101	0.6948	0.5667	0.5431	0.5031	0.3687
Predicted Value	2.3230	2.2541	2.2495	2.1760	2.1024	2.0932	2.0003	1.8940
Upper Limit	4.0220	3.8007	3.7889	3.6571	3.6382	3.6434	3.4974	3.4194

Figure 4.18: CK Heart Cold Samples—There is one outlier above the 95% PI range. Although there is only one outlier in this model, the data points are considerably more spread out than the outside samples in the previous graph. This graph displays a sharp decrease in velocity between the zero time point and the second knot, after which the average velocities show a trend toward overall increase in enzyme velocity until the last knot, when it again drops. PI values at the knots are given in Table 4.18. The knots are measured in hours, and the upper and lower limits and predicted value are measured in $\mu\text{moles/ml/mg}$ protein.

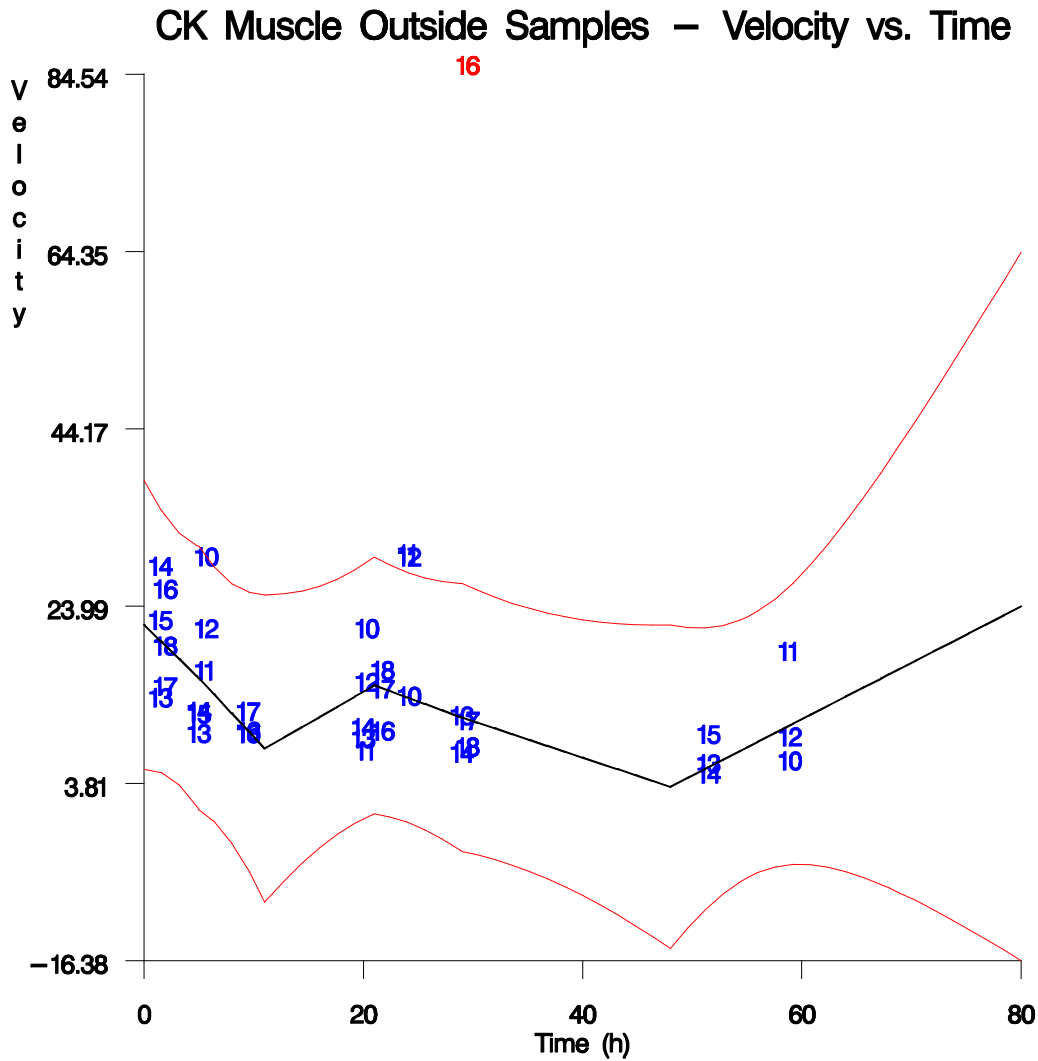


Figure 4.11: CK activity in outside muscle samples as a function of time. One data point that falls outside the 95% prediction interval is excluded from computation of the regression line. The regression line is shown in black, and the 95% prediction interval is denoted by the two outer red lines. Data points in blue were used in computation of the prediction interval, while data points in red were considered outliers and excluded from the formula. Velocity is measured in $\mu\text{moles}/\text{min}/\text{mg}$ protein.

Table 4.18: PI Values of Knots in Figure 4.18

Knot	1.5	5	11	21	29	48	55	68
Lower Limit	1.7830	1.4268	1.3993	0.8906	0.2511	0.1626	0.1864	0.1588
Predicted Value	4.0423	3.5348	3.5010	2.9597	2.4183	2.3507	2.2894	2.2194
Upper Limit	6.3016	5.6429	5.6027	5.0288	4.5856	4.5388	4.3924	4.2800

Figure 4.19: AST Heart Outside Samples—There are three outliers below the lower limit of the 95% PI for this graph. All the outliers are from Rat 12. There are numerous groupings of samples at various time points. Both AST heart graphs exhibit a smaller PI than those of the other two enzymes. This graph displays an overall increase in enzyme velocity. There are only three data points on which to base the trend for the latter part of the graph, but the data points have similar values to those in the first part of the graph, even though there is a sharp velocity increase seen there. PI values at the knots are given below in Table 4.19. The knots are measured in hours, and the upper and lower limits and predicted value are measured in $\mu\text{moles/ml/mg}$ protein.

Table 4.19: PI Values of Knots in Figure 4.19

Knot	1.5	5	11	21	29	48	55	68
Lower Limit	0.1670	0.1976	0.1982	0.1796	0.1060	0.0931	0.0301	0.0831
Predicted Value	0.9365	0.8962	0.8936	0.8506	0.8076	0.8022	0.7115	0.6078
Upper Limit	1.7061	1.5949	1.5889	1.5215	1.5092	15113	1.3929	1.2987

Figure 4.20: AST Heart Cold Samples—There are four outliers below the lower limit of the 95% PI for this set of data. There is a small increase in velocity through

CK Muscle Cold Room Samples – Velocity vs. Time

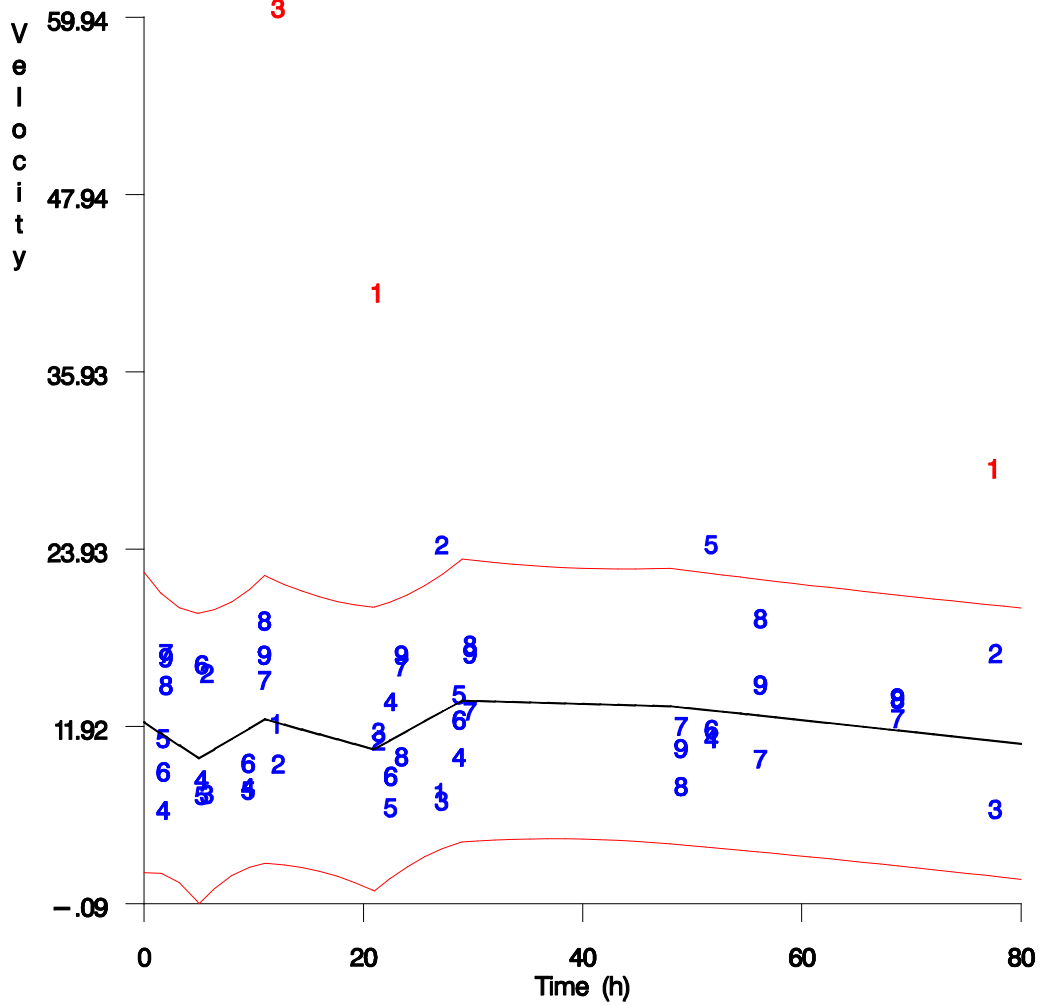


Figure 4.12: CK activity in cold room muscle samples as a function of time. Three data points that fall outside the 95% prediction interval are excluded from computation of the regression line. The regression line is shown in black, and the 95% prediction interval is denoted by the two outer red lines. Data points in blue were used in computation of the prediction interval, while data points in red were considered outliers and excluded from the formula. Velocity is measured in $\mu\text{moles}/\text{min}/\text{mg}$ protein.

around 30 hours, after which the velocity change is almost absent. This graph looks similar to the graph of the outside samples, especially in the beginning. The graphs would probably look more similar toward the ends if there were more data points in the graph of the outside samples to get a more accurate comparison. The data points are dispersed fairly evenly around the center line. Three of the four outliers fall very far outside the PI parameters; two of the four are from Rat 3. PI values at the knots are given below in Table 4.20. The knots are measured in hours, and the upper and lower limits and predicted value are measured in $\mu\text{moles/ml/mg}$ protein.

Table 4.20: PI values of Knots in Figure 4.20

Knot	1.5	5	11	21	29	48	55	68
Lower Limit	0.4445	0.3742	0.3683	0.2517	0.0940	0.0716	0.0806	0.0722
Predicted Value	1.0625	0.9490	0.9414	0.8203	0.6992	0.6840	0.6627	0.6384
Upper Limit	1.6805	1.5237	1.5145	1.3888	1.3044	1.2964	1.2448	1.2046

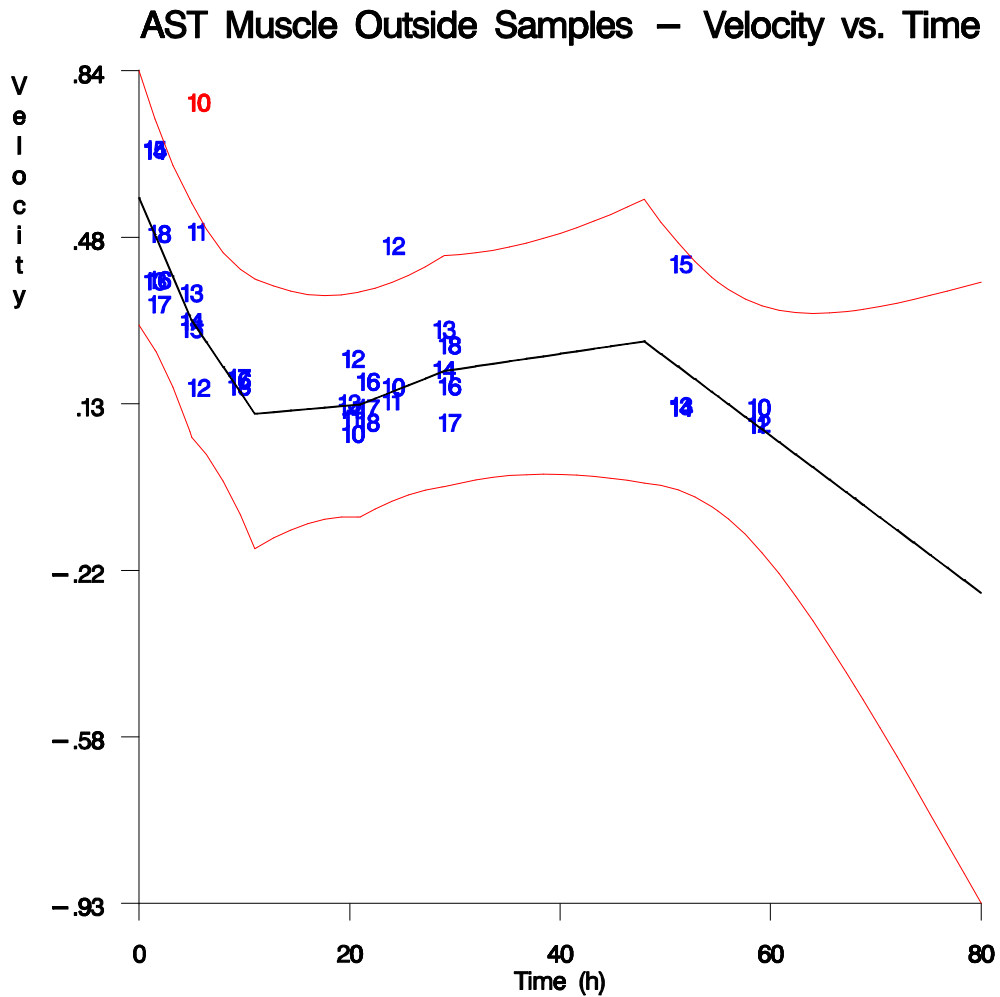


Figure 4.13: AST activity in outside muscle samples as a function of time. One data point that falls outside the 95% prediction interval is excluded from computation of the regression line. The regression line is shown in black, and the 95% prediction interval is denoted by the two outer red lines. Data points in blue were used in computation of the prediction interval, while data points in red were considered outliers and excluded from the formula. Velocity is measured in $\mu\text{moles}/\text{min}/\text{mg}$ protein.

LDH Heart Outside Samples – Velocity vs. Time

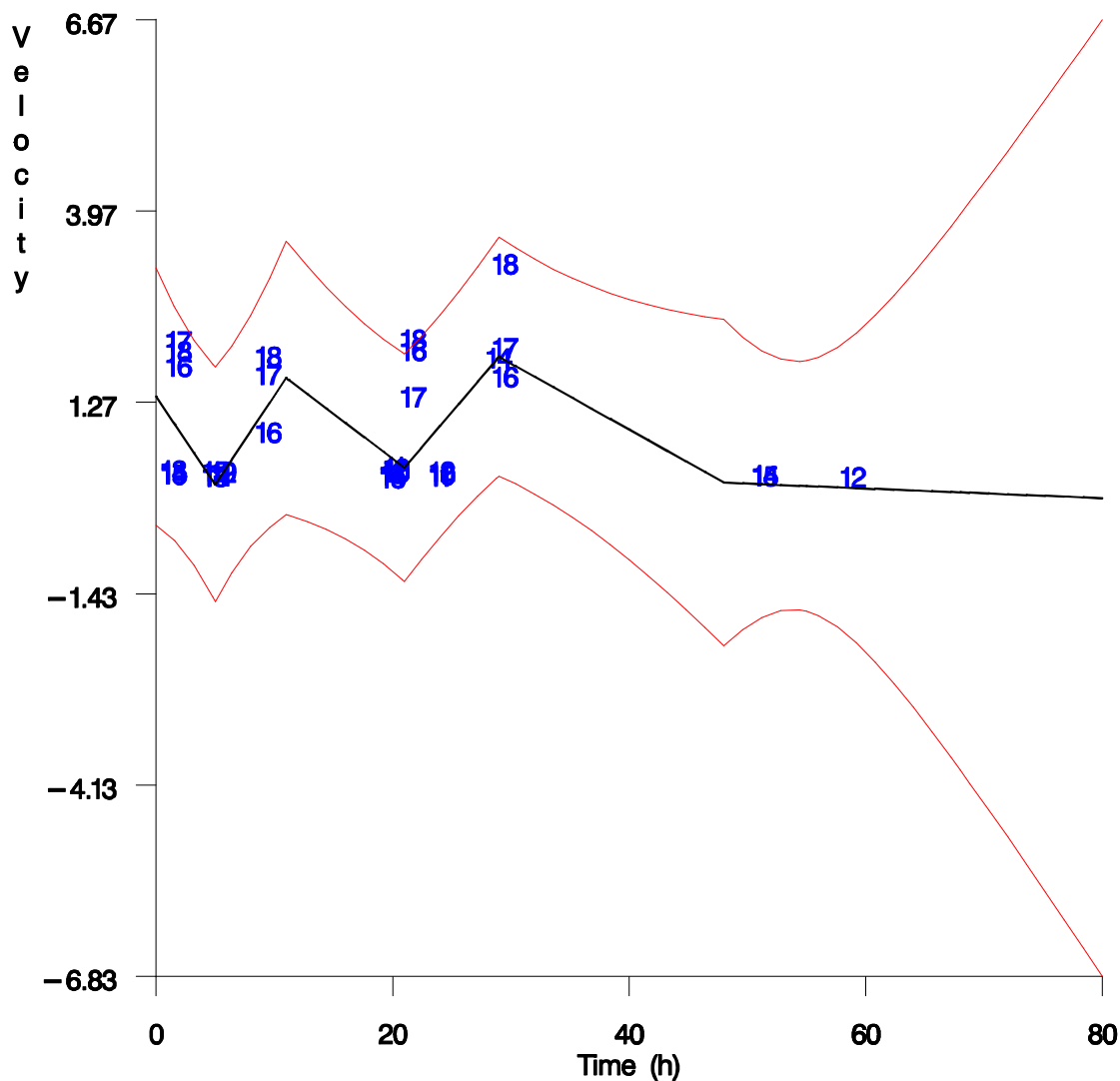


Figure 4.15: LDH activity in outside heart samples as a function of time. No data points fall outside the 95% prediction interval and none are excluded from computation of the regression line. The regression line is shown in black, and the 95% prediction interval is denoted by the two outer red lines. Data points in blue were used in computation of the prediction interval, while data points in red were considered outliers and excluded from the formula. Velocity is measured in $\mu\text{moles}/\text{min}/\text{mg}$ protein.

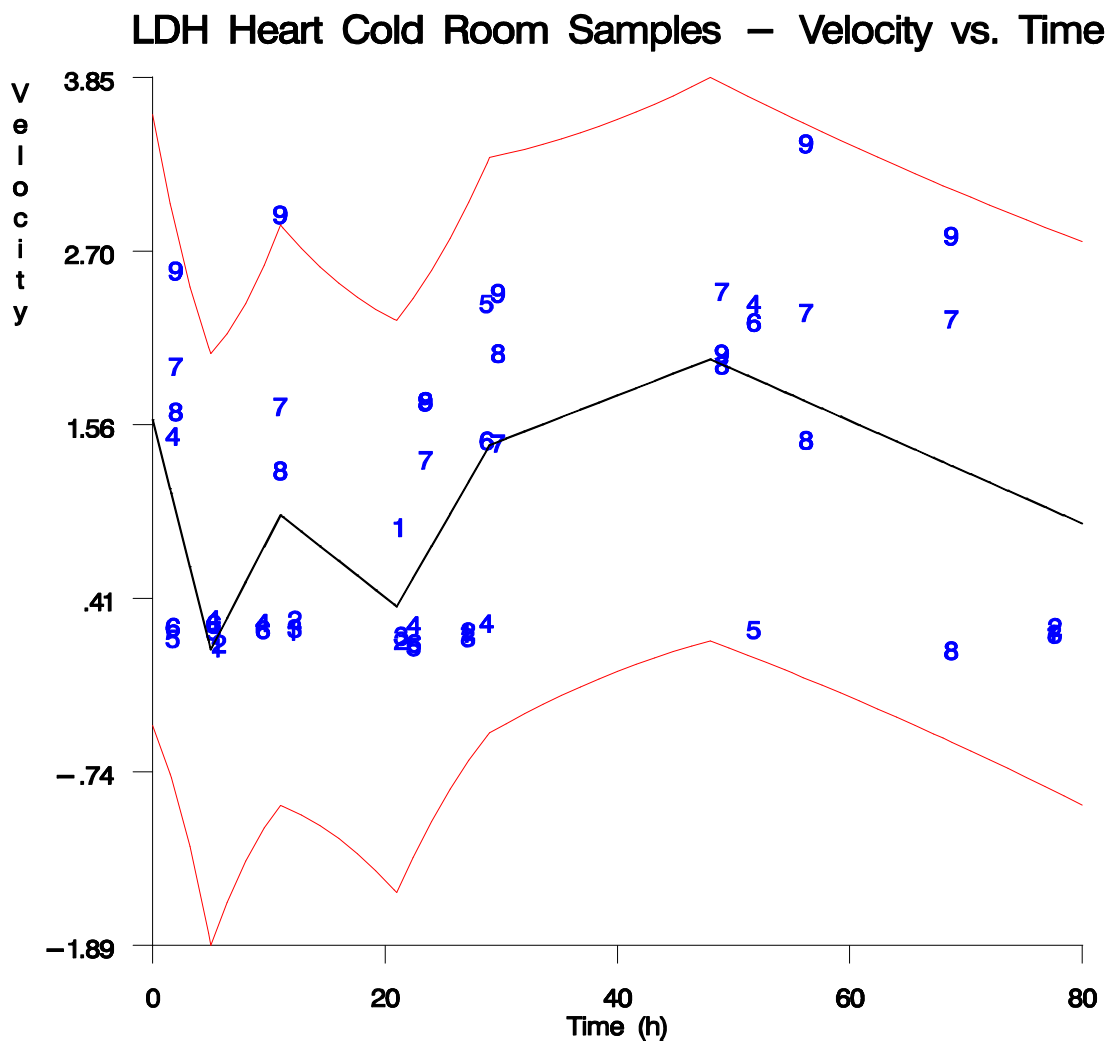


Figure 4.16: LDH activity in cold room heart samples as a function of time. No data points fall outside the 95% prediction interval and none are excluded from computation of the regression line. The regression line is shown in black, and the 95% prediction interval is denoted by the two outer red lines. Data points in blue were used in computation of the prediction interval, while data points in red were considered outliers and excluded from the formula. Velocity is measured in $\mu\text{moles}/\text{min}/\text{mg}$ protein.

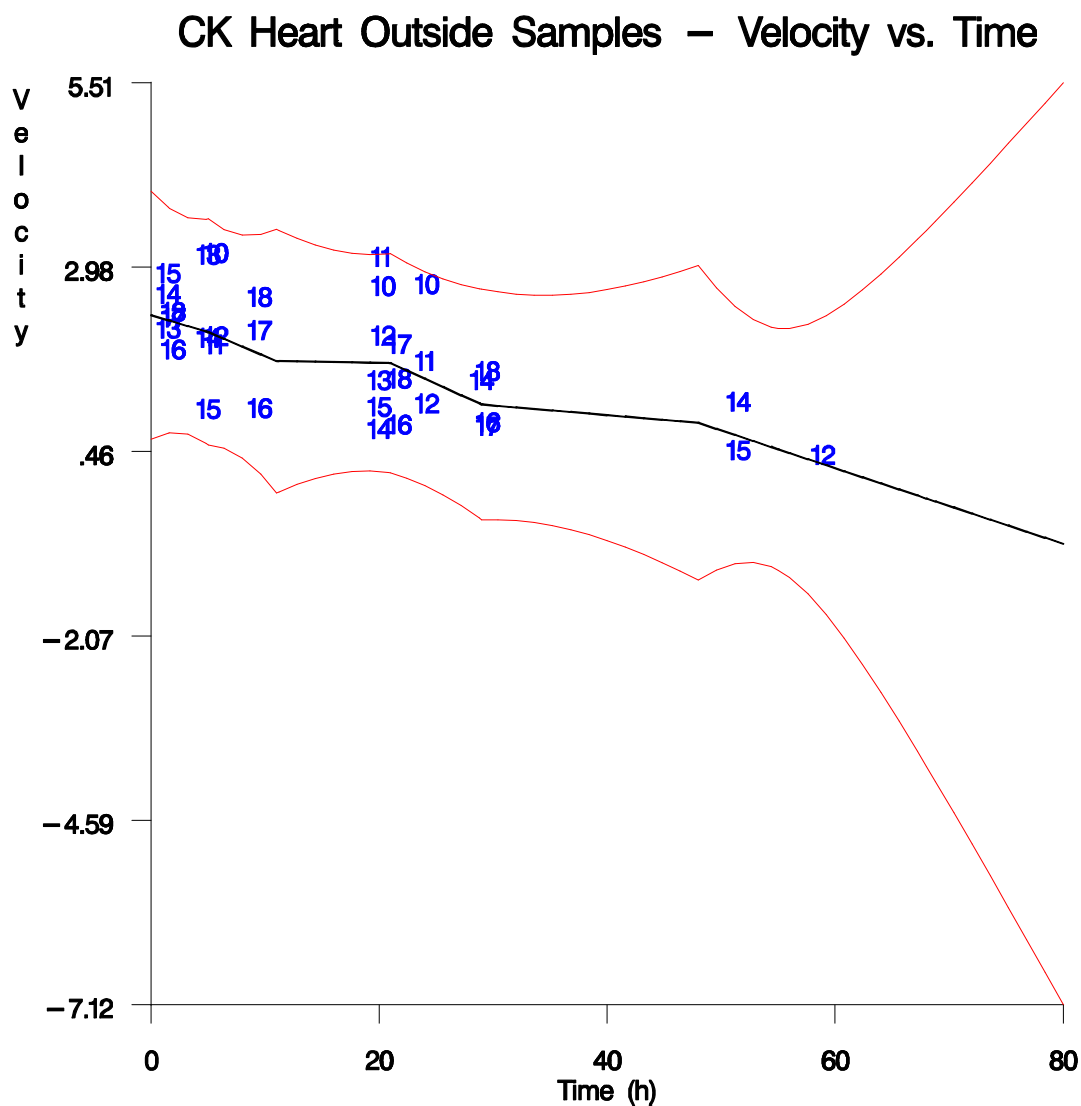


Figure 4.17: CK activity in outside heart samples as a function of time. No data points fall outside the 95% prediction interval and none are excluded from computation of the regression line. The regression line is shown in black, and the 95% prediction interval is denoted by the two outer red lines. Data points in blue were used in computation of the prediction interval, while data points in red were considered outliers and excluded from the formula. Velocity is measured in $\mu\text{moles}/\text{min}/\text{mg}$ protein.

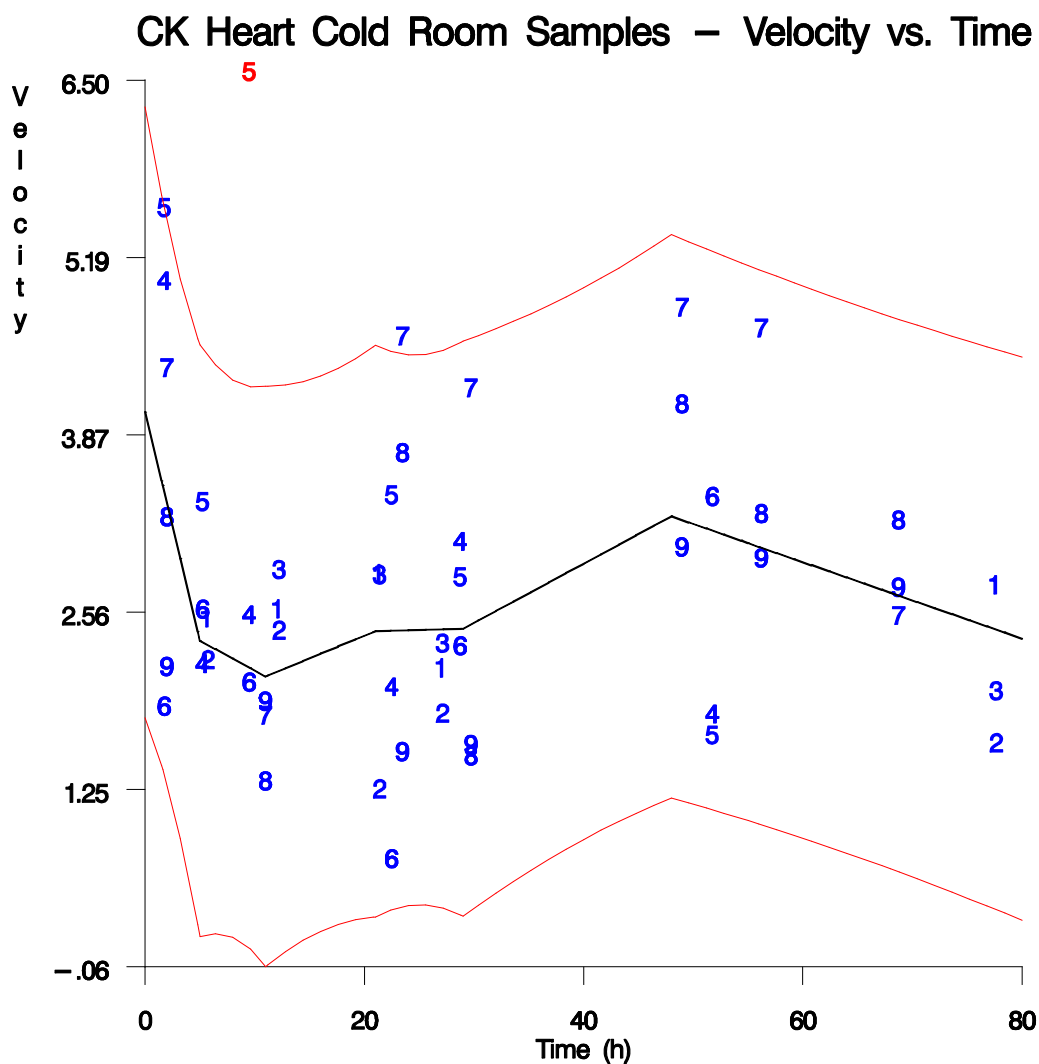


Figure 4.18: CK activity in cold room heart samples as a function of time. One data point that falls outside the 95% prediction interval is excluded from computation of the regression line. The regression line is shown in black, and the 95% prediction interval is denoted by the two outer red lines. Data points in blue were used in computation of the prediction interval, while data points in red were considered outliers and excluded from the formula. Velocity is measured in $\mu\text{moles}/\text{min}/\text{mg}$ protein.

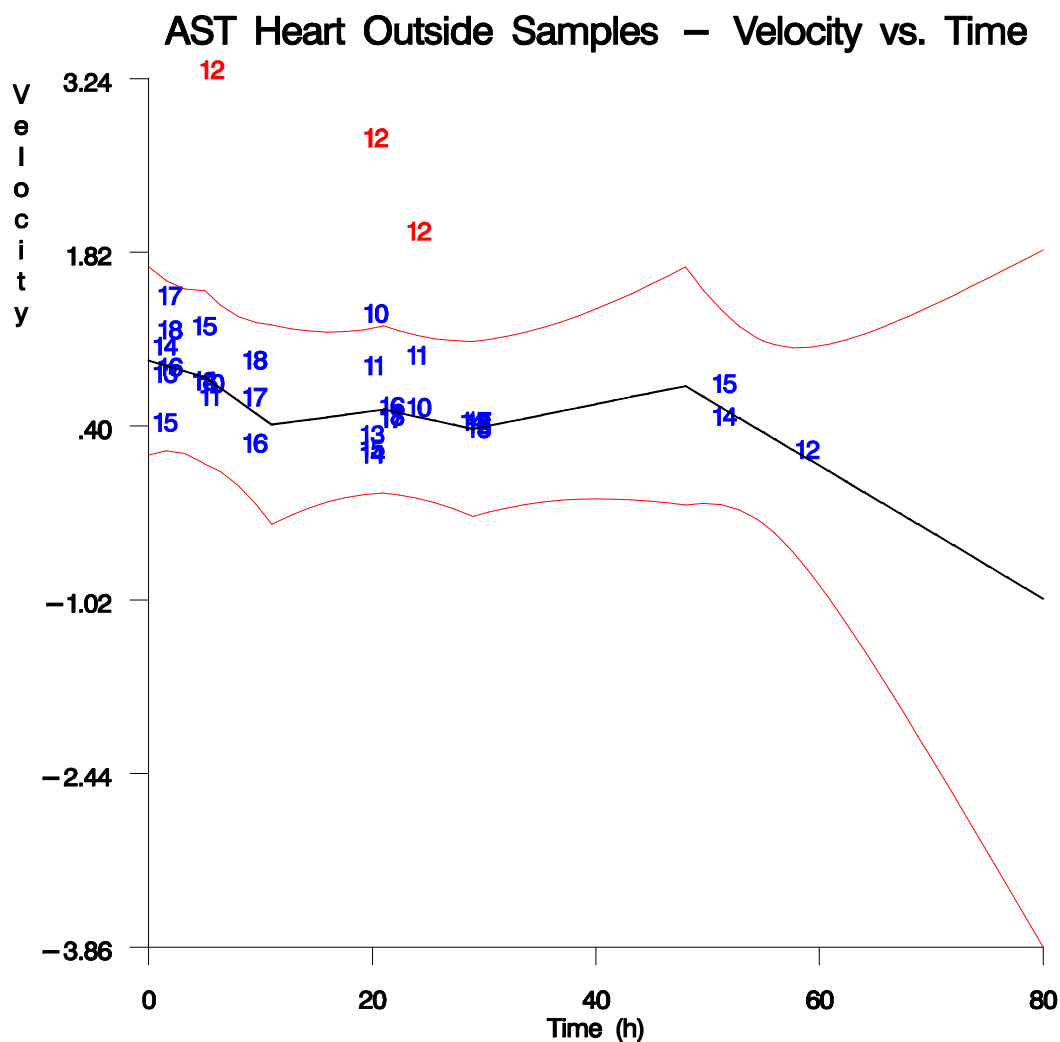


Figure 4.19: AST activity in outside heart samples as a function of time. Three data points that fall outside the 95% prediction interval are excluded from computation of the regression line. The regression line is shown in black, and the 95% prediction interval is denoted by the two outer red lines. Data points in blue were used in computation of the prediction interval, while data points in red were considered outliers and excluded from the formula. Velocity is measured in $\mu\text{moles}/\text{min}/\text{mg}$ protein.

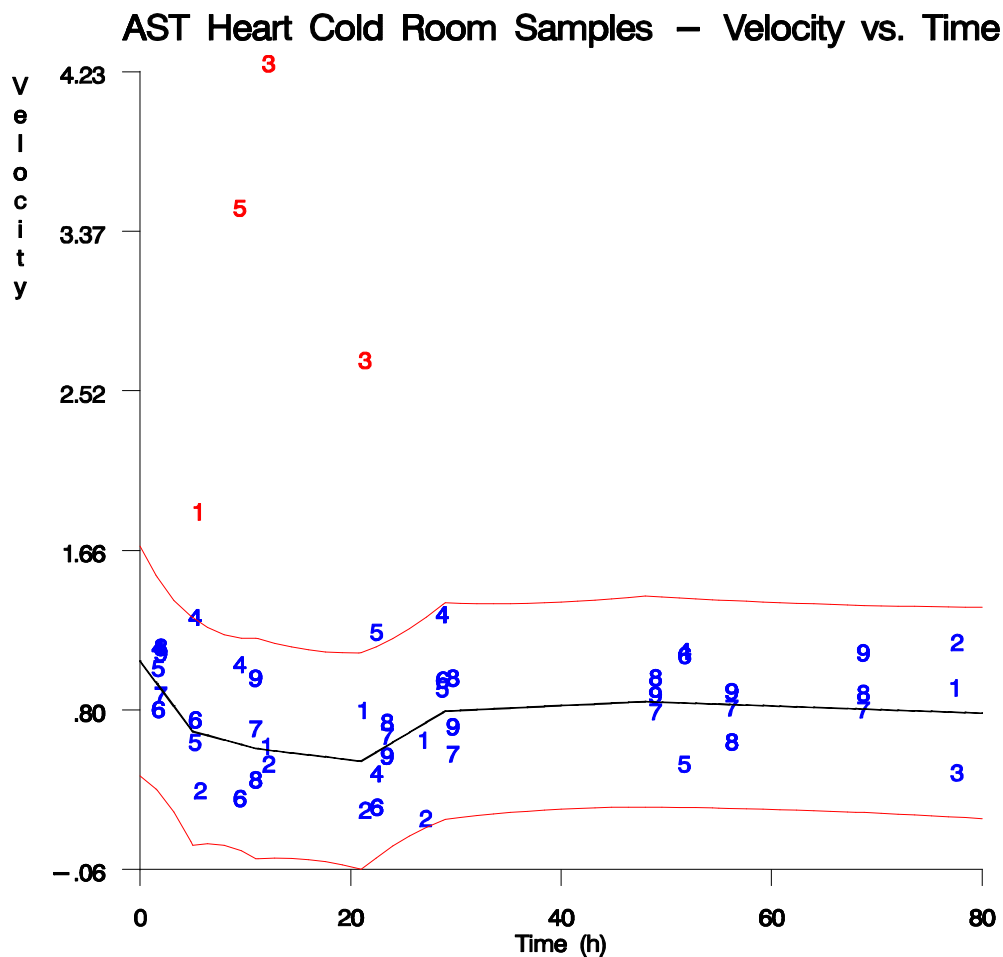


Figure 4.20: AST activity in cold room heart samples as a function of time. Four data points that fall outside the 95% prediction interval are excluded from computation of the regression line. The regression line is shown in black, and the 95% prediction interval is denoted by the two outer red lines. Data points in blue were used in computation of the prediction interval, while data points in red were considered outliers and excluded from the formula. Velocity is measured in $\mu\text{moles}/\text{min}/\text{mg}$ protein.

The graphs numbered 4.21 through 4.40 are plots of all rats' individual data points, rather than a combination of all data for a particular enzyme, tissue, and temperature. Each colored symbol represents data collected at a specific time point. No splines or knots are used in the graphs, and no data points are omitted from the plots (unless there was no data for a particular time point). Each rat's data points are plotted in a different color, and a legend is located to the right of the graph denoting the color and symbol that are assigned to each rat. For each enzyme a graph from the cold room samples and a graph from the outside samples are plotted, showing enzyme velocity (as micromoles/min/mg protein) vs. time (as hours after euthanasia). The information in graphs 4.21 through 4.40 is the individual data for each rat, which are compiled into the groups of data that are shown in the graphs numbered 4.1 through 4.20.

Lactate Dehydrogenase (Outside Liver Samples)

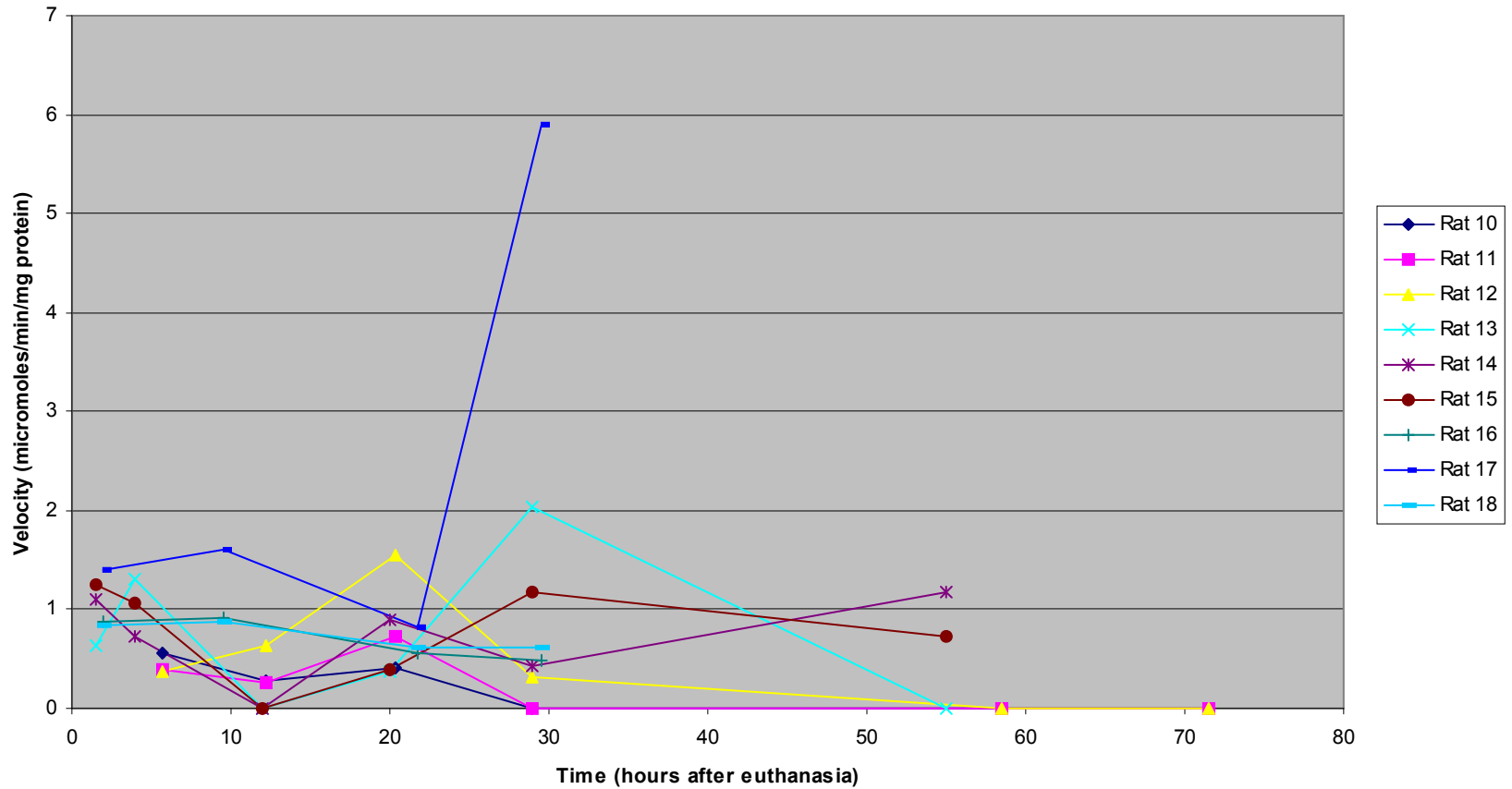


Figure 4.21: Lactate Dehydrogenase (Outside Liver Samples)—Each colored line represents data from one rat, and each symbol within the lines represents a sample collection at that particular time. A legend at the right shows the color that represents each rat.

Lactate Dehydrogenase (Cold Liver Samples)

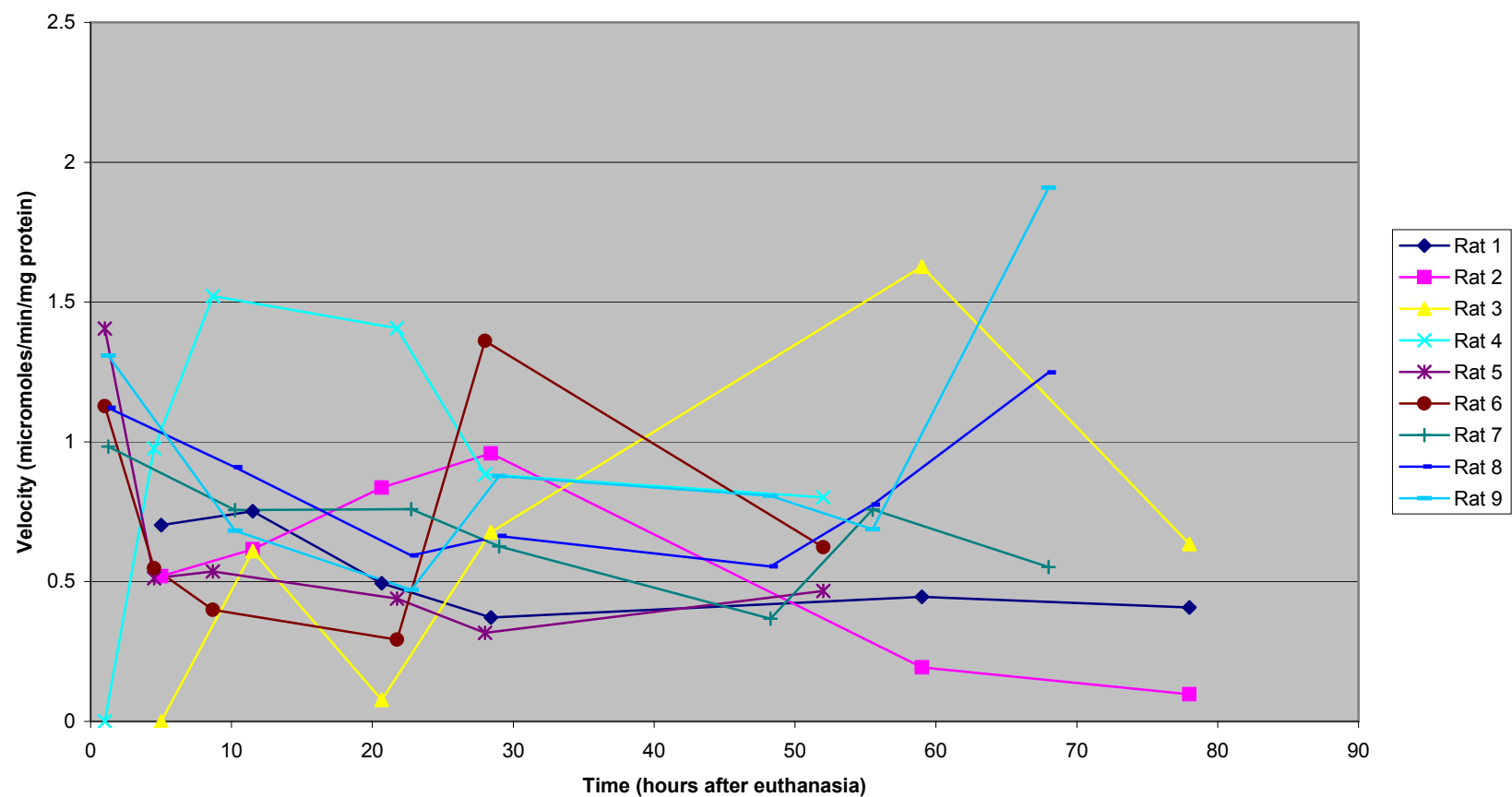


Figure 4.22: Lactate Dehydrogenase (Cold Liver Samples)—Each colored line represents data from one rat, and each symbol within the lines represents a sample collection at that particular time. A legend at the right shows the color that represents each rat.

Creatine Kinase (Outside Liver Samples)

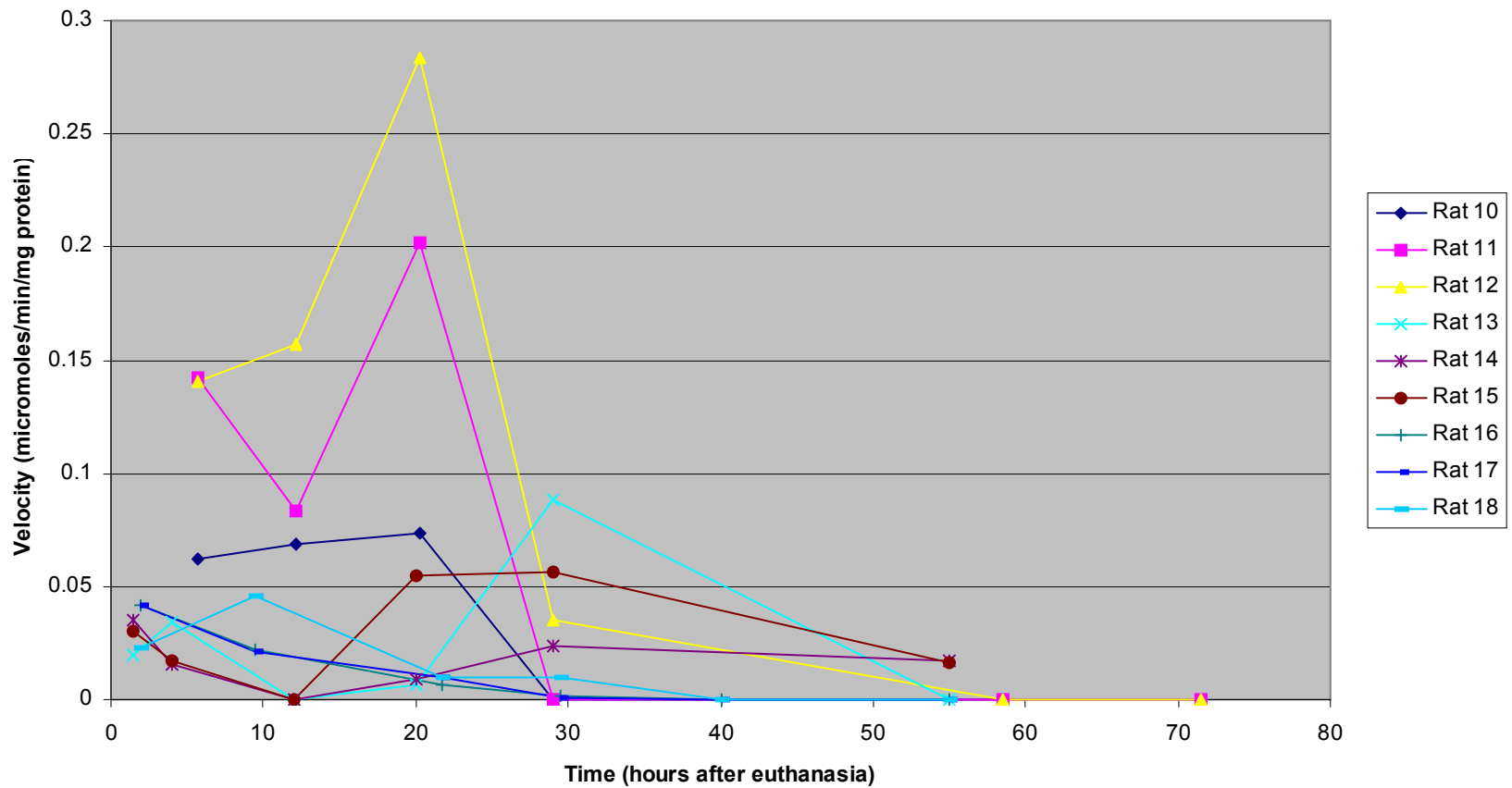


Figure 4.23: Creatine Kinase (Outside Liver Samples)—Each colored line represents data from one rat, and each symbol within the lines represents a sample collection at that particular time. A legend at the right shows the color that represents each rat.

Creatine Kinase (Cold Liver Samples)

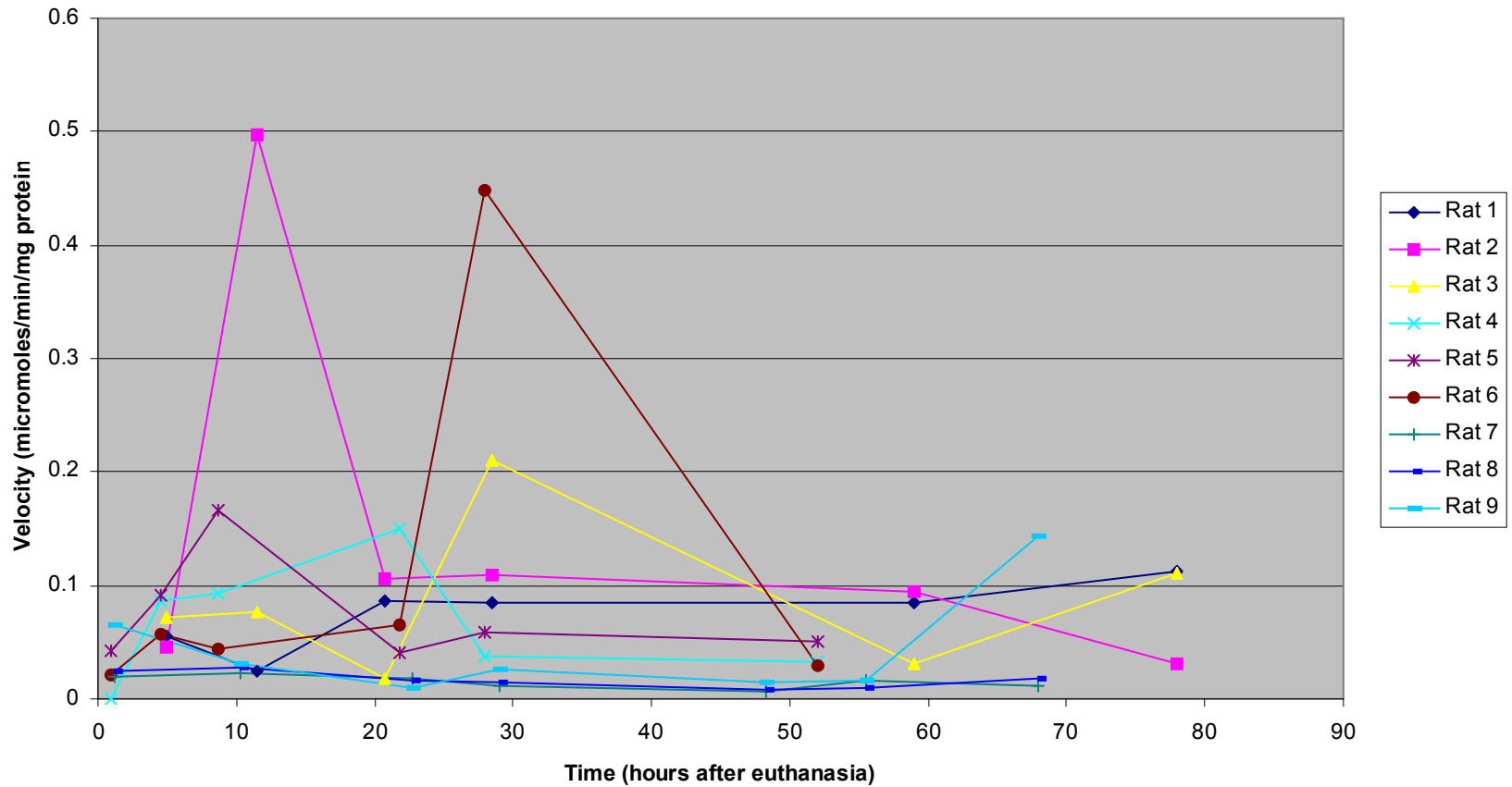


Figure 4.24: Creatine Kinase (Cold Liver Samples)—Each colored line represents data from one rat, and each symbol within the lines represents a sample collection at that particular time. A legend at the right shows the color that represents each rat.

Aspartate Aminotransferase (Outside Liver Samples)

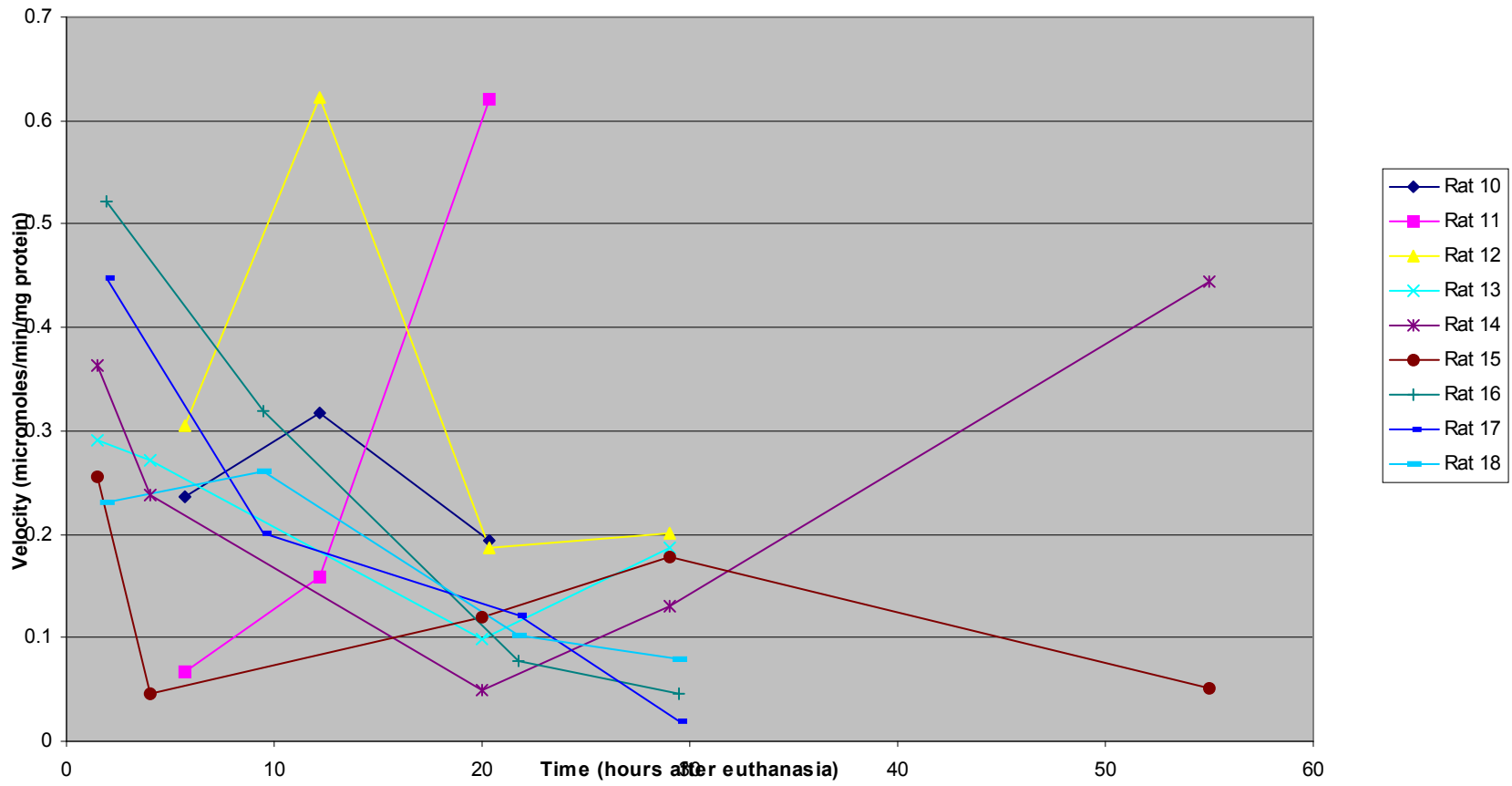


Figure 4.25: Aspartate Aminotransferase (Outside Liver Samples)—Each colored line represents data from one rat, and each symbol within the lines represents a sample collection at that particular time. A legend at the right shows the color that represents each rat.

Aspartate Aminotransferase (Cold Liver Samples)

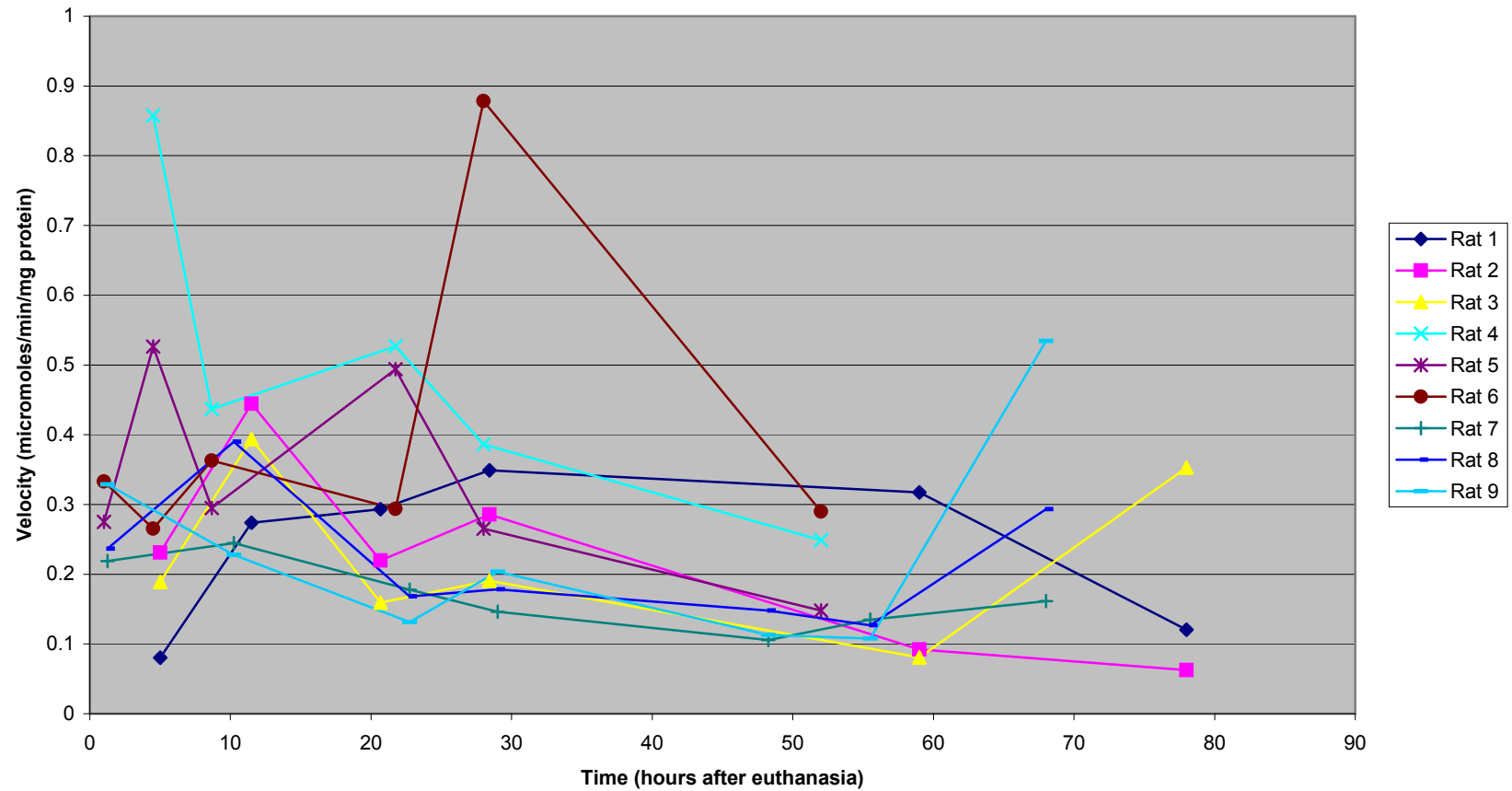


Figure 4.26: Aspartate Aminotransferase (Cold Liver Samples)—Each colored line represents data from one rat, and each symbol within the lines represents a sample collection at that particular time. A legend at the right shows the color that represents each rat.

Alcohol Dehydrogenase (Outside Liver Samples)

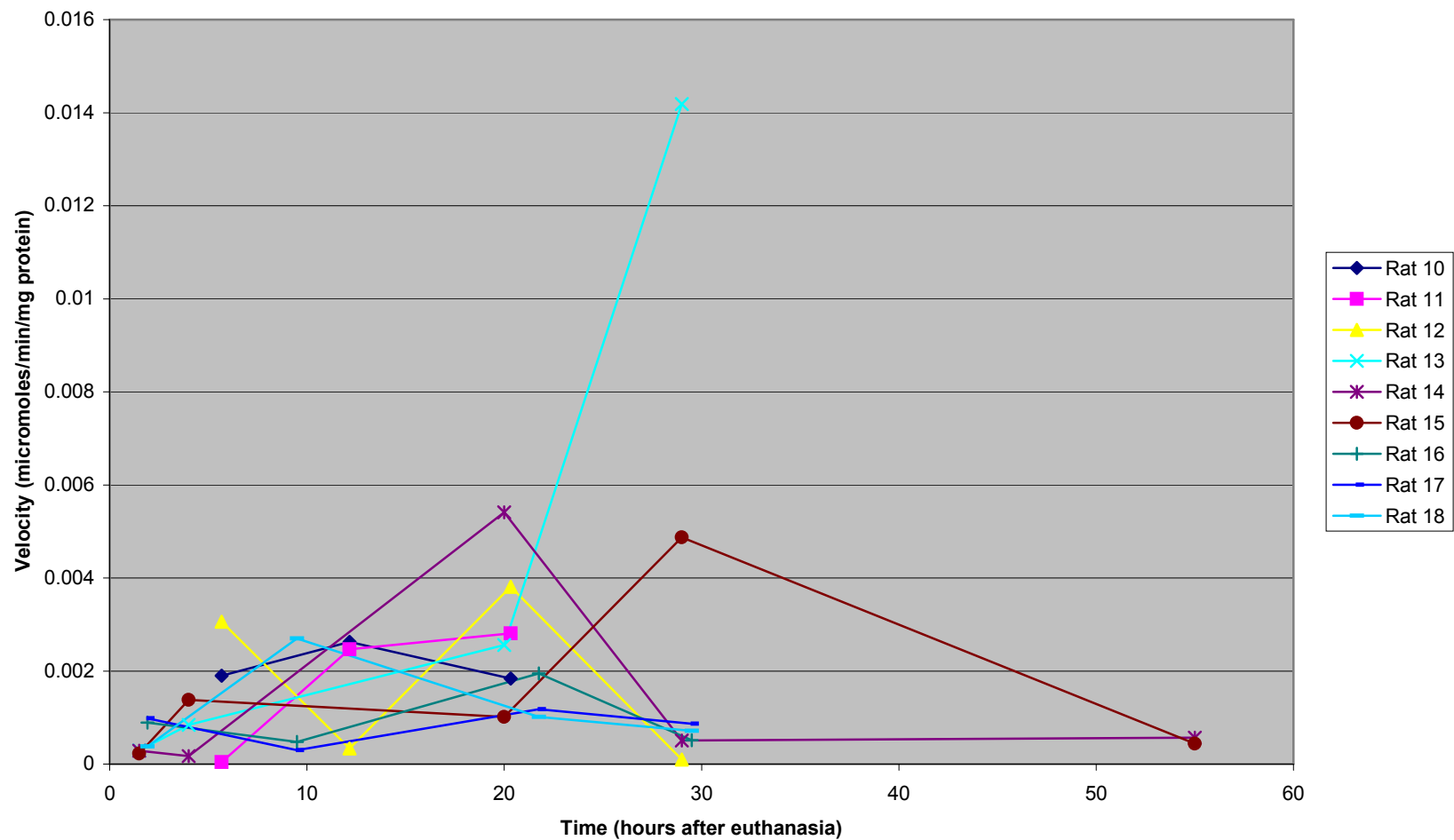


Figure 4.27: Alcohol Dehydrogenase (Outside Liver Samples)—Each colored line represents data from one rat, and each symbol within the lines represents a sample collection at that particular time. A legend at the right shows the color that represents each rat.

Alcohol Dehydrogenase (Cold Liver Samples)

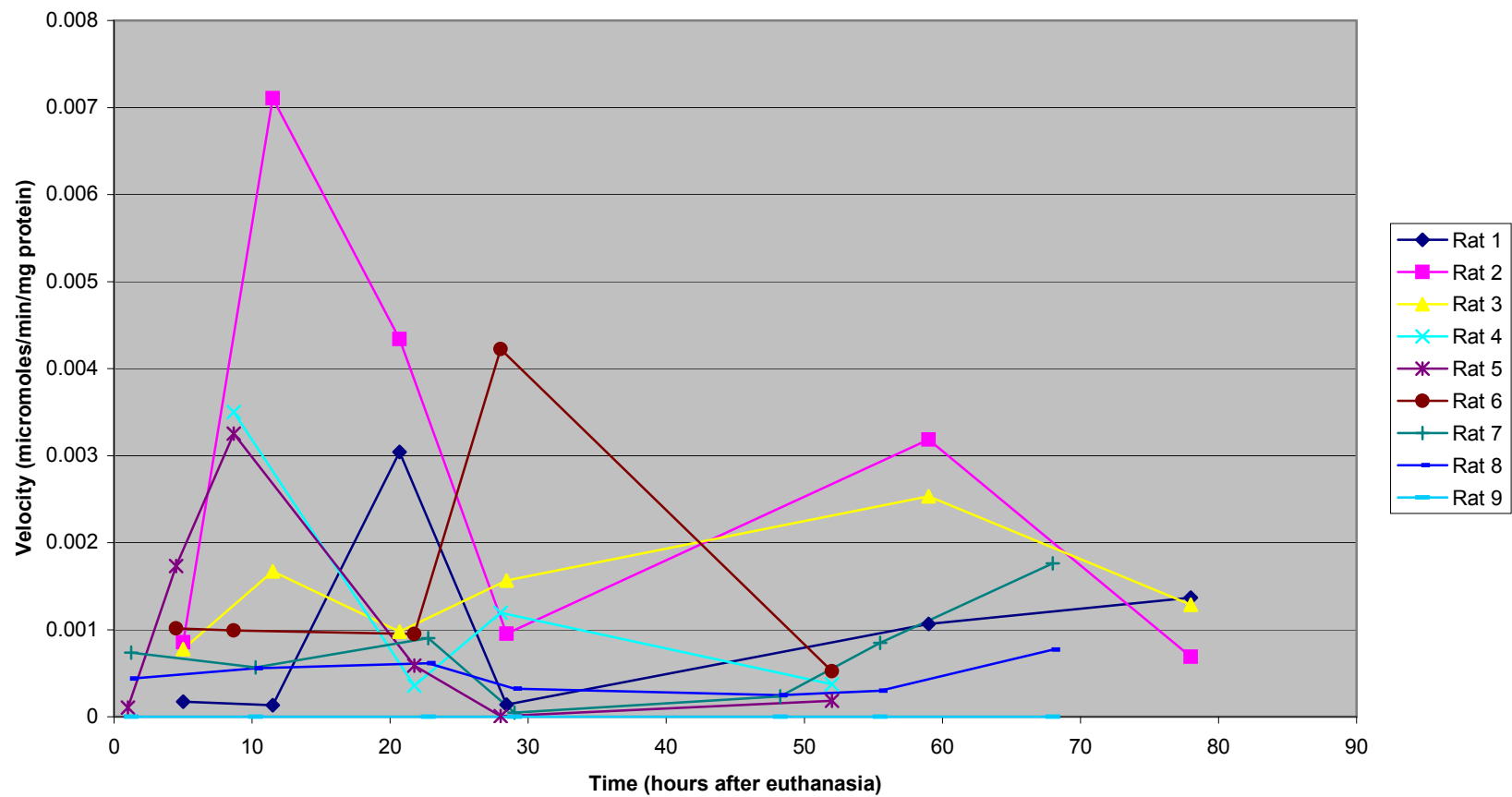


Figure 4.28: Alcohol Dehydrogenase (Cold Liver Samples)—Each colored line represents data from one rat, and each symbol within the lines represents a sample collection at that particular time. A legend at the right shows the color that represents each rat.

Lactate Dehydrogenase (Outside Muscle Samples)

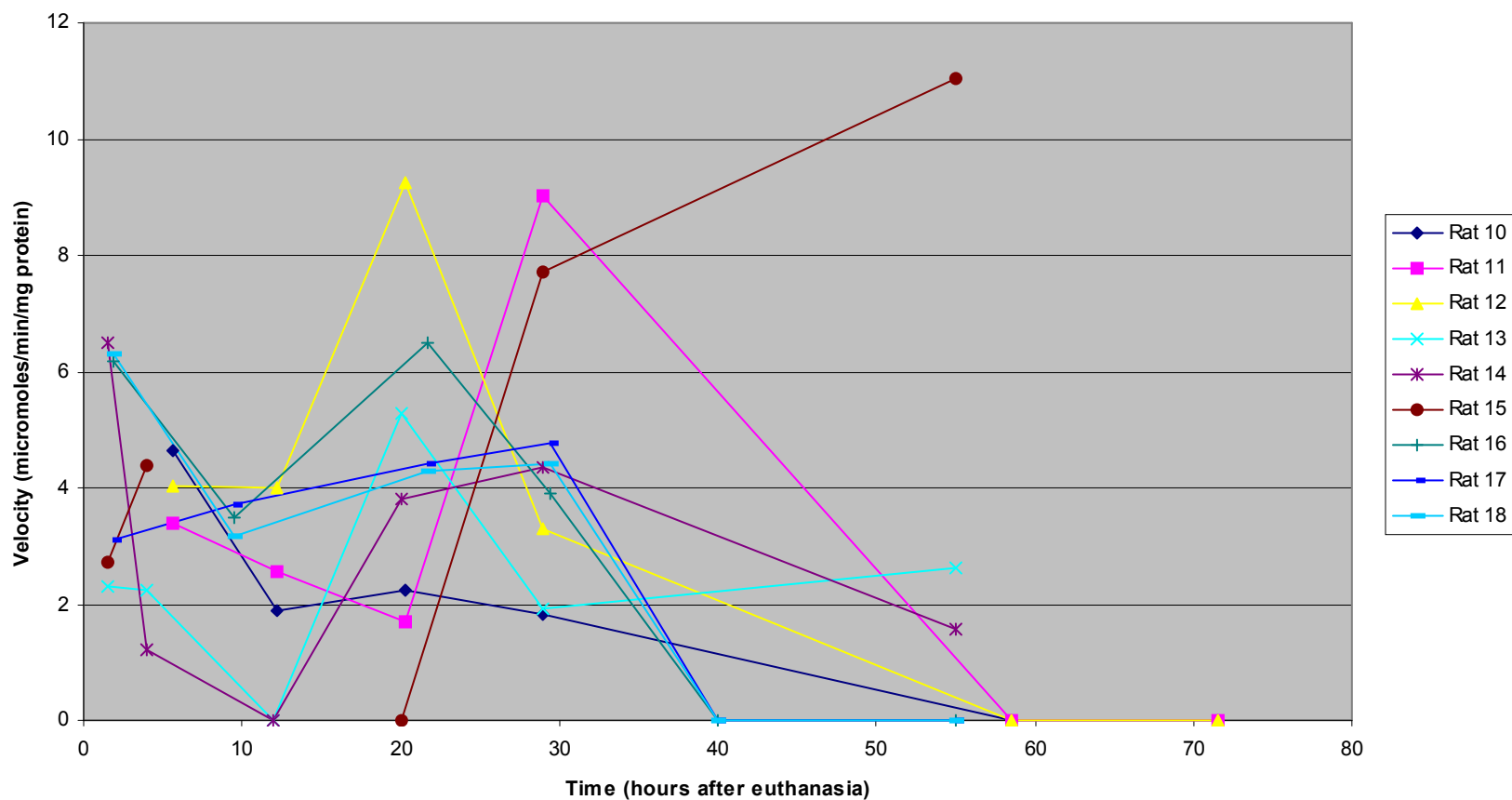


Figure 4.29: Lactate Dehydrogenase (Outside Muscle Samples)—Each colored line represents data from one rat, and each symbol within the lines represents a sample collection at that particular time. A legend at the right shows the color that represents each rat.

Lactate Dehydrogenase (Cold Muscle Samples)

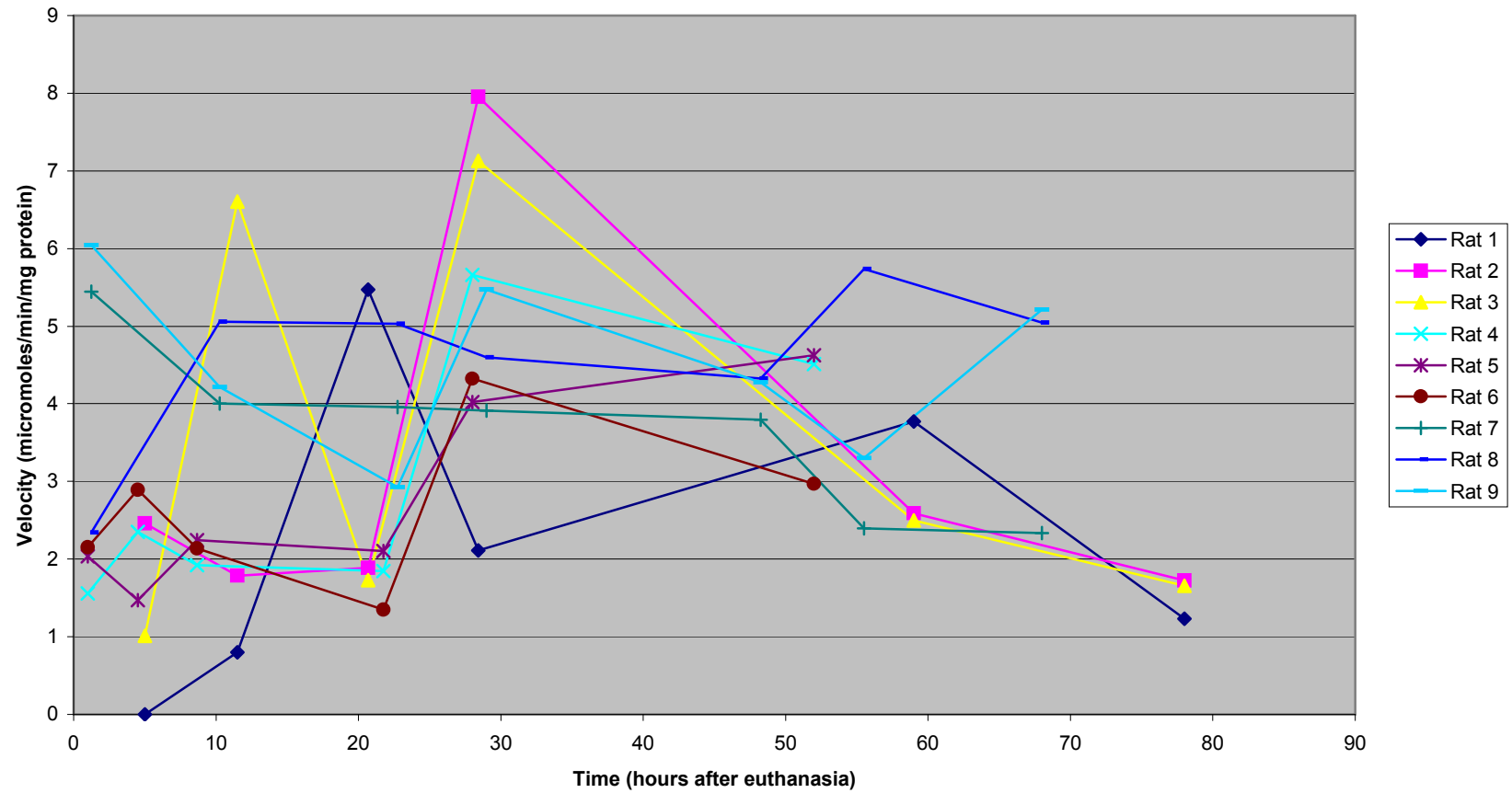


Figure 4.30: Lactate Dehydrogenase (Cold Muscle Samples)—Each colored line represents data from one rat, and each symbol within the lines represents a sample collection at that particular time. A legend at the right shows the color that represents each rat.

Creatine Kinase (Outside Muscle Samples)

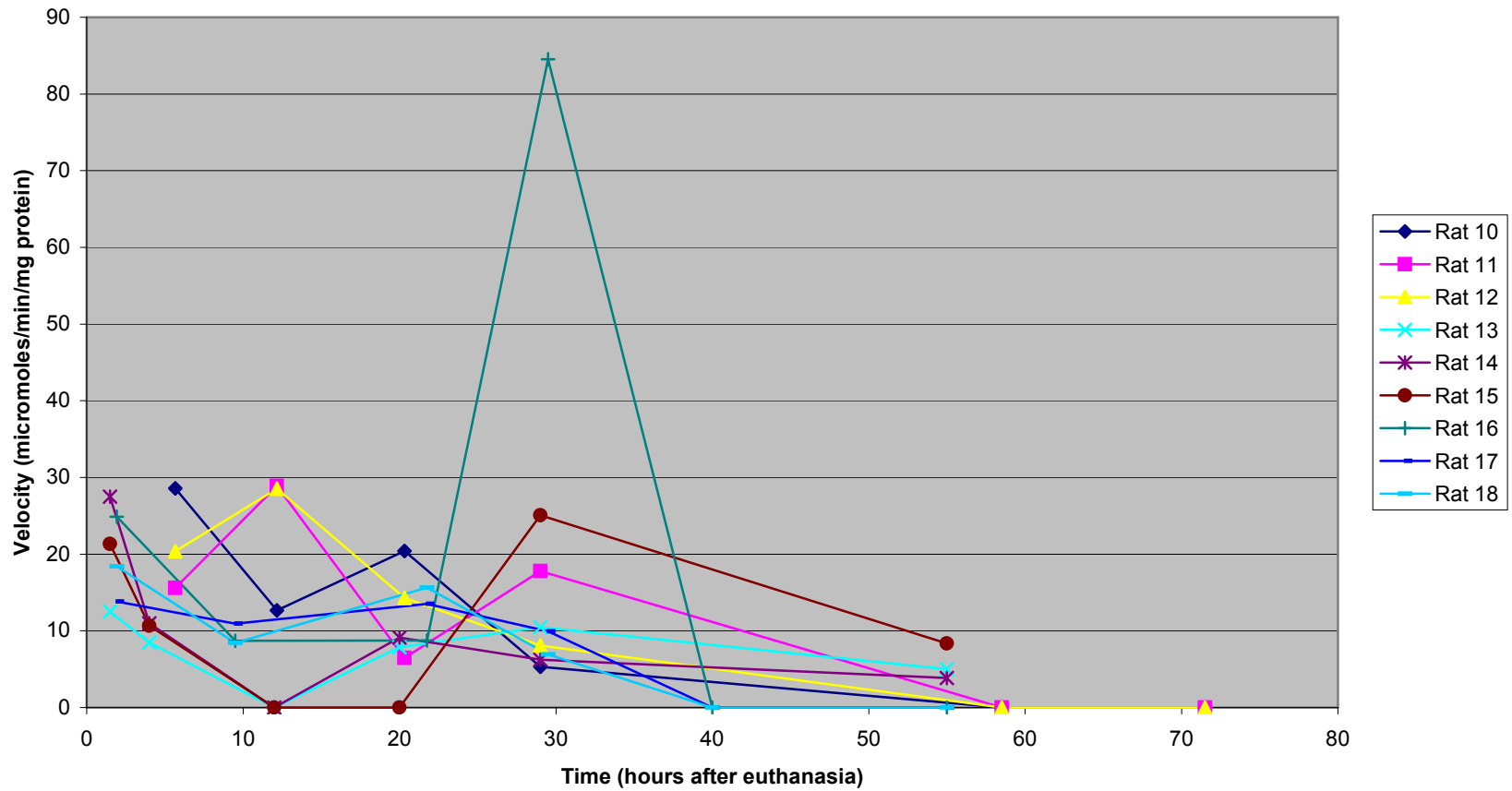


Figure 4.31: Creatine Kinase (Outside Muscle Samples)—Each colored line represents data from one rat, and each symbol within the lines represents a sample collection at that particular time. A legend at the right shows the color that represents each rat.

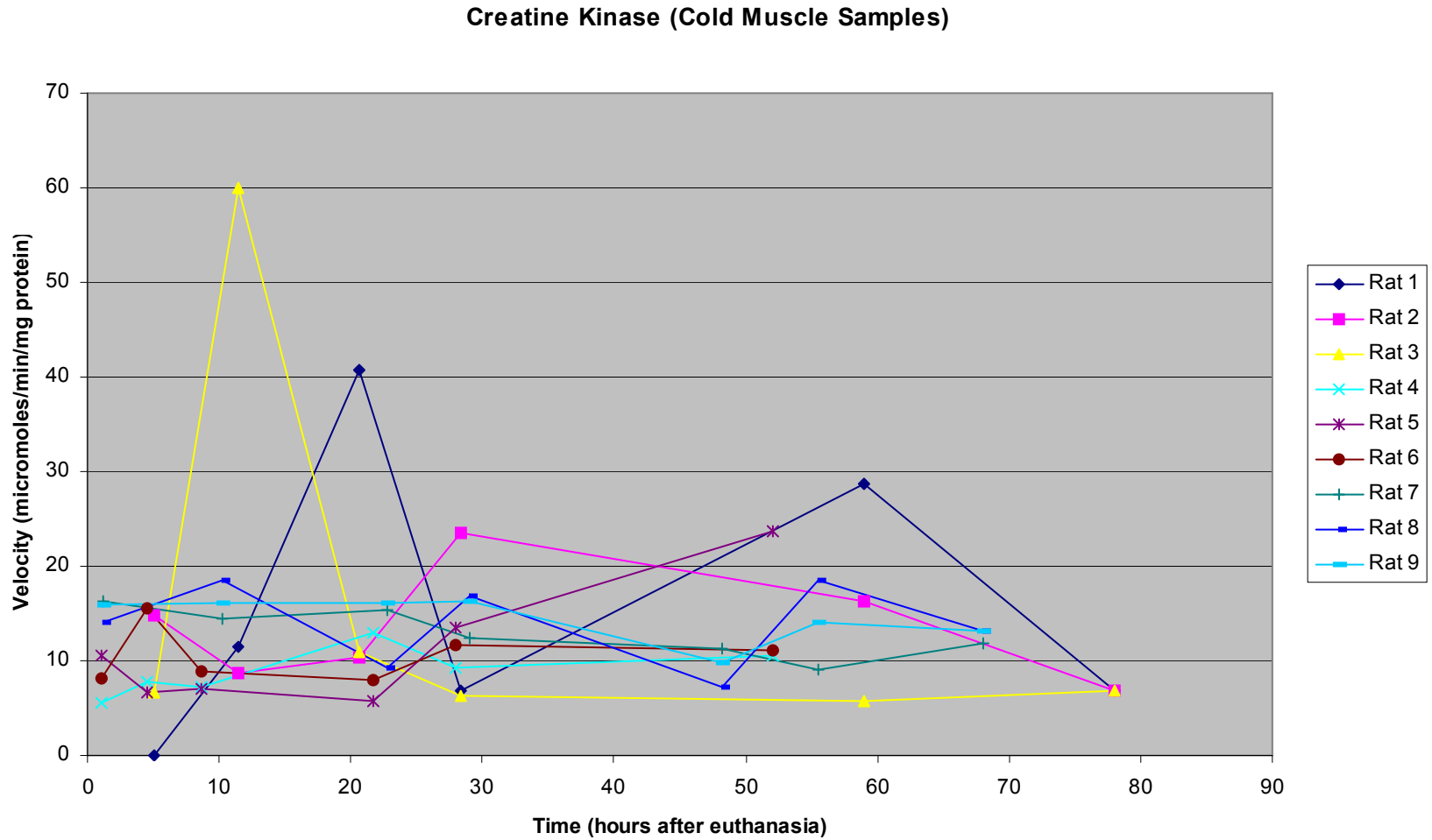


Figure 4.32: Creatine Kinase (Cold Muscle Samples)—Each colored line represents data from one rat, and each symbol within the lines represents a sample collection at that particular time. A legend at the right shows the color that represents each rat.

Aspartate Aminotransferase (Outside Muscle Samples)

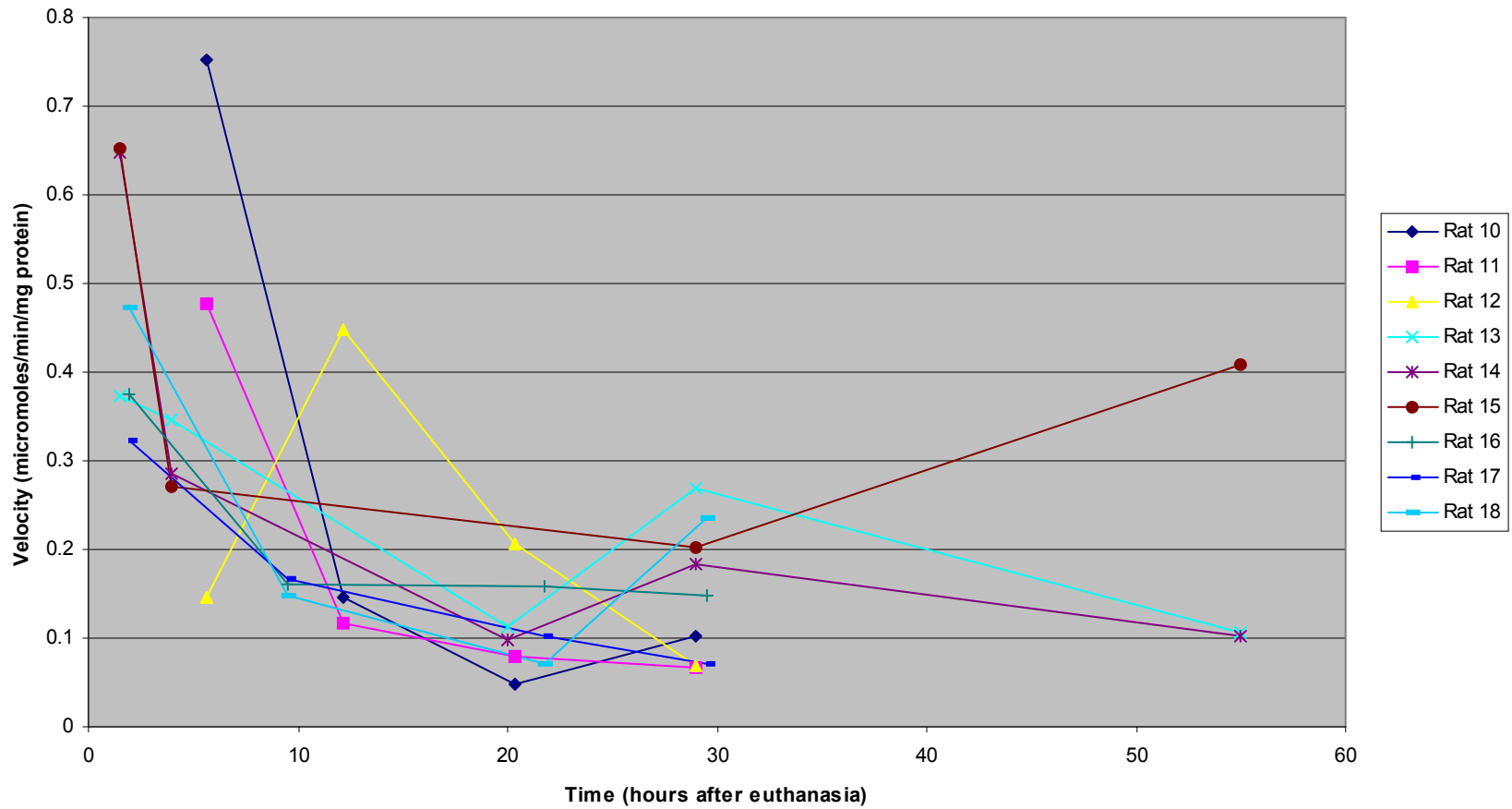


Figure 4.33: Aspartate Aminotransferase (Outside Muscle Samples)—Each colored line represents data from one rat, and each symbol within the lines represents a sample collection at that particular time. A legend at the right shows the color that represents each rat.

Aspartate Aminotransferase (Cold Muscle Samples)

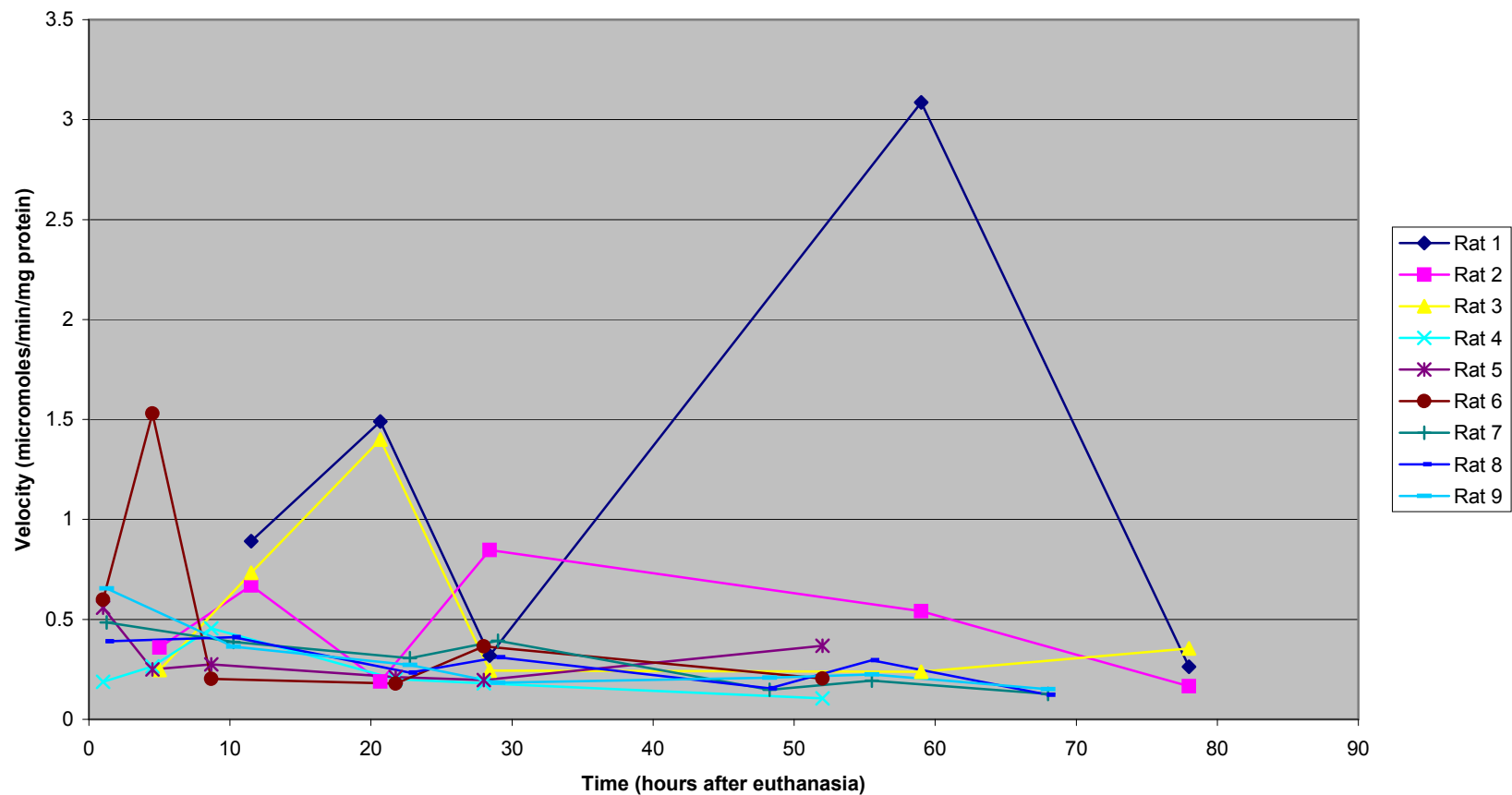


Figure 4.34: Aspartate Aminotransferase (Cold Muscle Samples)—Each colored line represents data from one rat, and each symbol within the lines represents a sample collection at that particular time. A legend at the right shows the color that represents each rat.

Lactate Dehydrogenase (Outside Heart Samples)

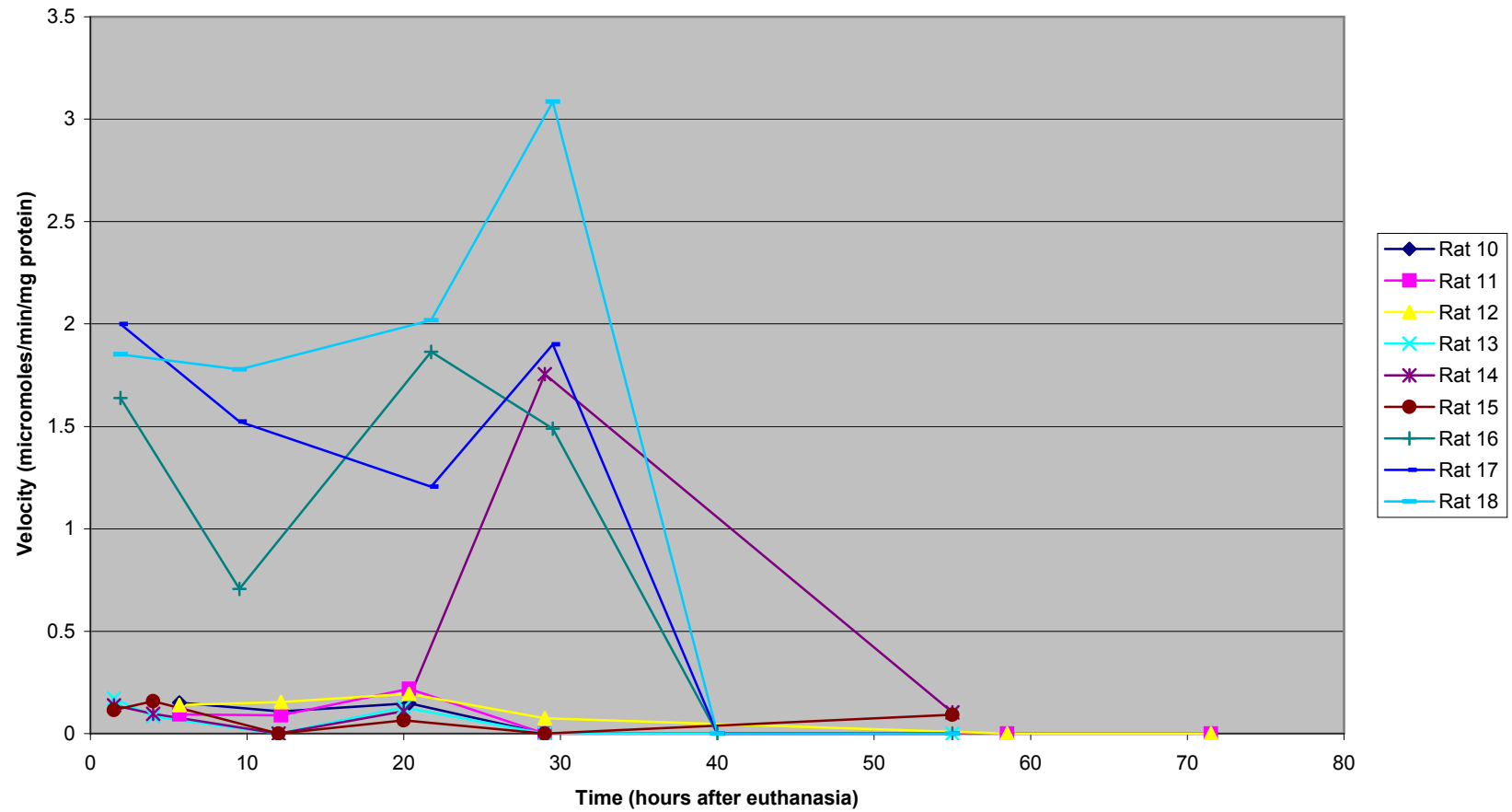


Figure 4.35: Lactate Dehydrogenase (Outside Heart Samples)—Each colored line represents data from one rat, and each symbol within the lines represents a sample collection at that particular time. A legend at the right shows the color that represents each rat.

Lactate Dehydrogenase (Cold Heart Samples)

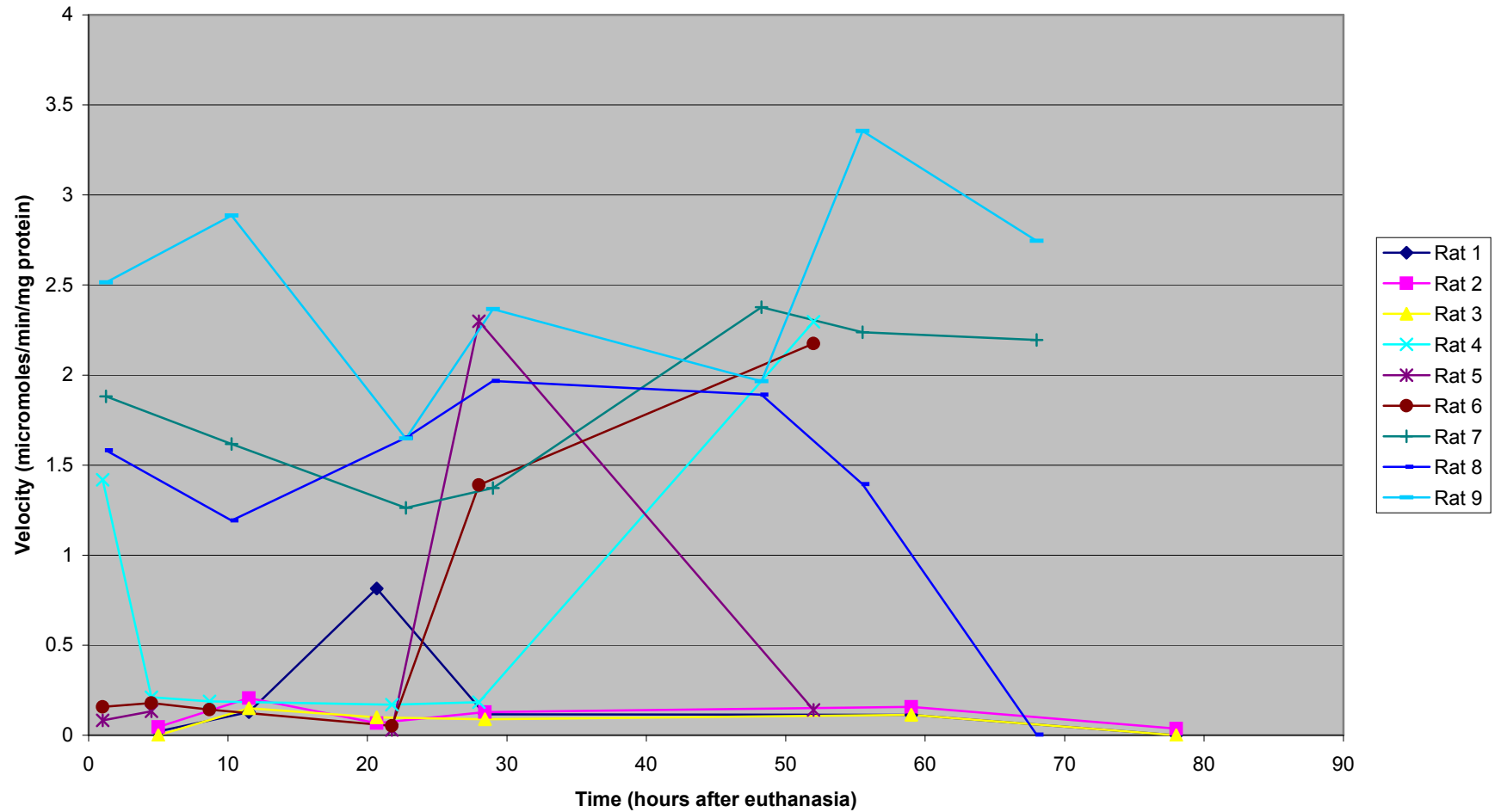


Figure 4.36: Lactate Dehydrogenase (Cold Heart Samples)—Each colored line represents data from one rat, and each symbol within the lines represents a sample collection at that particular time. A legend at the right shows the color that represents each rat.

Creatine Kinase (Outside Heart Samples)

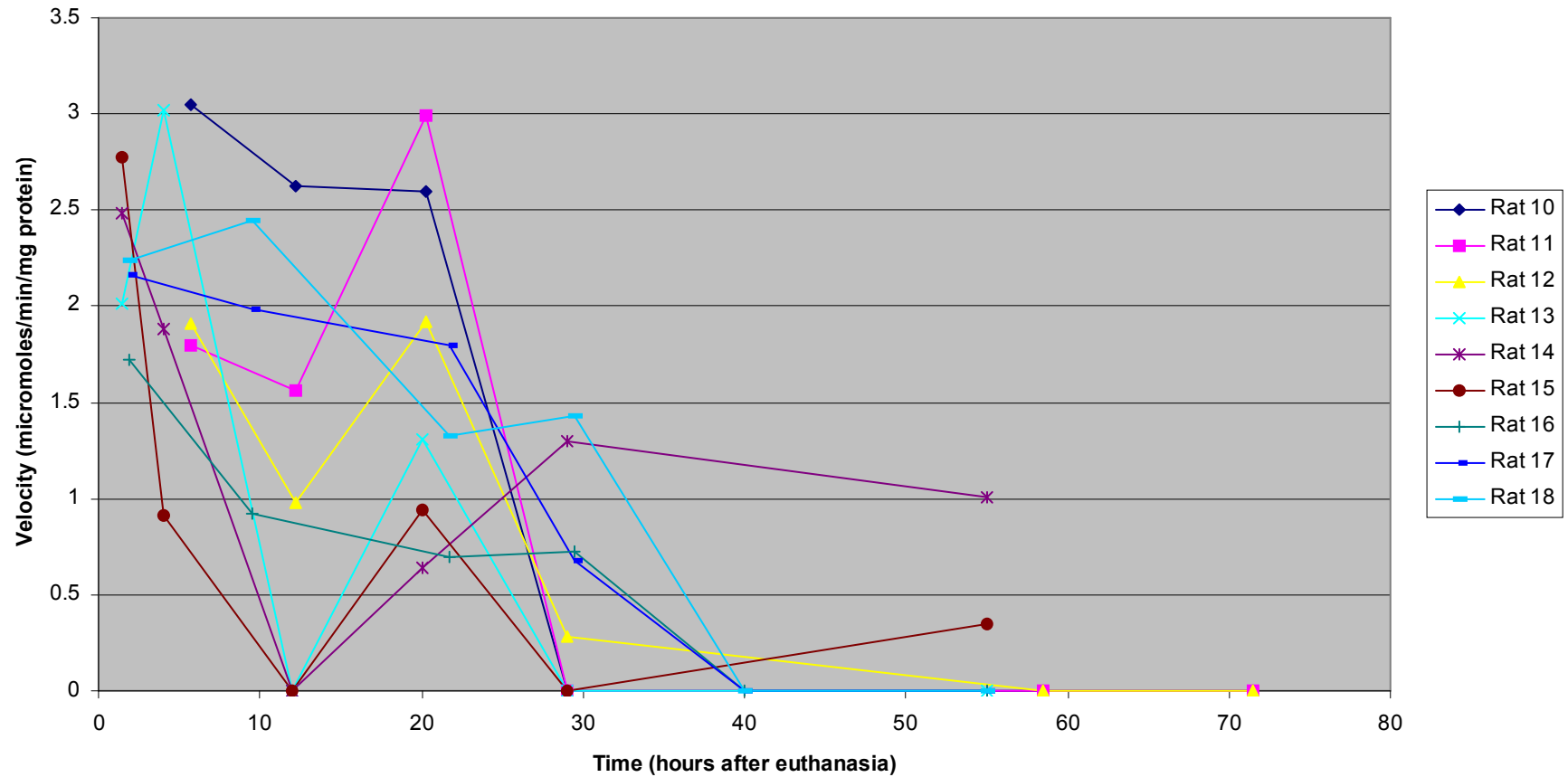


Figure 4.37: Creatine Kinase (Outside Heart Samples)—Each colored line represents data from one rat, and each symbol within the lines represents a sample collection at that particular time. A legend at the right shows the color that represents each rat.

Creatine Kinase (Cold Heart Samples)

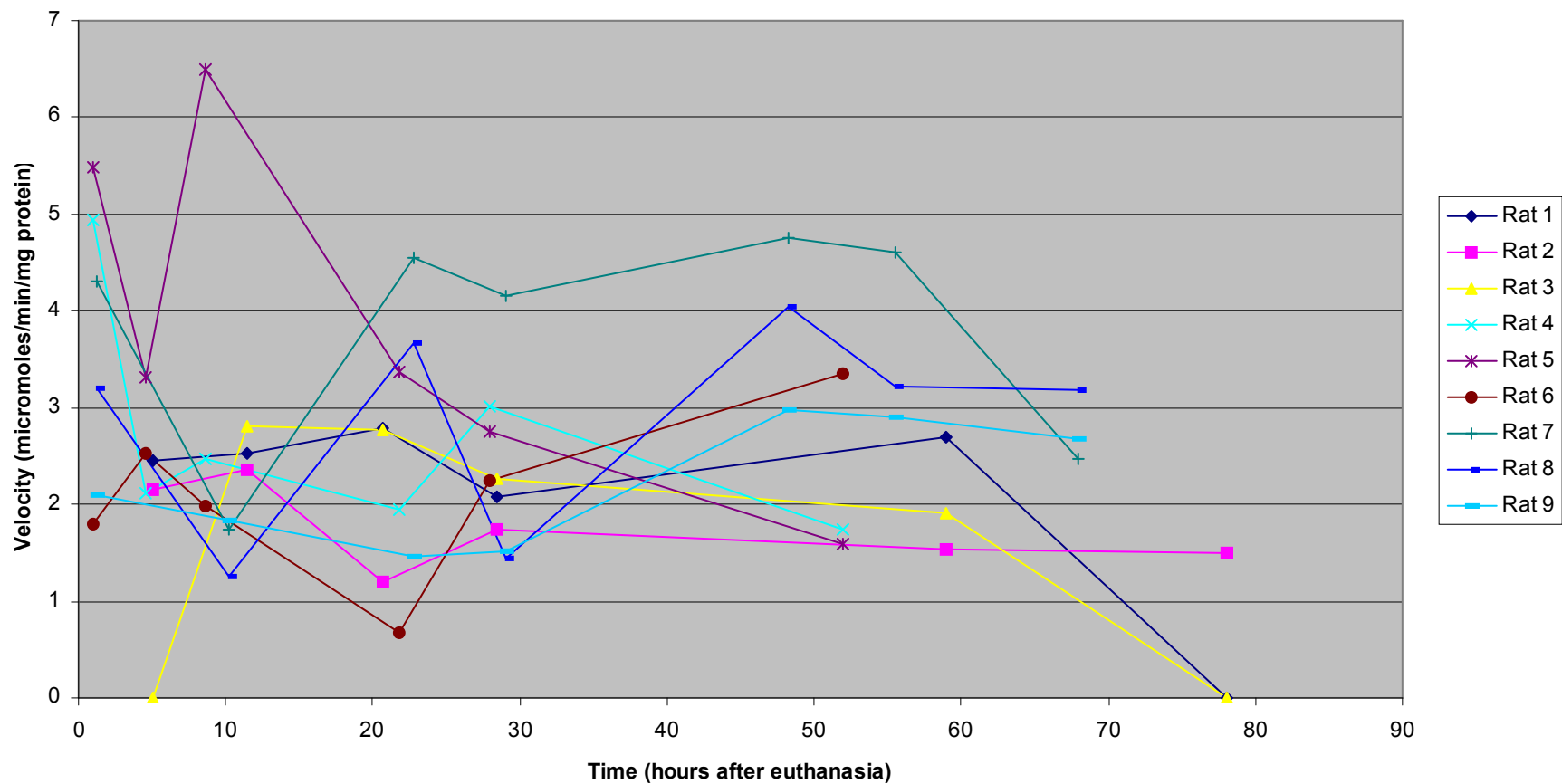


Figure 4.38: Creatine Kinase (Cold Heart Samples)—Each colored line represents data from one rat, and each symbol within the lines represents a sample collection at that particular time. A legend at the right shows the color that represents each rat.

Aspartate Aminotransferase (Outside Heart Samples)

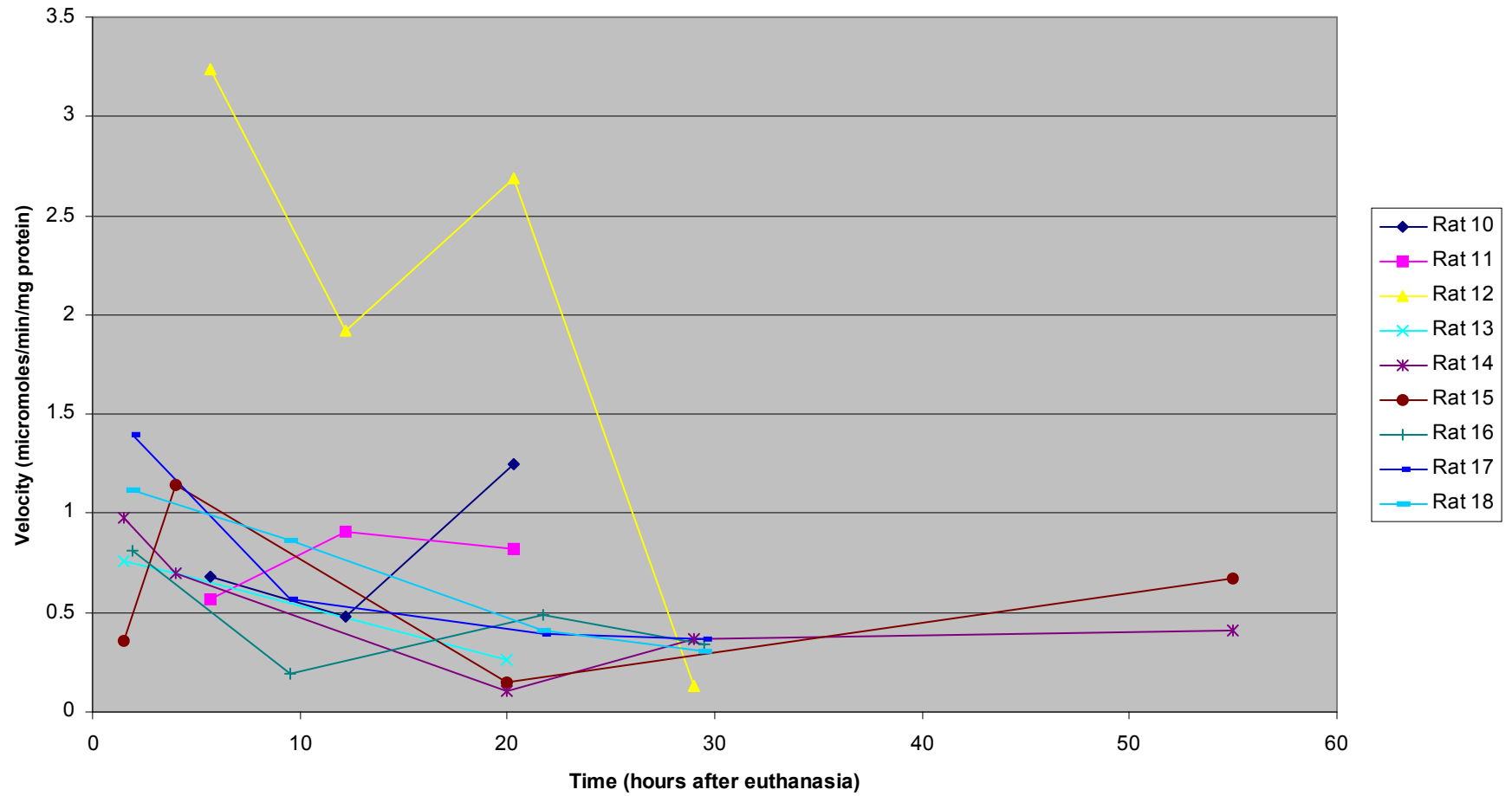


Figure 4.39: Aspartate Aminotransferase (Outside Heart Samples)—Each colored line represents data from one rat, and each symbol within the lines represents a sample collection at that particular time. A legend at the right shows the color that represents each rat.

Aspartate Aminotransferase (Cold Heart Samples)

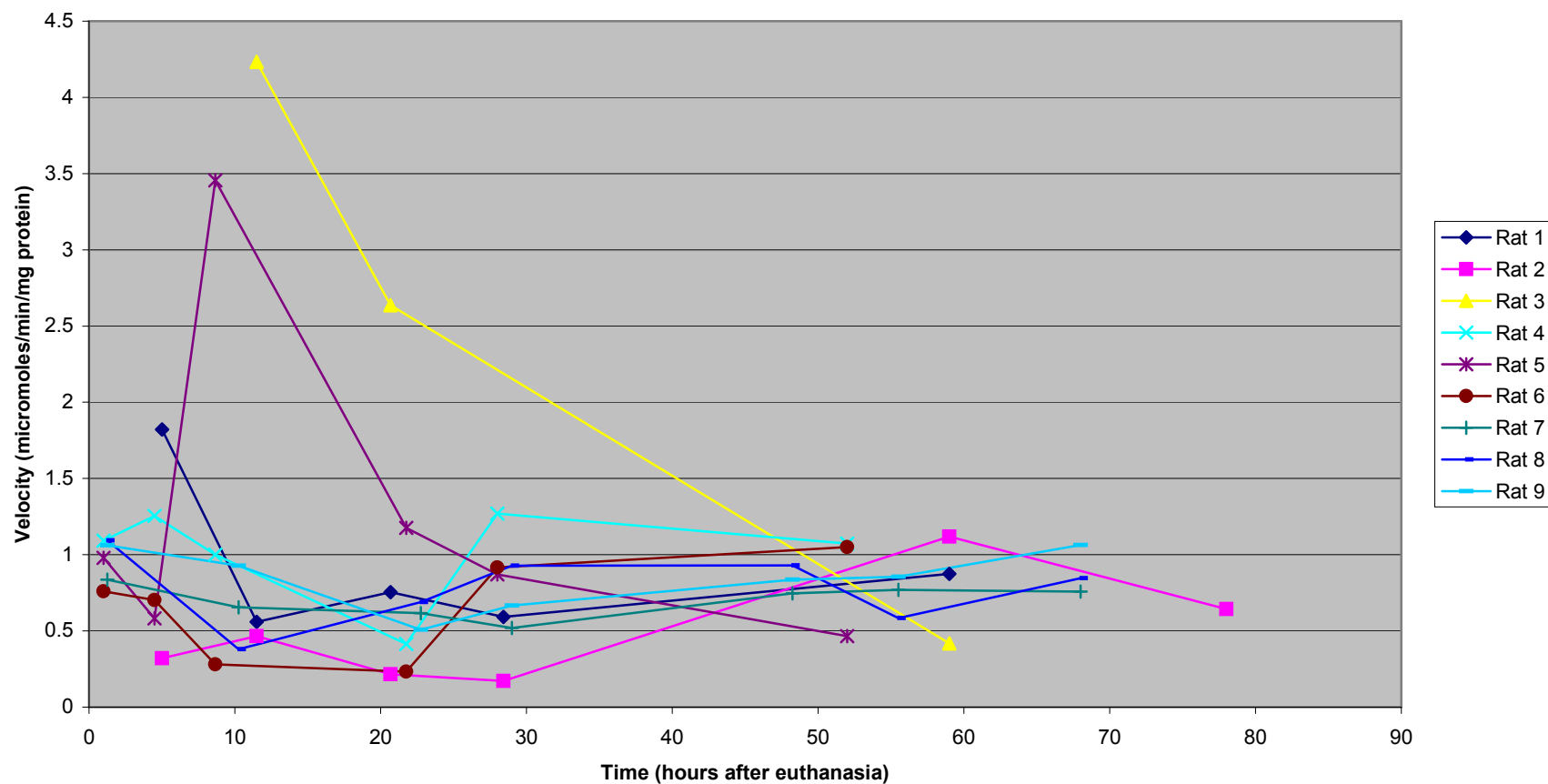


Figure 4.40: Aspartate Aminotransferase (Cold Heart Samples)—Each colored line represents data from one rat, and each symbol within the lines represents a sample collection at that particular time. A legend at the right shows the color that represents each rat.

DISCUSSION

The results of this study showed that the four enzymes chosen—ADH, AST, CK, and LDH—would likely not be of use for estimating PMI for the conditions under which this study was performed. Many variables could account for the apparent unreliability of these enzymes for PMI estimation. There could have been a problem with the procedure itself. For a useful procedure, what variables needed to be controlled or taken into account?

Outside temperatures on all three groups of rats were comparable, and temperature in the cold room stayed within a four to five degree range. All rats, both cold and outside, were positioned on their right sides with incisions made in the same places on all eighteen rats. Could this position have had an effect on enzyme distribution and activity? Could the postmortem mechanical injury (scalpel cuts) have played a part in enzyme concentrations? Micozzi (1986) did a study on mechanical injury and how freezing and thawing affect postmortem processes. These variables come into play in areas where seasonality affects PMI estimates. Micozzi showed that the rates of disarticulation in fresh killed animals were slower than in frozen-thawed animals, but the sequences did not differ. He wrote, “the extent to which postmortem processes in previously frozen-thawed tissues duplicates processes in freshly killed tissues is questionable and requires experimental validation” (Micozzi 1986, p 955). The mechanical injury undoubtedly played a significant role in the decomposition and maggot activity. Micozzi also found that, in general, the frozen-thawed animals were more susceptible to invasion by insects and outside microorganisms, whereas the fresh killed animals were more susceptible to putrefaction from within, rather than external decay.

Does it matter from which area of the tissues one takes a sample? Could samples from different areas of the tissues yield different enzyme velocities? One could argue either side of

this point, that is, whether enzyme concentration will initially increase or decrease after cell death. Once the cells lyse, they release their materials into the surrounding tissue. Should this matter, however, if the preparation process for sample analysis involves mechanical lysis of the cells? Perhaps it depends on how quickly the process of livor mortis sets in, which, in turn, depends on the environmental conditions into which the body is placed.

One could argue that the tissues would show an initial increase in enzyme velocity because the cells are lysing and releasing their intracellular products into the tissue directly surrounding the area of insult. This would be followed by a subsequent decrease in velocity because the process of livor mortis would set in and the cellular contents that were once suspended in the tissues directly surrounding the affected areas would now begin to leak out. In other words, one would see a steady increase in enzyme velocity until livor mortis set in, after which the spectrophotometer would show a decrease in absorbance (corresponding to a decrease in enzyme velocity). However, one could also make the argument that enzyme velocity should show a constant decrease from its starting point, stating that as the tissues die and cells lyse, enzyme is constantly being released from the cells and leaking out of the tissues as a result of gravity and livor mortis.

Yet another argument is that enzyme velocity would not change at all. Even though the tissues are dying and releasing their intracellular enzymes, the time for this to occur is longer than for the blood to coagulate; therefore, there would be no way by which the enzyme could leak out of the tissues (*i.e.*, they would remain stagnant wherever the cell lysed). Whatever the case, Coe (1974) stated, “as increasingly sophisticated studies on hormones, blood gases, and enzymes are carried out, it will undoubtedly become important to be able to accurately identify the source of the material to be analyzed” (p 26).

A researcher could find a basis for all three of the above arguments, but then she must consider how different or changing temperatures would affect the enzyme velocity differently. With regard to temperatures, one might expect to see a greater slope to the regression line for the outside rats and a more horizontal line for the cold room rats, because optimum temperature for most enzymes encountered in PMI estimations will be fairly high, around normal body temperature (Campbell 1999).

The sample size for this study was relatively small. Unless variables are controlled for differently, one would expect to see the same results in another study. All cold and outside rats seemed to yield similar results, respectively. There seemed to be no real change over time in the cold room rats' enzyme levels. The outside rats showed a greater degree of fluctuation overall, but no real predictable or repeatable trend. The cold room rats showed a fairly similar regression line; the velocity fluctuated unpredictably.

Repeated thawing and freezing could have affected the enzyme activity levels. Karkela (1993) stated this in his study of postmortem enzyme levels in cisternal fluid. Samples were thawed for each enzyme assay performed (a total of four times), and then refrozen after each assay was completed. Samples were allowed to thaw completely before being added to the cuvet; however, they were kept on ice to keep their temperatures as low as possible to prevent any possible continued enzyme activity. In future studies, a control substance with a known normal velocity/time function should be employed to determine whether the freeze/thaw process could also affect a change in the enzyme velocity. In this study, however, such a control was not available. Samples that were not thawed to exactly the same temperature could also have resulted in non-uniform changes in enzyme velocity.

One would expect the enzyme activity to be higher in the outside rats because of the higher temperature. Outside temperatures averaged in the 70-85°F between the night and day, whereas the cold room was kept at a constant temperature of 40-45°F. The higher temperatures found outside were closer to the optimum temperature for the enzyme activity; therefore, higher activity should be reflected in the velocities of the enzymes. However, this was not the case. The outside and cold room rats showed very similar velocities and velocity trends. This result leads one to believe that the enzyme activities were not affected by the temperatures. Further research should examine whether, or how much of, a difference is made by ambient temperature.

There were no studies found on whether or how maggot activity affects the activities of ADH, AST, CK, or LDH. Future studies may address this topic. Maggots found on the body could possibly alter the enzyme activity in the infested areas. Control animals could be subjected to all environmental conditions as the experimental ones, with the exception of insect infestation. Samples would be taken from approximately the same place on all rats and each sample prepared and assayed to determine enzyme velocity. If significant differences were found, one could infer that the difference was due to the maggots.

One important factor that must also be addressed is the possible interrelatedness of enzymes. If the activity or level of a particular enzyme changes, does that effect a change in another? Current research does not indicate if or how the enzymes in this study are affected by changes in one another, or even those not studied. Further research is also warranted to determine to what degree, if any, the ethanol treatments had on the study samples. However, there are also other factors discussed in this paper that should be accounted for before these enzymes are completely discounted as reliable PMI indicators.

Body size is an important consideration for correlation of data between rats and humans. Did size affect the outcome of the study? Are rats comparable to humans when analyzing such functions as those examined here? One might be tempted to say no because of the obvious differences in size. Coe (1974) stated that “while the animal experiments can be carefully controlled, they demonstrate considerable variation in concentrations of chemical constituents between the different species studied, and conclusions drawn from them are frequently at odds with data obtained from postmortem studies on human species” (p 22). But after considering all the scientific research that has been done on rats and other small animals, how could they not be deemed adequate for an initial study such as this? Basic biological functions are being studied here; activities that require higher brain function play no part. Hence, size should not be a factor in this study.

This study could not account for all possible biological reactions taking place antemortem, perimortem, and postmortem, but hopefully this study has shed some light on a few. The use of multiple PMI indicators will always be the most reliable method by which to estimate time since death. Hopefully, future studies will incorporate some of the suggestions and ideas proposed in this paper, and the field of forensic science will benefit from the results of this study. Camps (1959, p 78) put it well, stating that “estimating the time of death is not an exact science. The best we can achieve is a reasoned guess taking into account all the known factors, and our aim should be to limit the margin of error inherent in assessing their effects.”

WORKS CITED

- Backer, R.C., R.V. Pisano, and I.M. Sopher
1980 The Comparison of Alcohol Concentrations in Postmortem Fluids and Tissues. *Journal of Forensic Sciences* 25(2):327-331.
- Bass, W.M.
1984 Time Interval Since Death. A Difficult Decision, in *Human Identification: Case Studies in Forensic Anthropology*, Rathbun, T.A, and J.E. Buikstra, Eds., Charles C. Thomas, Springfield, Illinois.
- Bhagavan, N.V.
2002 *Medical Biochemistry*. Harcourt/Academic Press, San Diego.
- Bolliger, A., and A.L. Carrodus
1938 Creatine Retention in Blood and Cerebrospinal Fluid. *Medical Journal of Australia* 1(Jan 8):69-72.
- Briglia, E.J., J.H. Bidanset, and L.A. Dal Cortivo
1992 The Distribution of Ethanol in Postmortem Blood Specimens. *Journal of Forensic Sciences* 37(4):991-998.
- Budd, R.D.
1982 Ethanol Levels in Postmortem Body Fluids. *Journal of Chromatography* 252:315-318.
- Burton, J.F.
1974 Fallacies in the Signs of Death. *Journal of Forensic Sciences* 19(1):529-534.
- Campbell, N.
1999 *Biology*, 5th ed., Benjamin Cummings, New York.
- Camps, F.E.
1959 Establishment of the Time of Death—A Critical Assessment. *Journal of Forensic Sciences* 4(1):73-82.
- Coe, J.I.
1974 Postmortem Chemistry: Practical Considerations and a Review of the Literature. *Journal of Forensic Sciences* 19(1):13-32.
- Deitrich, R.A., and R.A. Harris
1996 How Much Alcohol Should I Use in My Experiments? *Alcoholism: Clinical and Experimental Research* 20(1):1-2.

- Devlin, T.M.
2002 Textbook of Biochemistry with Clinical Correlations, 5th ed., Wiley-Liss, New York.
- Enticknap, J.B.
1960 Biochemical Changes in Cadaver Sera in Fatal Acute Heart Attacks. *Journal of Forensic Medicine* 7(3):135-146.
- Erickson, R.J., and D.R. Morales
1961 Clinical Use of Lactate Dehydrogenase. *New England Journal of Medicine* 265(18):478.
- Gilliland, M.G.F., and R.O. Bost
1993 Alcohol in Decomposed Bodies: Postmortem Synthesis and Distribution. *Journal of Forensic Sciences* 38(6):1266-1274.
- Hennsge, C., B. Madea, B. Knight, L. Nokes, and T. Krompecher
1995 *The Estimation of the Time Since Death in the Early Postmortem Interval*, Arnold, London.
- Jetter, W.W.
1959 Postmortem Biochemical Changes. *Journal of Forensic Sciences* 4(3):330-341.
- Jetter, W.W., and R. McLean
1942 Biochemical Changes in Body Fluids After Death. Paper presented at the Twenty-First Annual Meeting of the American Society of Clinical Pathologists, Philadelphia, June 6.
- Kachmar, J.F., and D.W. Moss
1976 Enzymes, in *Fundamentals of Clinical Chemistry*, Tietz, N.W., Ed., Saunders, Philadelphia:652-660.
- Karkela, J.T.
1993 Critical Evaluation of Postmortem Changes in Human Autopsy Cisternal Fluid. Enzymes, Electrolytes, Acid-Base Balance, Glucose and Glycolysis, Free Amino Acids and Ammonia. Correlation to Total Brain Ischemia. *Journal of Forensic Sciences* 38(3):603-615.
- Lands, W.E.M.
1998 A Review of Alcohol Clearance in Humans. *Alcohol* 15(2):147-160.
- Lyle, H.P., K.L. Stemmer, and F.P. Cleveland
1958 Determination of the Time of Death. *Journal of Forensic Sciences* 4(2):167-175.

- Micozzi, M.S.
1986 Experimental Study of Postmortem Change Under Field Conditions: Effects of Freezing, Thawing, and Mechanical Injury. *Journal of Forensic Sciences* 31(3):953-961.
- Naumann, H.N.
1950 Studies on Postmortem Chemistry. *American Journal of Clinical Pathology* 20:314-324.
- Riveros-Rosas, H., A. Julian-Sanchez, and E. Pina
1997 Enzymology of Ethanol and Acetaldehyde Metabolism in Mammals. *Archives of Medical Research* 28(4):453-471.
- Schleyer, F.
1963 Determination of the Time of Death in the Early Postmortem Interval. *Methods of Forensic Science* 2:253-293.
- Stone, B.E., and P.A. Rooney
1984 A Study Using Body Fluids to Determine Blood Alcohol. *Journal of Analytical Toxicology* 8(2):95-96.
- Wells, J.D., and L.R. Lamotte
2001 Estimating the Postmortem Interval, in *Forensic Entomology: The Utility of Arthropods in Legal Investigations*, Byrd, J.H., and J.L. Castner, Eds., CRC Press, London:263-285.
- Young, D.S., L.C. Pestaner, and V. Gibberman
1975 Effects of Drugs on Clinical Laboratory Tests. *Clinical Chemistry* 21:1D.
- Zilva, J.F., and P.R. Pannall
1979 *Plasma Enzymes in Diagnosis in Clinical Chemistry in Diagnosis and Treatment*. Lloyd-Luke, London.
- Zimmerman, H.J., and J.B. Henry
1979 Clinical Enzymology, in *Clinical Diagnosis and Management by Laboratory Methods*, 16th ed., Henry, J.B, Ed., Saunders, Philadelphia:365-368.

VITA

Karly Laine Buras was graduated from St. Mary's Dominican High School in 1997 and received her Bachelor of Science in microbiology in December of 2001 from Louisiana State University. She is a member of the American Academy of Forensic Sciences, where she has participated in the Young Forensic Scientists Forum as an academic session chair and general planner. She is also a member of Lambda Alpha National Honor Society, National Society of Collegiate Scholars, and the Geography and Anthropology Society at Louisiana State University. She is currently employed as a forensic scientist at Louisiana State Police Crime Lab, and continues to use her background in microbiology and physical anthropology to complement her career in forensic science.

Karly is the daughter of Paul Buras, and of Dennis Beaver and Karla LaMarca Buras. She has one brother, Cody, and two sisters, Ann and Sara. She will be married this November to Paul Ridgell. She was born on November 3, 1979, and is a native of Plaquemines Parish, Louisiana.